Numerical Experiments in Homogeneous Turbulence

Robert S. Rogallo

September 1981

NASA

National Aeronautics and
Space Administration

Numerical Experiments in Homogeneous Turbulence

Robert S. Rogallo

September 1981

NUMERICAL EXPERIMENTS IN HOMOGENEOUS TURBULENCE

Robert S. Rogallo

Ames Research Center

SUMMARY

The direct simulation methods developed by Orszag and Patterson (1972) for isotropic turbulence have been extended to homogeneous turbulence in an incompressible fluid subjected to uniform deformation or rotation. The results of simulations for irrotational strain (plane and axisymmetric), shear, rotation, and relaxation toward isotropy following axisymmetric strain are compared with linear theory and experimental data. Emphasis is placed on the shear flow because of its importance and because of the availability of accurate and detailed experimental data. The computed results are used to assess the accuracy of two popular models used in the closure of the Reynolds-stress equations. Data from a variety of the computed fields and the details of the numerical methods used in the simulation are also presented.

INTRODUCTION

The turbulence problem has remained the greatest challenge to fluid dynamicists since its definition by Reynolds 100 years ago. The nonlinearity of the Navier-Stokes equations prevents statistical analysis of the dynamics of energetic turbulent fields, and as a result no theory has yet been devised that is devoid of assumptions beyond that of the validity of the Navier-Stokes equations themselves. Although statistical, tensorial, and dimensional analysis combined with the continuity condition provide constraints on the statistics of a turbulent field, our knowledge of the statistics themselves has been gained primarily through experiment.

The turbulent flows of interest in engineering, geophysics, and meteorology are complex even at the statistical level, but there are interesting flows with spatially homogeneous statistics that have been examined both theoretically and experimentally. Although these homogeneous flows do not have net diffusion of turbulence momentum or energy, they can be anisotropic and extract energy from the mean motion ; therefore, they provide a case for study intermediate in complexity between isotropic flows and general inhomogeneous flows. Although homogeneous flows are more difficult to achieve experimentally than inhomogeneous flows, such as jets, wakes, and pipe flow, they are considerably easier to simulate on a computer because of the absence of flow boundaries.

The method of direct numerical simulation of homogeneous turbulence in general use today is that of Orszag and Patterson (1972). The turbulence field is represented by the coefficients of a truncated three-dimensional Fourier series, or

equivalently by spatially periodic discrete values on a uniform mesh in physical space. Transformation between the two spaces (physical and wave) is accomplished by fast Fourier transforms. Differentiation is performed in wave space as multiplication by the wave number, and velocity products are carried out in physical space to avoid the expensive convolution sums required for that operation in wave space. The field can be time-advanced in either space by any algorithm appropriate for systems of ordinary differential equations.

There are two basic requirements that a direct simulation must meet if it is to represent turbulence. First, it must represent a solution of the Navier-Stokes equations. This means that all scales of motion must be adequately resolved, in the deterministic sense, by the computational mesh. In particular, the Reynolds number should be small enough to allow the mesh to accurately capture the viscous dissipation scales. The explicit use of Fourier series then implies a spatially periodic solution of the Navier-Stokes equation. The second requirement is that this periodic solution be sufficiently complicated, that is, it must provide adequate statistical resolution (large sample) of the set of all possible fluid motions allowed by the Navier-Stokes equations. The computational sample of a scale of motion is inversely proportional to the volume of the scale. Thus scales of motion comparable to the computational period have a very small sample (~1), and scales comparable to the mesh spacing have a large sample (~10^5 for a 128^3 mesh). The two requirements for a turbulence simulation conflict; the sample improves as the energy moves to smaller scales but the viscous resolution is degraded.

The range of scales (the ratio of the wavelength of the fundamental to that of the highest wave number carried) in a given direction is $M/2$, where M is the number of nodes in that direction. The largest computers available today allow 128 mesh cells in each direction, which limits the useful range of scales to about 10 or so. That is, the bulk of the total turbulent energy must be contained within one decade of scale. This is a severe constraint and it limits completely resolved direct simulation to very low Reynolds numbers. In practice we usually accept some error in order to obtain a higher Reynolds number. In some cases we sacrifice sample and shift the computed scale range toward the small scales , and in others we sacrifice resolution of the dissipation process and shift the computed range toward the large scales. For the current study we are most interested in the anisotropy of the Reynolds-stress tensor, and less interested in the details (such as intermittency) of the small scales, and we generally accept incomplete resolution of the dissipation scales. It appears, however, that the error in total dissipation is much less affected than is its spectral distribution because the total is determined primarily by energy transfer down-scale within the energetic scales; this in turn depends on how well the energetic scales themselves are resolved and not on how well the actual dissipative scales are resolved.

Computation and physical experiment complement each other rather well for homogeneous turbulence. The experimental difficulties are associated with setting up the mean motion, achieving a homogeneous turbulence field, and in the actual measurement of the various spectra, correlations, etc. There is no doubt that the physical experiment produces results at all scales in accordance with the Navier-Stokes equations, although frequency response (in both space and time) of the instrumentation can limit their measurement. The computation on the other hand has no difficulty setting up the mean flow or making measurements. The difficulty is that because of limited resolution (statistical accuracy at the large scales, numerical accuracy at the small scales), it is not always simple to relate computed quantities to those of the experiment at much higher Reynolds number. The goal of this study is to use experimental data to validate simulated turbulence fields, which

2

in turn provide measurements that are not available from experiment. The quantities measured here are primarily those volume averages appearing in the Reynolds-stress equations.

In the sections that follow we consider four cases of homogeneous turbulence, each being the evolution from an initially isotropic state caused by a mean velocity gradient uniform in space and time. The deformations considered are (1) irrotational plane strain, (2) irrotational axisymmetric strain, (3) uniform shear, and (4) uniform rotation. In the case of axisymmetric strain we allow the turbulence to relax back toward isotropy when the straining ceases. The only theory available to describe the evolution of these flows is a linear theory valid in the limit in which the time scale of all turbulence scales is much longer than the time scale given by the mean velocity gradient. This theory, due originally to Taylor (1935), has been developed for each case by various authors and is used, together with available experimental data, to establish (we hope) some credibility for the simulations. Then, as an example of how the detailed measurements of the simulated fields might be used to aid the turbulence-model maker, we have compared measured values from the fields with modeled values following recommendations of Rotta (1951) and Launder, Reece, and Rodi (1975).

Finally, more details are given in the appendixes, Appendix A presents in tabular form various raw data measured in each field, including the Reynolds-stress budget; Appendix B provides a more detailed exposition of the equations and numerical methods used in the simulations.

PLANE STRAIN

Nearly isotropic turbulence, subjected to a uniform strain in two directions, has been investigated experimentally by Townsend (1951) and by Tucker and Reynolds (1968) by passing grid-generated turbulence through a channel of changing cross section. Townsend imposed a total strain of 4 in directions transverse to the stream; Tucker and Reynolds imposed total strains of 6 in two different configurations, the first, like that of Townsend, was strained in the transverse directions and the second had one strain imposed in the flow direction. We follow the nomenclature of Townsend and take the flow direction to be x, imposing positive strain in the z direction and negative strain in the y direction. The results of Tucker and Reynolds indicate no significant difference between the two types of strain. The longitudinal strain does have the advantage, like the axisymmetric strain discussed in the next section, that the strain is given by direct measurement of the variation of mean flow velocity down the channel.

Results of four computed cases, all evolving from the same isotropic initial state are presented. The initial state itself is the result of an isotropic simulation so that the spectral transfer is established. The microscale Reynolds number $q\lambda_{11}/\nu$ of the initial field is ~35, and dimensionless strain rates aq^2/ε ~ .5, 1, 2, and 4 (where $a = d\bar{w}/dz = -d\bar{v}/dy$, $q^2 = \overline{u_i u_i}$, $\varepsilon = 2\nu\overline{u_{i,j} u_{i,j}}$) are imposed in cases B2D1, B2D2, B2D3, and B2D4, respectively. The total strain achieved is 4; higher strains result in inadequate resolution because the computational mesh moves with the mean flow and becomes excessively strained. At the initial state, the computational cell has $\Delta y = 2\Delta z$, and at a strain of 4, $\Delta z = 2\Delta y$.

3

Three independent dimensionless parameters can be formed from the time t, strain rate a, viscosity ν, and turbulent velocity and length scales q and L respectively. These are taken to be at, aL/q, qL/ν, the dimensionless time, ratio of turbulence and strain time scales, and a turbulence macroscale Reynolds number. No information on macroscales is directly available from the experiments, so we have instead estimated L by assuming $\varepsilon \sim q^3/L$ in the isotropic initial state. The initial conditions are then scaled by the dimensionless groups aq^2/ε and $q^4/\varepsilon\nu$. Estimates of the quantities for the experiments are as follows:

	aq^2/ε	$q^4/\nu\varepsilon$
Townsend .5 in. mesh	.45	95
1 in. mesh	.45	230
Tucker-Reynolds	.3	425
Present results	.5,1,2,4	129

Here the isotropic relation $\varepsilon = 10\nu q^2/\lambda_{11}^2$ has been used. For the Townsend experiment, the microscales are given and these are used to estimate ε; for the Tucker and Reynolds experiment we have estimated ε by fitting a power law, with exponent of -1.2, to the plotted energy history; these estimates are very rough indeed.

The linear theory of "sudden distortion" was originated by Taylor (1935) who considered the inviscid irrotational strain of a typical Fourier component of the velocity field. The effect of viscosity can be included by use of an integrating factor (Pearson (1959)). Batchelor and Proudman (1954) extended the inviscid theory to determine the effect of rapid irrotational strains on the energy tensor of an initially isotropic turbulence field, and the result is independent of the form of the energy spectrum E(k). Although viscosity can in principle be handled exactly, the necessary integrals over Fourier space contain exponential factors and probably cannot be evaluated in closed form. The result would depend on the initial spectrum.

A comparison of the linear theory, experimental, and computational results is presented in figures 1 through 3. The evolution of the normalized energy tensor is shown in figure 1, and the structure parameters introduced by Townsend are shown in figures 2 and 3. The computational results approach the linear theory consistently with increasing strain rate but, although they follow the trends of the experiment, quantitative agreement (particularly for K_1 and K_1') is lacking.

The differences between the two experiments are not consistent with our estimates of their dimensionless time scales and Reynolds numbers. At a given level of strain, the structure parameter K_1 should increase with strain rate but decrease with increasing Reynolds number. Our estimates of the dimensionless strain rates and Reynolds numbers of the experiments would cause us to expect higher K_1 values from the the Townsend experiment than from the Tucker and Reynolds experiment, but that is not the case.

AXISYMMETRIC STRAIN

Turbulence in an axisymmetric strain field is the simplest anisotropic flow. Because it occurs often in engineering applications, it has been studied in a number of experiments. We will compare the computational results with the experimental data of Uberoi (1956) and Hussain and Ramjee (1976), who achieved total strains up to 16 at a wide range of Reynolds numbers. Unfortunately, information concerning the dissipation rate and length scales was not presented, and we are unable to determine with any confidence the turbulence Reynolds numbers or time scales of the turbulence prior to straining.

Simulations were made with four constant strain rates applied at each of two viscosity values. The dimensionless strain rates aq^2/ε, where $a = d\bar{u}/dx = -2d\bar{v}/dy = -2d\bar{w}/dz$, were 0.3, 0.6, 1.2, and 2.4, and the initial Reynolds numbers $q^4/\nu\varepsilon$ were 15 and 56. The evolution of the longitudinal and transverse component energies, normalized by their initial values for five of the eight simulated cases, the inviscid linear theory, and the experimental results of Uberoi and Hussain-Ramjee, are shown in figure 4. The computational results approach rapid-distortion theory consistently with increasing strain rate and Reynolds number, and the differences between computation and experiment seem to indicate a higher experimental strain rate. Beyond a strain of 4, the experimental component energy u^2 grows because of the redistribution of energy by the pressure-strain correlation, and the computational data (appendix A) indicate that this is a result primarily of the growth of the "slow-pressure-strain" term with increasing strain.

HOMOGENEOUS SHEAR

Homogeneous shear turbulence is the closest structurally to flows of engineering interest and has been extensively investigated by experimenters. In a series of papers from Johns Hopkins University, Rose (1966), Champagne, Harris and Corrsin (1970), Harris, Graham and Corrsin (1977), and Tavoularis and Corrsin (1981) (hereafter TC) have provided extensive documentation of the development of turbulence subjected to uniform shear. The results of Mulhearn and Luxton (1975) are in substantial agreement with the earlier work of the Johns Hopkins group. On the other hand, the linear theory of homogeneous shear turbulence has been worked out by Deissler (1961, 1970, 1972), and Fox (1964); their results are consistent with the initial stage of development of the experimentally observed turbulence.

The linear theory can be worked out in a somewhat simpler way than that of Deissler, who worked directly with the equations for the spectrum tensor after dropping out the triple correlations. Written in a coordinate system moving with the mean shear, the linearized Navier-Stokes equations are

$$u_t + sv + p_x = \nu\nabla u$$

$$v_t - stp_x + p_y = \nu\nabla v$$

$$w_t + p_z = \nu\nabla w$$

$$u_x - stv_x + v_y + w_z = 0$$

5

where

$$s = \frac{d\bar{u}}{dy} \quad \text{and} \quad \mathscr{D} = \frac{\partial^2}{\partial x^2} + \left(\frac{\partial}{\partial y} - st\frac{\partial}{\partial x}\right)^2 + \frac{\partial^2}{\partial z^2}$$

Upon taking the Fourier transform of these equations and solving the remaining ordinary differential equations for the time variation, we obtain

$$F\tilde{u} = -Ak_3 + B\left\{k_3^2 \tan^{-1}\eta - k_1^2 \frac{\eta}{1 + \eta^2}\right\}$$

$$F\tilde{v} = Bk_1 \sqrt{k_1^2 + k_3^2} \frac{1}{1 + \eta^2}$$

$$F\tilde{w} = Ak_1 - Bk_1k_3\left\{\tan^{-1}\eta + \frac{\eta}{1 + \eta^2}\right\}$$

where F is the integrating factor

$$\log F = \frac{-\nu}{ks} (k_1^2 + k_3^2)^{3/2}\left(\eta + \frac{1}{3}\eta^3\right)$$

$$\eta = \frac{k_2 - k_1 st}{\sqrt{k_1^2 + k_3^2}}$$

and $A(\underline{k})$, $B(\underline{k})$ are determined from the initial conditions. The evolution of the spectrum tensor from an isotropic state is determined by solving for AA^*, AB^*, and BB^*, using the isotropic form at $st = 0$.

$$\tilde{u}_i\tilde{u}_j^* = \frac{E(k)}{4\pi k^4} (k^2\delta_{ij} - k_ik_j)$$

Deissler (1970) has carried out the analysis for the spectrum function

$$E(k) \sim k^4 e^{-(k/k_0)^2}$$

integrating (numerically) over wave space to determine the time history of the energy tensor. The solution depends only on the dimensionless time st and on the Reynolds number $s/\nu k_0^2$. For small Reynolds numbers, the energy decreases at all times, but for large enough Reynolds numbers the energy increases for a finite time and then decays. The $\overline{v^2}$ energy component decays at all times, as can be readily seen in the solution for $\tilde{v}$ above. This in turn causes the cross correlation $\overline{uv}$ to decay, after some growth from its zero initial value, and the resulting loss of production ($-s\ \overline{uv}$) eventually leads to viscous decay.

This linear picture of the development of shear turbulence is consistent with

6

the experimental evidence at small times (st < 4) and predicts (surprisingly well) the magnitude of the shear stress correlation $\overline{uv}/u'v'$ and the ordering $u' > w' > v'$ of the component energies. It has been determined experimentally, however, that the v component eventually grows, gaining energy through the pressure-strain correlation caused by the nonlinear transport terms in the Navier-Stokes equations; this in turn leads to growth in $\overline{uv}$ and the energy. The ultimate fate of the turbulence is currently a speculative issue, but there is evidence of a self-similar evolution. The energy is still growing at the largest times observed in both the experiments and computation, and the ratios of component energies and integral scales are still varying, although rather slowly. If the turbulence approaches a self-similar state with single velocity scale q and single length scale L, its attributes depend only upon t, q, L, s, and v. Dimensional analysis then requires

$$\frac{sL}{q} = f\left(st, \frac{qL}{v}\right)$$

If the velocity and length scales both grow monotonically at large times, sL/q must approach a finite nonzero constant, because if $sL/q \to \infty$, linear theory is valid and predicts the ultimate decay of q; similarly, if $sL/q \to 0$, the flow approaches isotropy and q decays. With nonzero s the flow can not become isotropic in any case because for isotropic flow there is strong experimental evidence that $L \sim q^3/\varepsilon$ and $q \sim t^{-n}$ from which it follows that $d(sL/q)/d(st) > 0$.

Four shear flows were simulated, three of them (BSH9, BSH10, and BSH11) from the same initial conditions. The initial energy spectrum for these runs was simply a square pulse $E(k) = 1$ for $16 < k < 32$, a wave-number band containing roughly a quarter million Fourier modes. The initial spectrum for the fourth case (BSH12) was a square pulse at $10 < k < 20$, the lower wave number allowing a higher Reynolds number to be attained.

The shear rates and viscosity used are as follows:

Case	Spectrum (E(k)=1)	s	Viscosity
BSH9	16<k<32	$20\sqrt{2}$	$.01/\sqrt{2}$
BSH10	16<k<32	$20\sqrt{2}$	$.02/\sqrt{2}$
BSH11	16<k<32	$40\sqrt{2}$	$.02/\sqrt{2}$
BSH12	10<k<20	20	.005

The velocity-scale history of the four runs is shown in figure 5(a). As observed experimentally, the energy decays at first but later grows monotonically for the remainder of the observed time; the growth beyond st~10 appears to be exponential. The growth of the integral scales is shown in figure 5(b), with obvious anomalies beyond c~10. The strange behavior, especially for BSH9, is caused by the fact that the two-point correlation is forming a rather broad negative region that diminishes the growth of its integral because of the lengthening positive portion, as shown by figure 6. Similar behavior is observed in the other correlations for run BSH9 in figures 7 - 9. By st~10, the largest scales of the simulation (roughly the size of the computational period) have attained sufficient energy that they dominate the integral scale. The evolution of the three-dimensional energy spectrum of run BSH9, which illustrates the point, is shown in figure 10. The sample in each spherical shell is proportional to k^2 so that as the spectrum develops toward the large-scale end, more and more of the energy is contained in fewer and fewer Fourier modes. At st~10 the number of these energy-rich modes no longer provides an adequate

7

statistical sample, and although the simulation is still a periodic solution of the Navier-Stokes equations, it is not representative, at the large scales, of turbulence. However the smaller scales still retain a good sample, and statistics from them (e.g., microscales) show no anomalous behavior. As shown in figure 11, the dissipation scales are adequately sampled throughout the run, but for st~12 the spectrum does not decay with wave number rapidly enough to allow complete resolution of the dissipation scales. All four cases appear to be adequately resolved at st ~ 8; BSH9 and BSH12 are marginal at st = 10 ; and BSH10 and BSH11 are marginal at st = 12.

The primary dimensionless flow parameters are presented in figures 12 and 13. We have used the longitudinal integral scale $L_{11,1}$ in the streamwise direction (x) as the length scale and $q = \overline{(u_i u_i)}^{1/2}$ as the velocity scale. The mean shear s provides the time scale of the shear. In figure 12, the experimental data of TC indicate that the growth of velocity and length scales has equilibrated at st~8; this is prevented in the computation by the peculiar growth of the integral scale. The turbulence Reynolds number shown in figure 13 indicates that the experimental data are consistent with exponential growth in both velocity and length scales, having roughly the same growth rate as the computation. The experimental Reynolds numbers are simply not attainable with the available computational resolution but we hope that the Reynolds numbers attained are high enough for the statistics of the energetic scales to achieve nearly asymptotic values. The classical mixing length (fig. 14) is formed from velocity scales of the turbulence and the (constant for each run) time scale of the shear; it appears to grow exponentially at earlier times than does q (fig. 5(a)).

The distribution of energy among the velocity components is presented in figure 15; it suggests the possibility that the component energies approach fixed ratios. If such a structural equilibrium occurs between the tendency of the shear to produce anisotropy and the tendency of the turbulence to become isotropic, the anisotropy measure of the equilibrium should depend on sL/q and (probably weakly) on qL/ν. This is shown more clearly in figure 16 where an adhoc linear scaling of the anisotropy is shown which collapses the data reasonably well. The discrepancy between computation and experiment could be a Reynolds-number effect similar to that in the shear-stress correlation shown in figure 17. The Reynolds number shown there was chosen because it is the only dimensionless group independent of L and t. Although it seems physically reasonable to eliminate explicit dependence on time, the elimination of L simply allows us to avoid the use of the measured integral scales. The rapid rise of the shear-stress correlation from its initial isotropic value of zero is evident. The shear-stress correlation is equally well collapsed by microscale Reynolds number. The reduction of the shear-stress correlation with increasing Reynolds number is primarily due to the fact that the contribution to $\overline{uv}$ of the small scales increases less rapidly with the increase of small-scale energy than does the contribution to the normalizing factor (u'v'); this is because of the tendency toward isotropy of small scales. The explicit use of Reynolds-number to collapse correlations for medium and large scales was first used by Stewart and Townsend (1951) in isotropic turbulence. In the shear flow, unlike isotropic flow, we have a direct energy measure, $\overline{uv}$, that is relatively Reynolds number insensitive, and this can be used to advantage to normalize velocity autocorrelations.

The autocorrelations presented in figure 18 are normalized by the single energy measure $\overline{uv}$, and plotted against the separation, normalized by the single length scale $L_{11,1}$, the integral scale of $R_{11}(r,0,0)$. The experimental points are from the Tavoularis and Corrsin data at X/H = 11. If the turbulence were in exact structural equilibrium this scaling would collapse all of the data, except near r = 0 where

8

viscous effects appear. At infinite Reynolds number the collapse would be complete. Perfect collapse requires that ratios of the component energies and ratios of the macroscales be universal constants. This is too much to expect here, however, for we have already seen that ratios of the component energies in both the experiment and computation are still varying slowly with sL/q and qL/ν; moreover the integral scales of the computation are not as reliable as we would like because of the small sample of the largest energetic scales.

The microscales measured by TC did not vary after $st = 8.65$, but the computed microscales are growing slowly at $st = 8$, as shown in figure 19, with the growth rate diminishing with increasing Reynolds number.

TABLE 1. – COMPARISON OF EXPERIMENTAL AND COMPUTED TURBULENCE FIELDS

Quantity		Tavoularis-Corrsin X/H=11	Case BSH9 st=10	Case BSH12 st=10
$\overline{u_1^2}/q^2$	(Component energies)	.535	.508	.485
$\overline{u_2^2}/q^2$		.186	.185	.209
$\overline{u_3^2}/q^2$		.279	.307	.306
$-\overline{uv}/u'v'$	(Shear-stress correlation)	.45	.49	.49
$L_{11,2}/L_{11,1}$	(Integral scale ratios)	.33	.44	.59
$L_{11,3}/L_{11,1}$		.25	.17	.14
$L_{22,1}/L_{11,1}$		.23	.41	.33
$L_{33,1}/L_{11,1}$		.34	.23	.17
$L_{12,1}/L_{11,1}$		.90	.88	.88
$L_{12,2}/L_{11,1}$		.40	.69	.74
$\lambda_{12}/\lambda_{11}$	(Microscale ratios)	.67	.65	.76
$\lambda_{13}/\lambda_{11}$		.68	.69	.79
$\lambda_{21}/\lambda_{11}$		.68	.86	.80
$\lambda_{31}/\lambda_{11}$		.79	.88	.85
σ_a/σ_b	(Principal stress ratios)	4.3	4.8	4.0
σ_a/σ_c		2.1	1.9	1.8
$\alpha_a(^\circ)$	(Principal axis orientation)	20	22	24
$\nu_T/\nu = (-\overline{uv})/\nu s$	(Dimensionless measures)	179	16	38
$R_\lambda = u'\lambda_{11}/\nu$		266	76	104
$sL_{11,1}/q$		2.83	2.23	1.96
$qL_{11,1}/\nu$		3581	219	472
$\ell/L_{11,1} = (-\overline{uv})/sL_{11,1}\nu$		.116	.167	.174

A summary of the TC data at $X/H = 11$ ($st \sim 12.6$) and of the computational results at $st = 10$ from cases BSH9 and BSH12 (our highest Reynolds numbers) is presented in table 1. The results of the computation agree well with the experimental data,

9

except for the integral scale ratios (and quantities containing viscosity explicitly). Part of this discrepancy is due to the fact that TC measured the scales by integrating to the first zero of the correlations and that we integrated over the negative portions as well; but this affects only $L_{11,3}$ in the experimental data. The main cause of the discrepancy is that the integral scale, as stated by Batchelor (1953), is not as representative of the scales of motion containing the energy as we would like; it overemphasizes the largest scales where our sample is poor. In the experiment, a large sample of the largest eddies is swept past the probes by the mean flow, but in the computation we move with the mean flow and always observe the same large scales.

There is some evidence in both the computational and experimental results that the turbulence approaches a structural equilibrium, with length and velocity scales growing exponentially. The experimental evidence, stated by Tavoularis and Corrsin themselves, although they seem to expect linear rather than exponential growth, is that the measured downstream transport Dq^2/Dt and the production $-\overline{suv}$ of the turbulence are in a fixed ratio, within the experimental error, for $7.5 \leq X/H \leq 11$. This implies that the dissipation rate is also in a fixed ratio to the transport; and this relationship was checked independently by measurement of the velocity derivative variances. This is equivalent to the fact that both the shear-stress correlations and microscales are constant. The energy growth rate is then proportional to the energy, and the growth is exponential. In table 2 we present a check of the experimental data for consistency with linear and exponential growth by using the data at $X/H = 7.5$ and $X/H = 9.5$ to predict the data at $X/H = 11$. Although either growth form extrapolated to $X/H = 11$ probably lies within the experimental error, the exponential form is consistently closer to the published values. The computations clearly indicate that the energy of periodic perturbations of a uniform shear grows exponentially, but the turbulence macroscale is bounded by the computational period. Unfortunately, by the time the computational velocity is clearly growing exponentially, the integral scales indicate an insufficient sample at the largest scales, and the relevance of the exponential growth to turbulence (as opposed to periodic solutions of the Navier-Stokes equations) is suspect.

TABLE 2. – DATA PREDICTED AT X/H = 11
BASED ON DATA AT X/H = 7.5 AND X/H = 9.5

Data predicted at X/H = 11

Quantity	Measured	Linear growth	Exponential growth
$\overline{u^2}$	.475	.465	.478
$\overline{v^2}$	.165	.163	.167
$\overline{w^2}$	.248	.242	.247
q^2	.888	.870	.892
$L_{11,1}$	57	56	57
ε	3.42	3.26	3.35

10

The decay of turbulence in a region in uniform (solid-body) rotation presents a rather special problem to the turbulence modeler because in the Reynolds stress equations the net production term (production plus fast-pressure-strain) vanishes when the turbulence is isotropic. This is an artificial situation in the sense that it is probably impossible physically to generate isotropic turbulence in a fluid rotating as a whole, but mathematically it is simply a matter of specifying isotropic initial conditions. At the Reynolds-stress level it is not possible to determine whether initially isotropic turbulence will remain isotropic. The experimental and computational results indicate that the turbulence does become slightly anisotropic, and this is consistent with the linear theory valid at low Rossby number.

At small Rossby numbers $(q/\Omega L)$ the mean rotation (Ω) causes plane waves $e^{i\underline{k}\cdot\underline{x}}$ to propagate with phase speed $2\Omega\cdot\underline{k}/k$, giving the Fourier modes some physical "wave" significance (unlike most turbulent fields in which the wave space is purely a mathematical convenience). The nonlinear terms can then be viewed as direct wave interactions. The bilinear convection term in the Navier-Stokes equation is interpreted in wave space as the interaction between wave vectors $\underline{k}'$ and $\underline{k}''$ to give the convective contribution to the time derivative at wave vector $\underline{k}'+\underline{k}''$ so that the time derivative at $\underline{k}$ is determined by the convolution sum over all wave vectors $\underline{k}'$, $\underline{k}''$ satisfying $\underline{k}'+\underline{k}'' = \underline{k}$. Taking the y-axis as the axis of rotation, the Fourier modes at low Rossby number have the form

$$\underline{\tilde{u}}(\underline{k},t) = \underline{\tilde{A}}\left(\underline{k}, \frac{qt}{L}\right)e^{i(2k_2/k)\Omega t} + \underline{\tilde{B}}\left(\underline{k}, \frac{qt}{L}\right)e^{-i(2k_2/k)\Omega t}$$

This is a classical "two-time-scale" problem at low Rossby numbers; the "long-time" is qt/L where q and L are representative of the turbulence and the "short-time" is Ωt. We are interested in the long-time variation of the spectrum tensor, and this requires that we integrate the wave interactions over times (T) much larger than the short-time scale but much smaller than the long-time scale. The correlation over this intermediate time between $\underline{\tilde{u}}(\underline{k})$ and the contribution to its time-derivative due to the interaction between $\underline{\tilde{u}}(\underline{k}')$ and $\underline{\tilde{u}}(\underline{k}'')$ is proportional to

$$\frac{\sin\omega T}{\omega T} \quad\text{where}\quad \omega = 2\Omega\left(\frac{k_2}{k} \pm \frac{k_2'}{k'} \pm \frac{k_2''}{k''}\right)$$

For very small Rossby numbers, only interactions between waves $\underline{k}'$, $\underline{k}''$ having $k_2/k \pm k_2'/k' \pm k_2''/k'' \ll 1$ are significant on the long-time scale. Rotation then acts to attenuate the effectiveness of the nonlinear interactions, which in isotropic flow move energy to higher wave numbers and enhance the dissipation; this explains the experimentally observed reduction (Wigeland and Nagib (1978)) of the dissipation from its value without rotation. This argument only requires that rotation attenuate interactions and assumes nothing about which directions in wave space or which

11

velocity components suffer the reduced energy flow. However the experimental data of Wigeland and Nagib (1978) indicate that the energy is redistributed among the velocity components with the ratio of energies reaching an equilibrium when the transverse macroscale begins to grow at a faster rate than the longitudinal macroscale.

We have simulated the flow at five rotation rates, but with a microscale Reynolds number of only about 3, because of a program input error. As a result, dissipation dominates the Reynolds-stress equations. The dissipation rate is nevertheless reduced slightly (~25 percent at the highest rotation rate) at early times, as shown in figure 20. A structure parameter indicating component energy anisotropy is shown in figure 21; the longitudinal component $\overline{v^2}$ gains energy through the slow-pressure-strain term. As the tables in appendix A indicate, the contribution of the fast-pressure-strain term varies widely in magnitude and takes both signs, indicating that it is oscillating. The slow-pressure term, on the other hand, varies slowly and always works to enhance $\overline{v^2}$. The experimental data show higher anisotropy, but this could well be a result of the anisotropic initial conditions of the experiment or to the Reynolds number disparity.

In figure 22 the anisotropy at the dissipation scale is also shown to reach an equilibrium, and the correlation with Ωt, rather than νt, indicates that this is not entirely a viscous effect.

TURBULENCE MODELS

The results of the numerical simulations can be used to aid the construction of turbulence models at any level, from simple algebraic models of the Reynolds stresses to spectral models such as the quasi-normal approximation. Appendix A contains information at the Reynolds-stress level for a sample of the computed fields discussed in the previous sections. In this section we illustrate how these data might be used to test proposed models or to determine "model constants" for some of the modeled terms in the Reynolds-stress equations.

THE REYNOLDS-STRESS EQUATIONS

When the turbulence field is homogeneous, the Reynolds-stress equations become

$$\frac{d}{dt}\,(\overline{u_i u_j}) = \underbrace{-U_{i,k}\overline{u_j u_k} - U_{j,k}\overline{u_i u_k}}_{\text{production}} + \underbrace{2\overline{p s_{ij}}}_{\substack{\text{pressure-}\\\text{strain}}} - \underbrace{2\nu\overline{u_{i,k} u_{j,k}}}_{\text{dissipation}}$$

where the mean flow gradient $U_{i,j}$ depends only on time, and s_{ij} is the turbulent strain-rate tensor $s_{ij} = (u_{i,j}+u_{j,i})/2$. The over-bar denotes an average over physical space. Pressure is decomposed into its so-called "fast" and "slow" parts given by

$$\nabla^2 p^{(1)} = -u_{i,j}u_{j,i} \qquad \text{(slow pressure)}$$

$$\nabla^2 p^{(2)} = -2U_{i,j}u_{j,i} \qquad \text{(fast pressure)}$$

The terms "fast" and "slow" refer to the fact that $p^{(2)}$ depends directly on mean flow gradients and can therefore have its time scale imposed directly by the mean strain rate. The slow term, on the other hand, responds indirectly through changes in turbulence structure. For homogeneous flows we have exactly

$$\overline{2p^{(2)}s_{ij}} = a^{mi}_{\ell j} U_{\ell,m}$$

where

$$a^{mi}_{\ell j} = 2 \sum_{\underline{k}} \frac{k_\ell k_j}{k^2} \hat{u}_i(\underline{k})\hat{u}^*_m(\underline{k})$$

The sum indicated is over all Fourier modes. The fourth rank tensor $\underline{\underline{a}}$ has the obvious symmetry

$$a^{mi}_{\ell j} = a^{im}_{\ell j} = a^{mi}_{j\ell}$$

and the continuity condition, $k_i\hat{u}_i = 0$, implies

$$a^{mi}_{\ell i} = 0$$

In addition, the contraction $a^{mi}_{jj} = 2\overline{u_i u_m}$ provides a convenient scaling factor, and as a factor of the mean deformation rate it emphasizes the close relation between the production and fast-pressure-strain terms in the stress equations. In essence, the production and fast-pressure terms sum to produce the "net" production. Tables of the tensor $\underline{\underline{a}}$, shortened by use of its symmetry, are included for each recorded field in appendix A, with the budget of the stress equations above.

In the Reynolds-stress equations only the production term can be computed directly from the stress tensor. The dissipation and fast-pressure terms are second-order velocity moments like the stress; however, they contain velocity derivatives and thus depend on the spectral distribution of stress (the spectrum tensor) and not merely on its average value. They must be modeled along with the slow-pressure term, which is a third-order velocity moment.

We consider first the slow-pressure-strain and dissipation terms, following the analysis of Lumley and Newman (1977) who combine the slow-pressure-strain tensor with

13

the deviator of the dissipation tensor. Lumley writes

$$2p^{(1)}s_{ij} - 2\nu\overline{u_{i,k}u_{j,k}} + \frac{2}{3}\,\varepsilon\delta_{ij} = -\varepsilon\phi_{ij}$$

where ϕ is a traceless tensor and ε is the dissipation rate of kinetic energy

$$\varepsilon = \nu\overline{u_{i,j}u_{i,j}}$$

which must be modeled. The approximation (Rotta (1951)) that ϕ depends only on the tensor $\underline{b}$,

$$b_{ij} = \frac{\overline{u_i u_j}}{q^2} - \frac{1}{3}\,\delta_{ij}$$

and on scalar attributes of the flow, requires for proper tensor invariance that ϕ be an isotropic function of $\underline{b}$,

$$\phi_{ij} = \beta b_{ij} + \gamma\left(b_{ik}b_{kj} + \frac{1}{6}\,II\delta_{ij}\right)$$

The coefficients β and γ are functions of scalar invariants of the field such as Reynolds number, $q^4/\nu\varepsilon$, II, III,

where $\qquad -2II = b_{ij}b_{ji}, \qquad 3III = b_{ij}b_{jk}b_{ki}$

are the invariants of $\underline{b}$ (the third independent invariant, b_{ii} is zero by the definition of $\underline{b}$). Lumley and Newman show that for high Reynolds numbers, $\gamma\to 0$, if slightly anisotropic flows are to return to isotropy.

We will retain for our purposes here only the linear term of the model. Some information about the coefficient of the linear term β can be determined by considering limiting cases. In the absence of a mean flow (for example the "return to isotropy" following an applied strain), $\beta \geq 2$ if the anisotropy is to decay. For any anisotropy $\beta\to 2$ as the Reynolds number vanishes since in that case the velocity components all decay in proportion to their magnitudes and the anisotropy $\underline{b}$ is constant. Lumley and Newman fit the slightly anisotropic data of Comte-Bellot and Corrsin (1966) and find that, again, $\beta\to 2$ as the anisotropy vanishes at high Reynolds number in the absence of a mean flow. In later papers, Lumley (1978, 1979) shows that in order to force the energy tensor predicted by the model to be realizable (have positive definite component energies in principle axes) $\beta\to 2$ as a component energy vanishes. Lumley found a function of the invariants

14

$$G(II,III) = 1/9 + 3III + II$$

that vanishes if and only if a component energy vanishes, and he suggests that this function be explicitly included in the model to ensure realizability. For example,

$$\beta = 2 + \beta'G(II,III)$$

where β' is a function of scalar invariants.

The relaxation toward isotropy of turbulence subjected to axisymmetric strain has been simulated, taking as initial conditions fields at total strains $2^{1/3}$, 2, and 4 from the set of axisymmetric strain runs discussed earlier. In figure 23 we show the variation of ϕ and its pressure-strain and dissipation terms with the anisotropy b. In this flow only the normal stresses are significant, and two of them are nearly equal, the deviation being a result of the finite sample. The two families of points in the pressure-strain plot correspond to the two values of viscosity in the simulations, indicating the Reynolds-number dependence of the coefficient β. This Reynolds-number effect is more apparent in the dissipation and pressure-strain parts than in their sum ϕ, indicating the advantage of treating these terms together. This is done by default when experimental data are used to determine model constants, because the dissipation is assumed to be isotropic in order to find the pressure-strain (plus dissipation deviator) from the Reynolds-stress equations. The model coefficient β for each field was found by least-square fitting the measured ϕ to the measured b. The fit is nearly perfect for each field. This is expected since ϕ and b are both diagonal, traceless, and axisymmetric and thus can be related exactly by a single coefficient. The resulting coefficients for all of the fields are plotted against a Reynolds number $q^4/9\nu\varepsilon$ and $G(II,III)$ in figures 24 and 25. Although the scatter in the coefficients is large, the trends are consistent with Lumley's predictions. The Rotta model applied to the axisymmetric strain runs, during the straining period, gives essentially the same results.

In figure 26 we present the data from the plane-strain cases discussed earlier, the groups of four points being associated with the four strain rates applied. The single degree of freedom of the linear model does not fit the two degrees of freedom of the data well, but the fit improves as the strain rate decreases. The nonlinear model, having two degrees of freedom, would fit the data exactly.

The anisotropy of the shear cases is plotted in figure 27. The fit achieved by the Rotta model is shown in figure 28 as a plot of the measured ϕ for each field against the ϕ predicted for that field by the linear model, using the measured b and the coefficient β giving the least-square fit for that field. Although this would appear to be a more difficult case than the two-dimensional strain, since four elements of the stress tensor are active, the model seems to fit the data fairly well. The coefficient grows with Reynolds number (fig. 29) as predicted by Lumley, but its variation with $G(II,III)$ is uncertain (fig. 30).

The modeled terms for the uniform rotation cases are presented in figure 31. The dissipation anisotropy is correlated with the stress anisotropy, but the pressure strain is negatively correlated with it. The pressure-strain term is evidently the source of the anisotropy in this case, contrary to its usual role as the "return to isotropy" mechanism.

The performance of the Rotta model must be judged by how well it fits the elements of the tensor ϕ at each field and how well the coefficient for each field

15

can be fitted to the scalar invariants of the field. With the exception of the plane-strain runs, which seem to be sensitive to strain rate, the linear model provides a fairly good fit to the data with coefficients that vary (qualitatively) with Reynolds number and anisotropy level in accordance with Lumley's predictions. The results do suggest, as has Lumley, that the time-scale ratio between the turbulence and mean deformation be included in the list of invariants determining the Rotta coefficient.

It would seem that modeling the tensor

$$a_{\ell j}^{mi} = 2 \sum_{\underline{k}} \frac{k_\ell k_1}{k^2} \tilde{u}_1(\underline{k}) \tilde{u}_m^*(\underline{k})$$

would be an easier task than modeling the slow-pressure term which is a third-order velocity moment; however, this has not proved to be the case. The most widely used model of the tensor $\underline{\underline{a}}$ is that of Launder, Reece, and Rodi (1975) (LRR hereafter) which has the form

$$a_{\ell j}^{mi} = A_{\ell j}^{mi} + C B_{\ell j}^{mi}$$

where C is a coefficient to be determined (again, a function of invariants) and $\underline{\underline{A}}$ and $\underline{\underline{B}}$ are fourth-rank tensors of known form that depend linearly on the Reynolds-stress tensor, satisfy the symmetry required of $\underline{\underline{a}}$, and vanish when contracted over ij. The contraction over $1j$ gives

$$A_{jj}^{mi} = 2\overline{u_i u_m} , \qquad B_{jj}^{mi} = 0$$

When the turbulence is isotropic

$$\overline{u_i u_j} = \frac{1}{3} \overline{u_\ell u_\ell} \delta_{ij} \equiv \frac{2E}{3} \delta_{ij}$$

in which case

$$B_{\ell j}^{mi} = 0$$

and

$$a_{\ell j}^{mi} = A_{\ell j}^{mi} = \frac{2E}{15} (4\delta_{mi}\delta_{\ell j} - \delta_{m\ell}\delta_{ij} - \delta_{mj}\delta_{i\ell})$$

which gives the exact result for an isotropic flow regardless of the value of C. The model has certain failings, as do all models. Some of these have been pointed

out by Lumley (1978), who shows that the model can not meet the realizability condition, and by Leslie (1980), who demonstrates that the model is too simple in form to represent the general fourth-rank tensors $\underline{\underline{a}}$ that might occur. This latter argument is easily verified by noting that regardless of the coefficient C, the model produces the following spurious symmetries (no summation implied)

$$a^{ki}_{kj} = a^{kj}_{ki} \qquad i \neq j \neq k$$

$$a^{ii}_{ij} = a^{jj}_{ji}$$
$$\qquad\qquad i \neq j$$
$$a^{ji}_{jj} = a^{ij}_{ii}$$

The addition of nonlinear terms (higher-order products of the tensor) would remove these spurious symmetries and introduce more coefficients, and as noted by Lumley, might allow the model to meet the realizability constraint. The justification for nonlinear dependence on the stress-tensor, when $\underline{\underline{a}}$ is linear (formally) in the spectrum tensor, is that $\underline{\underline{a}}$ depends also on the distribution of energy over wave space, a dependence lost when integrating the spectrum tensor to the stress tensor. The idea that the anisotropy of the spectrum tensor with respect to $\underline{k}$ might be expressible in terms of the anisotropy of the stress itself leads to the possibility of nonlinear dependence on the stress tensor, and, as suggested by Lumley, the connection might be made using the theory of rapid-distortion. In view of the difficulties associated with the LRR model, several authors (e.g. Leslie (1980)) have suggested modeling the rapid-pressure-strain term, or even the total pressure-strain, as a unit. This avoids the detailed constraints on the model imposed by the formal definition of $\underline{\underline{a}}$, but the ability to handle flows with large variations of imposed mean strain would be lost.

We compare the results of the LRR model with the computational data for the shear runs in figure 32. The 36 different elements of the tensor $\underline{\underline{a}}$ are each normalized by q^2. The constant for each field, found by least-square fit to the data, is plotted against Reynolds number in figure 33, and against G(II,II) in figure 34. The model succeeds rather well in fitting the 36 different elements with a single constant for each field, and the constant appears to be related to the anisotropy level, if not to the Reynolds number.

The least-square procedure, which was used simply to illustrate how well the models fit the data, indicates that there is room for improvement. The use of the data to determine the coefficients of a postulated model can be done in a number of ways. For example, rather than finding coefficients for the Rotta and LRR models separately, they can be found simultaneously by fitting the sum of the individually modeled terms. This is how experimental data are used for the shear flow (Leslie (1980)). When this procedure is used on the computed results, model coefficients very close to the "recommended values" are found.

The real value of the data of appendix A however, is not that it allows model coefficients to be determined in a more precise way than does experimental data, but that it provides the detail needed to determine the range of validity of a model and, it is hoped, to suggest how the model might be modified to increase that range.

CONCLUSIONS

The large-scale direct simulation of homogeneous turbulence begun by Orszag and Patterson a decade ago, has advanced with increases in computer power to the point where today it is possible to capture the statistics of the energetic scales of motion at low Reynolds number for moderate imposed mean deformations. Further advances in hardware and method will permit higher resolution in the future, but the resolution available today is adequate to allow the extraction of information useful to both model builders and "pure" theoreticians.

The relevance of the simulation to real turbulence has been established, in this author's opinion, to the point that the results can be used to fill in the gaps in the experimental database, and it is hoped that the information included for this purpose in appendix A will lead to closer scrutiny of the fundamental assumptions implicit in turbulence models.

LISTING OF DATA FROM A VARIETY OF COMPUTED TURBULENCE FIELDS

The "raw data" of a variety of computed turbulence fields is presented here in tabular form. Fields from the following (deforming mean) runs are included.

Run	Deformation	Rate (T^{-1})	Viscosity (L^2T^{-1})	Initial Condition
B2D1	(Plane strain)	4.5	$.01/\sqrt{2}$	(Developed
B2D2	$-(d\bar{v}/dy)$ ⎫	9	$.01/\sqrt{2}$	isotropic
B2D3	$d\bar{w}/dz$ ⎬	18	$.01/\sqrt{2}$	field)
B2D4	⎭	36	$.01/\sqrt{2}$	
CD11	(Axisymmetric	10	$.01/\sqrt{2}$	(Developed
CD12	contraction)	20	$.01/\sqrt{2}$	isotropic
CD13		40	$.01/\sqrt{2}$	field)
CD14		5	$.01/\sqrt{2}$	
CD21	$d\bar{u}/dx$ ⎫	10	$.02/\sqrt{2}$	(Developed
CD22	$-2(d\bar{v}/dy)$ ⎬	20	$.02/\sqrt{2}$	isotropic
CD23	$-2(d\bar{w}/dz)$ ⎭	40	$.02/\sqrt{2}$	field)
CD24		5	$.02/\sqrt{2}$	
BSH9	(Shear)	$20\sqrt{2}$	$.01/\sqrt{2}$	(Undeveloped
BSH10		$20\sqrt{2}$	$.02/\sqrt{2}$	isotropic field,
BSH11	$d\bar{u}/dy$	$40\sqrt{2}$	$.02/\sqrt{2}$	square spectrum)
BSH12		20	$.005$	
BR1	(Rotation)	2.5	$.01/\sqrt{2}$	(Developed
BR2		5	$.01/\sqrt{2}$	isotropic
BR3	$d\bar{u}/dz$ ⎫	10	$.01/\sqrt{2}$	field)
BR4	$-(d\bar{w}/dx)$ ⎬	20	$.01/\sqrt{2}$	
BR6	⎭	40	$.01/\sqrt{2}$	

Fields from these runs are named using the run name above followed by a letter designating the individual field. The plane strain fields are given at nominal strains of $\sqrt{2}$, 2, $2\sqrt{2}$, and 4, with suffixes A, B, C, and D, respectively. The axisymmetric-strain fields are given for nominal strains of $3\sqrt{2}$, 2, and 4, with suffixes A, C, and F, respectively. For the shear runs, the suffixes are not consistent from run to run, but for all runs the fields are given for st = 2, 4, 6, 8... The rotation fields are taken more or less evenly in time and are labeled sequentially A, B, C, D, E, and F for each run.

Runs named RX... are relaxation-to-isotropy cases for each of which two fields are given; for example, RX24A2 and RX24A4 are fields from the run using as initial conditions the turbulence field CD24A but setting the strain rate to zero. Thus the data of field CD24A with net production set to zero provide a third field of the relaxation run.

The following data are presented for each field:

$T = $ time $\qquad$ with units $[T]$

$VISC = \nu \qquad$ (Kinematic viscosity) $\qquad [L^2 T^{-1}]$

$RII = \overline{u_i u_i} \equiv q^2 \qquad$ (Velocity variance = $\qquad [L^2 T^{-2}]$
$\qquad\qquad\qquad\qquad$ 2*kinetic energy)

$PII = 2U_{i,j}\overline{u_i u_j} \qquad$ (Net production of RII) $\quad [L^2 T^{-3}]$

$DII = 2\epsilon = 2\nu\overline{u_{i,j}u_{i,j}}$ (Net dissipation of RII) $\quad [L^2 T^{-3}]$

$II = b_{ij}b_{ji} \qquad$ (Invariant of anisotropy tensor)

$III = b_{ij}b_{jk}b_{ki} \qquad$ (Invariant of anisotropy tensor)

MEAN DEFORMATION $\quad DU/DX$ etc. $\quad [T^{-1}]$

INTEGRAL SCALES

$$L_{11,1} = \int_0^\pi R_{11}(r,0,0)dr \qquad [L]$$

MICROSCALES

$$\lambda_{11} = \left(\frac{\overline{u^2}}{\overline{(\partial u/\partial x)^2}}\right)^{1/2} \qquad [L]$$

$$\lambda_{21} = \left(\frac{\overline{v^2}}{\overline{(\partial v/\partial x)^2}}\right)^{1/2} \qquad [L]$$

(Note the absence of 2's in these length definitions.)

REYNOLDS-STRESS BUDGET

$IJ = ij \qquad\qquad\qquad\qquad$ Stress component

$RIJ/RII = \overline{u_i u_j}/\overline{u_k u_k} \qquad$ Component energy ratio

$RATE = \dfrac{1}{2\epsilon}\dfrac{d}{dt}(\overline{u_i u_j}) \qquad$ Net time rate

$PROD = \dfrac{-1}{2\epsilon}(U_{i,k}\overline{u_j u_k} + U_{j,k}\overline{u_i u_k}) \qquad$ Production

$P2S = \dfrac{1}{\epsilon}\overline{p^{(2)}s_{ij}} \qquad$ Fast-pressure-strain

$P1S = \dfrac{1}{\epsilon}\overline{p^{(1)}s_{ij}} \qquad$ Slow-pressure-strain

$DISS = \dfrac{-\nu}{\epsilon}\overline{u_{i,k}u_{j,k}} \qquad$ Dissipation

"FAST" PRESSURE-STRAIN TENSOR

$mi \longrightarrow$

$1j \downarrow$

$a^{mi}_{\ell j}/q^2$

Each panel below contains the headings: MEAN DEFORMATION RATE (X, Y, Z), INTEGRAL SCALES / MICROSCALES (X, Y, Z), REYNOLDS-STRESS BUDGET (IJ, RIJ/RII, RATE, PROD, P2S, P1S, DISS), and "FAST" PRESSURE-STRAIN TENSOR (IJ/RI, 11, 12, 13, 22, 23, 33).

B201A

T	7.535E-02
VISC	7.071E-03
RII	4.513E 00
PII	6.566E 00
OII	3.701E 01
II	1.324E-02
III	-1.449E-04

MEAN DEFORMATION RATE
	X	Y	Z
U	0.00	0.00	0.00
V	0.00	-4.50	0.00
W	0.00	0.00	4.50

INTEGRAL SCALES / MICROSCALES
	X	Y	Z	X	Y	Z
U	.1902	.0418	.1238	.0697	.0375	.0776
V	.0704	.1803	.1114	.0642	.0935	.0796
W	.1077	.0539	.1377	.0627	.0583	.0910

REYNOLDS-STRESS BUDGET
IJ	RIJ/RII	RATE	PROD	P2S	P1S	DISS
11	0.341	-0.289	0.000	0.081	-0.021	-0.348
12	0.000	-0.002	0.000	-0.002	-0.000	0.001
13	-0.000	-0.002	0.000	-0.001	-0.001	-0.000
22	0.411	-0.164	0.451	-0.259	-0.022	-0.385
23	-0.001	-0.000	0.000	-0.002	0.002	0.000
33	0.248	-0.319	-0.273	0.178	0.063	-0.287

"FAST" PRESSURE-STRAIN TENSOR
IJ/RI	11	12	13	22	23	33
11	0.1401	-.0016	-.0004	0.3780	-.0010	0.1732
12	-.0007	-.1068	0.0010	0.0021	0.0002	-.0004
13	-.0000	-.0008	-.0133	-.0012	-.0005	0.0001
22	0.3518	0.0012	0.0009	0.1712	0.0004	0.2361
23	0.0016	0.0068	-.0005	0.0013	-.0444	-.0014
33	0.1895	0.0006	-.0007	0.2724	-.0005	0.0977

B201B

T	1.543E-01
VISC	7.071E-03
RII	3.063E 00
PII	8.791E 00
OII	1.825E 01
II	5.094E-02
III	5.094E-04

MEAN DEFORMATION RATE
	X	Y	Z
U	0.00	0.00	0.00
V	0.00	-4.50	0.00
W	0.00	0.00	4.50

INTEGRAL SCALES / MICROSCALES
	X	Y	Z	X	Y	Z
U	.1590	.0309	.1423	.1006	.0392	.1032
V	.0674	.2307	.1497	.0769	.1131	.1118
W	.1521	.0479	.1165	.0715	.0587	.1019

REYNOLDS-STRESS BUDGET
IJ	RIJ/RII	RATE	PROD	P2S	P1S	DISS
11	0.327	-0.286	0.000	0.191	-0.026	-0.371
12	-0.002	-0.004	-0.001	0.000	0.001	0.001
13	-0.001	0.000	0.000	-0.000	-0.000	0.000
22	0.496	-0.167	0.769	-0.404	-0.067	-0.385
23	-0.001	0.000	0.000	-0.003	0.004	0.000
33	0.177	-0.208	-0.768	0.213	0.093	-0.244

"FAST" PRESSURE-STRAIN TENSOR
IJ/RI	11	12	13	22	23	33
11	0.1476	-.0037	-.0005	0.5089	-.0011	0.1087
12	0.0011	-.1369	0.0005	0.0004	-.0001	0.0002
13	-.0000	-.0017	0.0137	-.0020	-.0008	0.0006
22	0.3701	-.0007	-.0003	0.2022	0.0000	0.1497
23	0.0023	0.0006	-.0004	0.0030	-.0051	-.0003
33	0.1397	0.0005	-.0005	0.2815	-.0012	0.0760

B201C

T	2.316E-01
VISC	7.071E-03
RII	2.692E 00
PII	9.935E 00
OII	1.136E 01
II	8.537E-02
III	2.490E-03

MEAN DEFORMATION RATE
	X	Y	Z
U	0.00	0.00	0.00
V	0.00	-4.50	0.00
W	0.00	0.00	4.50

INTEGRAL SCALES / MICROSCALES
	X	Y	Z	X	Y	Z
U	.1123	.0206	.2614	.1128	.0658	.1979
V	.0621	.2656	.2439	.0890	.1392	.1525
W	.2072	.0646	.0629	.0832	.0656	.1211

REYNOLDS-STRESS BUDGET
IJ	RIJ/RII	RATE	PROD	P2S	P1S	DISS
11	0.314	-0.304	0.000	0.349	-0.023	-0.222
12	-0.004	-0.004	-0.005	-0.007	0.009	0.001
13	-0.000	0.002	0.000	-0.001	0.003	-0.000
22	0.549	0.049	1.173	-0.410	-0.100	-0.413
23	-0.001	-0.002	0.000	-0.004	0.004	-0.000
33	0.137	-0.110	-0.293	0.265	0.123	-0.205

"FAST" PRESSURE-STRAIN TENSOR
IJ/RI	11	12	13	22	23	33
11	0.1581	-.0037	-.0005	0.6179	-.0016	0.0745
12	0.0023	-.1599	0.0005	0.0035	0.0001	0.0705
13	-.0008	-.0021	0.0018	-.0036	-.0017	0.0003
22	0.3725	-.0023	0.0001	0.2228	-.0000	0.1369
23	0.0025	0.0012	-.0001	0.0035	-.0629	-.0004
33	0.0969	-.0007	-.0004	0.2573	-.0013	0.0611

B201D

T	3.069E-01
VISC	7.071E-03
RII	2.156E 00
PII	1.151E 01
OII	8.881E 00
II	1.108E 01
III	3.266E 03

MEAN DEFORMATION RATE
	X	Y	Z
U	0.00	0.00	0.00
V	0.00	-4.50	0.00
W	0.00	0.00	4.50

INTEGRAL SCALES / MICROSCALES
	X	Y	Z	X	Y	Z
U	.1171	.0356	.3590	.1242	.0710	.1812
V	.0496	.1278	.3598	.0988	.1538	.2031
W	.2492	.0356	.0797	.0627	.0712	.1439

REYNOLDS-STRESS BUDGET
IJ	RIJ/RII	RATE	PROD	P2S	P1S	DISS
11	0.313	-0.113	0.000	0.424	-0.015	-0.397
12	-0.005	-0.003	-0.007	-0.009	0.015	-0.001
13	-0.000	0.002	-0.004	-0.006	0.004	-0.001
22	0.576	0.245	1.405	-0.865	-0.129	-0.426
23	-0.002	0.008	0.000	-0.008	0.000	-0.000
33	0.111	-0.062	-0.310	0.281	0.144	-0.177

"FAST" PRESSURE-STRAIN TENSOR
IJ/RI	11	12	13	22	23	33
11	0.1727	-.0016	-.0003	0.7034	-.0008	0.0385
12	0.0020	-.1803	0.0005	0.0080	0.0007	-.0001
13	-.0015	-.0024	0.0077	-.0023	-.0005	0.0001
22	0.3832	-.0018	0.0004	0.2345	-.0008	0.1173
23	0.0024	0.0020	-.0002	0.0045	-.0541	0.0003
33	0.0706	-.0004	-.0005	0.2134	-.0021	0.0445

B202A

T	3.411E-02
VISC	7.071E-03
RII	6.154E 00
PII	1.665E 01
OII	5.557E 01
II	1.438E-02
III	2.452E-04

MEAN DEFORMATION RATE
	X	Y	Z
U	0.00	0.00	0.00
V	0.00	-9.00	0.00
W	0.00	0.00	9.00

INTEGRAL SCALES / MICROSCALES
	X	Y	Z	X	Y	Z
U	.1450	.0356	.1242	.0851	.0530	.0797
V	.0620	.1677	.1006	.0691	.0866	.0785
W	.1011	.0404	.1340	.0626	.0484	.0903

REYNOLDS-STRESS BUDGET
IJ	RIJ/RII	RATE	PROD	P2S	P1S	DISS
11	0.365	-0.212	0.000	0.189	-0.033	-0.352
12	-0.000	-0.003	-0.000	-0.005	0.003	0.002
13	-0.000	-0.001	0.000	-0.002	-0.000	-0.001
22	0.412	-0.242	0.821	-0.478	-0.010	-0.376
23	-0.001	-0.002	0.000	-0.001	0.001	0.000
33	0.243	-0.410	-0.485	0.309	0.060	-0.274

"FAST" PRESSURE-STRAIN TENSOR
IJ/RI	11	12	13	22	23	33
11	0.1464	-.0018	-.0000	0.3191	-.0019	0.1648
12	-.0009	-.1136	0.0008	0.0023	0.0005	-.0002
13	-.0005	-.0005	-.0288	-.0016	-.0005	-.0004
22	0.3739	0.0016	0.0007	0.1168	0.0003	0.2300
23	0.0011	0.0003	-.0005	0.0013	-.0631	0.0010
33	0.1735	0.0000	-.0003	0.2573	-.0009	0.0919

B202B

T	7.827E-02
VISC	7.071E-03
RII	5.205E 00
PII	2.989E 01
OII	4.282E 01
II	5.099E-02
III	-6.666E-04

MEAN DEFORMATION RATE
	X	Y	Z
U	0.00	0.00	0.00
V	0.00	-9.00	0.00
W	0.00	0.00	9.00

INTEGRAL SCALES / MICROSCALES
	X	Y	Z	X	Y	Z
U	.1294	.0215	.1844	.0851	.0479	.1000
V	.0539	.2629	.1611	.0842	.0933	.1056
W	.1373	.0314	.1067	.0628	.0489	.0946

REYNOLDS-STRESS BUDGET
IJ	RIJ/RII	RATE	PROD	P2S	P1S	DISS
11	0.342	-0.133	0.000	0.312	-0.049	-0.356
12	-0.002	-0.007	-0.002	-0.006	-0.001	0.001
13	-0.000	0.001	0.000	-0.001	0.001	-0.000
22	0.489	0.084	1.089	-0.590	-0.040	-0.376
23	-0.001	-0.001	0.000	-0.004	0.004	-0.000
33	0.170	-0.231	-0.371	0.278	0.089	-0.229

"FAST" PRESSURE-STRAIN TENSOR
IJ/RI	11	12	13	22	23	33
11	0.1553	-.0034	-.0005	0.5196	-.0016	0.1006
12	-.0000	-.1488	0.0007	0.0038	0.0002	-.0002
13	-.0003	-.0013	-.0064	-.0013	-.0005	0.0003
22	0.4122	0.0005	0.0002	0.2045	0.0000	0.1718
23	0.0022	0.0003	-.0005	0.0025	-.0604	-.0008
33	0.1161	-.0005	-.0002	0.2485	-.0009	0.0668

B202C

T	1.162E-01
VISC	7.071E-03
RII	5.065E 00
PII	3.788E 01
OII	3.344E 01
II	8.844E-02
III	6.905E-05

MEAN DEFORMATION RATE
	X	Y	Z
U	0.00	0.00	0.00
V	0.00	-9.00	0.00
W	0.00	0.00	9.00

INTEGRAL SCALES / MICROSCALES
	X	Y	Z	X	Y	Z
U	.1173	.0133	.2417	.0900	.0400	.1285
V	.0451	.2301	.2340	.0706	.1056	.1412
W	.1780	.0306	.0822	.0602	.0503	.1063

REYNOLDS-STRESS BUDGET
IJ	RIJ/RII	RATE	PROD	P2S	P1S	DISS
11	0.333	-0.018	0.000	0.486	-0.051	-0.417
12	-0.005	-0.015	-0.007	-0.010	0.000	0.001
13	0.000	-0.006	-0.000	-0.001	0.001	-0.000
22	0.541	0.231	1.475	-0.777	-0.073	-0.399
23	-0.002	0.006	0.000	-0.008	0.002	-0.000
33	0.126	-0.110	-0.392	0.291	0.124	-0.168

"FAST" PRESSURE-STRAIN TENSOR
IJ/RI	11	12	13	22	23	33
11	0.1696	-.0006	-.0004	0.6357	-.0019	0.0681
12	0.0016	-.1737	0.0009	0.0076	0.0002	0.0003
13	-.0007	-.0024	0.0046	-.0015	-.0009	0.0032
22	0.4165	-.0012	0.0003	0.2241	-.0007	0.1321
23	0.0028	0.0007	-.0004	0.0037	-.0546	-.0000
33	0.0809	-.0019	-.0000	0.2183	-.0013	0.3510

B202D

T	1.540E-01
VISC	7.071E-03
RII	5.489E 00
PII	4.867E 01
OII	2.411E 01
II	1.117E-01
III	4.157E-04

MEAN DEFORMATION RATE
	X	Y	Z
U	0.00	0.00	0.00
V	0.00	-9.00	0.00
W	0.00	0.00	9.00

INTEGRAL SCALES / MICROSCALES
	X	Y	Z	X	Y	Z
U	.1037	.0077	.3058	.0842	.0539	.1666
V	.0337	.2697	.3421	.0765	.1178	.1880
W	.2231	.0304	.0863	.0714	.0536	.1257

REYNOLDS-STRESS BUDGET
IJ	RIJ/RII	RATE	PROD	P2S	P1S	DISS
11	0.331	0.214	0.000	0.686	-0.042	-0.431
12	-0.008	-0.017	-0.016	-0.011	0.036	0.001
13	-0.000	-0.004	0.031	-0.008	0.001	0.000
22	0.571	0.444	1.957	-0.971	-0.137	-0.413
23	-0.001	-0.001	0.000	-0.008	0.002	0.000
33	0.098	-0.058	-0.334	0.285	0.149	-0.156

"FAST" PRESSURE-STRAIN TENSOR
IJ/RI	11	12	13	22	23	33
11	0.1844	-.0022	-.0005	0.7268	-.0018	0.0513
12	0.0041	-.1931	0.0012	0.0100	0.0010	0.0004
13	-.0014	-.0027	0.0189	-.0006	-.0010	-.0003
22	0.4207	-.0046	-.0001	0.2590	-.0017	0.1080
23	0.0015	0.0015	-.0003	0.0066	-.0479	0.0005
33	0.0671	-.0015	-.0003	0.2000	0.0017	0.0375

B203A

T	2.072E-02
VISC	7.071E-03
RII	7.315E 00
PII	4.588E 01
OII	6.843E 01
II	1.452E-02
III	-3.386E-04

MEAN DEFORMATION RATE
	X	Y	Z
U	0.00	0.00	0.00
V	0.00	-18.00	0.00
W	0.00	0.00	18.00

INTEGRAL SCALES / MICROSCALES
	X	Y	Z	X	Y	Z
U	.1393	.0720	.1274	.0134	.0504	.0841
V	.0571	.1613	.1092	.0568	.0811	.0795
W	.0987	.0404	.1317	.0660	.0530	.0923

REYNOLDS-STRESS BUDGET
IJ	RIJ/RII	RATE	PROD	P2S	P1S	DISS
11	0.368	-0.051	0.000	0.360	-0.035	-0.356
12	-0.000	-0.004	-0.000	-0.008	0.002	0.001
13	0.000	-0.004	-0.001	-0.004	0.001	-0.000
22	0.413	0.275	1.384	-0.932	0.040	-0.382
23	-0.001	-0.004	0.000	-0.006	0.003	0.000
33	0.239	-0.576	-0.914	0.572	0.030	-0.267

"FAST" PRESSURE-STRAIN TENSOR
IJ/RI	11	12	13	22	23	33
11	0.1454	-.0015	0.0000	0.3441	-.0008	0.1571
12	-.0007	-.1186	0.0007	0.0021	0.0006	-.0001
13	-.0007	-.0002	-.0250	-.0017	-.0004	-.0000
22	0.3914	0.0012	0.0000	0.1809	0.0002	0.2332
23	0.0006	0.0007	-.0005	0.0012	-.0621	-.0009
33	0.1813	-.0000	-.0001	0.2673	-.0011	0.0871

B203B

T	5.065E-02
VISC	7.071E-03
RII	7.210E 00
PII	8.043E 01
OII	7.412E 01
II	4.996E-02
III	-1.020E-03

MEAN DEFORMATION RATE
	X	Y	Z
U	0.00	0.00	0.00
V	0.00	18.00	0.00
W	0.00	0.00	18.00

INTEGRAL SCALES / MICROSCALES
	X	Y	Z	X	Y	Z
U	.1168	.0315	.1854	.0751	.0417	.1373
V	.0439	.1926	.1501	.0574	.0821	.1039
W	.1501	.0320	.1100	.0627	.0463	.0980

REYNOLDS-STRESS BUDGET
IJ	RIJ/RII	RATE	PROD	P2S	P1S	DISS
11	0.358	0.071	0.000	0.586	-0.040	-0.474
12	0.001	-0.009	-0.003	-0.009	0.001	0.002
13	-0.000	0.001	0.000	-0.002	0.001	-0.000
22	0.477	0.171	1.739	-0.481	-0.007	-0.370
23	-0.002	0.003	0.000	-0.006	0.002	0.000
33	0.165	-0.112	-0.452	0.341	0.151	-0.138

"FAST" PRESSURE-STRAIN TENSOR
IJ/RI	11	12	13	22	23	33
11	0.1600	-.0017	-.0004	0.6201	-.0016	0.0625
12	0.0005	-.1639	0.0006	0.0036	0.0001	-.0002
13	-.0005	-.0000	-.0027	-.0011	-.0001	0.0002
22	0.4377	-.0000	0.0000	0.2117	-.0009	0.1791
23	0.0012	0.0007	-.0003	0.0210	-.0008	-.0004
33	0.0897	-.0009	-.0002	0.2135	-.0011	0.0594

B203C

T	7.726E-02
VISC	7.071E-03
RII	1.145E 02
PII	1.145E 02
OII	2.777E 01
II	8.026E-02
III	-3.135E-03

MEAN DEFORMATION RATE
	X	Y	Z
U	0.00	0.00	0.00
V	0.00	-18.00	0.00
W	0.00	0.00	18.00

INTEGRAL SCALES / MICROSCALES
	X	Y	Z	X	Y	Z
U	.0914	.0042	.2465	.1158	.0392	.1366
V	.0334	.2467	.2317	.0595	.0856	.1429
W	.1843	.0241	.0832	.0652	.0414	.1042

REYNOLDS-STRESS BUDGET
IJ	RIJ/RII	RATE	PROD	P2S	P1S	DISS
11	0.358	0.192	0.000	0.766	0.000	-0.472
12	-0.004	-0.017	-0.018	-0.013	0.032	0.002
13	-0.000	-0.000	0.000	-0.002	0.001	0.000
22	0.561	0.708	2.636	-1.280	-0.061	-0.388
23	-0.002	-0.000	0.000	-0.005	0.001	0.000
33	0.113	-0.152	-0.452	0.341	0.151	-0.138

"FAST" PRESSURE-STRAIN TENSOR
IJ/RI	11	12	13	22	23	33
11	0.1747	-.0003	-.0004	0.6388	-.2073	0.2384
12	0.0005	-.1814	0.0016	-.0046	0.0003	-.0010
13	-.0006	-.0018	0.0077	-.0011	-.0003	0.0002
22	0.4719	-.0002	-.0002	0.2360	-.0004	0.1294
23	0.0017	0.0000	-.0005	0.0010	-.0446	-.0000
33	0.0691	-.0010	-.0002	0.1740	-.0011	0.0408

B203D

T	9.759E-02
VISC	7.071E-03
RII	8.081E 00
PII	1.527E 02
OII	7.341E 01
II	1.159E-01
III	-4.054E-03

MEAN DEFORMATION RATE
	X	Y	Z
U	0.00	0.00	0.00
V	0.00	-18.00	0.00
W	0.00	0.00	18.00

INTEGRAL SCALES / MICROSCALES
	X	Y	Z	X	Y	Z
U	.0784	.0042	.3102	.0773	.0406	.1931
V	.0245	.2300	.3377	.0626	.0920	.1942
W	.2005	.0190	.0653	.0660	.0422	.1237

REYNOLDS-STRESS BUDGET
IJ	RIJ/RII	RATE	PROD	P2S	P1S	DISS
11	0.357	0.393	0.000	0.990	-0.074	-0.492
12	-0.007	-0.025	-0.015	-0.015	0.000	0.001
13	-0.001	-0.004	0.001	-0.006	0.000	-0.000
22	0.561	0.780	2.636	-1.280	-0.061	-0.388
23	-0.002	-0.003	0.000	-0.008	0.001	0.000
33	0.082	-0.177	-0.357	0.282	0.118	-0.120

"FAST" PRESSURE-STRAIN TENSOR
IJ/RI	11	12	13	22	23	33
11	0.1888	-.0051	-.0007	0.7386	-.0022	0.0403
12	0.0012	-.2016	0.0018	0.0098	0.0008	0.0002
13	-.0012	-.0023	0.0108	0.0001	-.0303	-.0001
22	0.4541	-.0024	-.0001	0.2474	-.0016	0.0846
23	0.0021	0.0015	0.0002	0.0053	-.0378	0.0003
33	0.0616	-.0010	-.0001	0.1394	-.0010	0.0270

82C4A

T	1.071E-02	MEAN DEFORMATION RATE			
VISC	7.071E-03		X	Y	Z
RII	8.002E 00	U	0.00	0.00	0.00
PII	1.014E 02	V	0.00	-36.00	0.00
DII	7.619E 01	W	0.00	0.00	36.00
II	1.594E-02				
III	-3.082E-04				

	INTEGRAL SCALES			MICROSCALES		
	X	Y	Z	X	Y	Z
U	.1571	.0306	.1291	.0027	.0402	.0873
V	.0548	.1985	.1100	.0555	.0814	.0603
W	.0976	.0426	.1350	.0838	.0923	.0944

REYNOLDS-STRESS BUDGET

IJ	RIJ/RII	RATE =	PROD +	P2S +	P1S +	DISS
11	0.350	0.347	0.000	0.741	-0.035	-0.359
12	-0.000	-0.017	-0.000	-0.015	-0.003	0.001
13	0.000	-0.007	-0.000	-0.008	0.002	-0.000
22	0.413	0.505	3.120	-1.445	0.016	-0.384
23	-0.001	-0.011	0.000	-0.012	0.001	0.000
33	0.237	-0.425	-1.792	1.104	0.019	-0.255

"FAST" PRESSURE-STRAIN TENSOR

IJ/RI	11	12	13	22	23	33
11	0.1445	-.0014	0.0001	0.4014	-.0007	0.1537
12	-.0004	-.1213	0.0001	0.0018	0.0004	-.0001
13	-.0007	.0000	-.0232	-.0010	-.0004	-.0007
22	0.4008	0.0011	0.0002	0.1827	0.0001	0.2358
23	0.0004	0.0007	-.0005	0.0012	-.0014	-.0007
33	0.1952	0.0080	-.0000	0.2408	-.0012	0.0844

82C4B

T	1.482E-02	MEAN DEFORMATION RATE			
VISC	7.071E-03		X	Y	Z
RII	8.426E 00	U	0.00	0.00	0.00
PII	1.938E 02	V	0.00	-36.00	0.00
DII	9.348E 01	W	0.00	0.00	36.00
II	9.089E-02				
III	-2.717E-03				

	INTEGRAL SCALES			MICROSCALES		
	X	Y	Z	X	Y	Z
U	.1049	.0137	.1091	.0148	.0384	.1107
V	.0916	.1734	.1422	.0541	.0785	.1098
W	.1283	.0291	.1193	.0657	.0420	.1028

REYNOLDS-STRESS BUDGET

IJ	RIJ/RII	RATE =	PROD +	P2S +	P1S +	DISS
11	0.371	8.315	0.000	1.092	-0.068	-0.450
12	-0.002	-0.015	-0.006	-0.014	-0.001	0.002
13	-0.000	-0.002	0.001	-0.005	0.002	0.000
22	0.476	0.477	3.126	-1.797	0.014	-0.366
23	-0.001	-0.008	0.000	-0.010	0.001	0.000
33	0.156	-0.477	-1.092	0.705	0.034	-0.164

"FAST" PRESSURE-STRAIN TENSOR

IJ/RI	11	12	13	22	23	33
11	0.1653	-.0034	.0004	0.5236	-.0017	0.0837
12	-.0001	-.1138	0.0008	0.0034	0.0005	-.0001
13	-.0005	-.0005	0.0005	-.0011	-.0000	-.0001
22	0.4916	0.0006	0.0001	0.2112	-.0005	0.1802
23	0.0006	0.0007	-.0003	0.0010	-.0033	-.0003
33	7.0870	-.0004	-.0001	0.3002	-.0013	0.0528

82C4C

T	2.089E-02	MEAN DEFORMATION RATE			
VISC	7.071E-03		X	Y	Z
RII	8.881E 00	U	0.00	0.00	0.00
PII	2.009E 02	V	0.00	-36.00	0.00
DII	1.181E 02	W	0.00	0.00	36.00
II	8.619E-02				
III	-6.085E-03				

	INTEGRAL SCALES			MICROSCALES		
	X	Y	Z	X	Y	Z
U	.0036	.0062	.2595	.0491	.0331	.1518
V	.0506	.1816	.2381	.0938	.0747	.1905
W	.1018	.0204	.0903	.0661	.0571	.1194

REYNOLDS-STRESS BUDGET

IJ	RIJ/RII	RATE =	PROD +	P2S +	P1S +	DISS
11	0.383	0.417	0.000	1.235	-0.091	-0.528
12	-0.004	-0.028	-0.011	-0.018	-0.000	0.002
13	-0.000	-0.001	0.001	-0.004	0.002	0.000
22	0.511	1.050	3.080	-1.699	0.021	-0.344
23	-0.002	-0.004	0.000	-0.008	0.000	0.000
33	0.105	-0.224	-0.634	0.464	0.070	-0.128

"FAST" PRESSURE-STRAIN TENSOR

IJ/RI	11	12	13	22	23	33
11	0.1854	-.0031	-.0004	0.6303	-.0023	0.0490
12	0.0007	-.1422	0.0609	0.0061	0.0003	-.0001
13	-.0008	-.0014	0.0018	-.0009	0.0000	0.0001
22	0.5307	-.0004	0.0001	0.2387	-.0011	0.1281
23	0.0008	0.0010	-.0003	0.0023	-.0434	0.0001
33	0.0507	-.0010	-.0002	0.1534	-.0011	0.0336

82C4D

T	9.843E-02	MEAN DEFORMATION RATE			
VISC	7.071E-03		X	Y	Z
RII	1.198E 01	U	0.00	0.00	0.00
PII	4.080E 02	V	0.00	-36.00	0.00
DII	1.450E 02	W	0.00	0.00	36.00
II	1.148E-01				
III	-8.892E-03				

	INTEGRAL SCALES			MICROSCALES		
	X	Y	Z	X	Y	Z
U	.0621	.0027	.3334	.0660	.0315	.1936
V	.0202	.2046	.3527	.0541	.0752	.2091
W	.1972	.0143	.0867	.0670	.0357	.1346

REYNOLDS-STRESS BUDGET

IJ	RIJ/RII	RATE =	PROD +	P2S +	P1S +	DISS
11	0.387	0.715	0.000	1.378	-0.045	-0.570
12	-0.006	0.034	-0.019	-0.019	0.002	0.002
13	-0.001	0.004	0.002	-0.007	0.001	0.000
22	0.544	1.228	3.233	-1.486	0.022	-0.344
23	-0.002	0.004	0.000	-0.005	0.001	0.000
33	0.069	-0.119	-0.413	0.308	0.073	-0.086

"FAST" PRESSURE-STRAIN TENSOR

IJ/RI	11	12	13	22	23	33
11	0.2085	-.0091	-.0005	0.7248	-.0024	0.0307
12	0.0027	-.2201	0.0013	0.0090	0.0305	-.0030
13	-.0011	-.0020	0.0116	0.0004	0.0000	-.0001
22	0.5949	-.0027	-.0002	0.2518	-.0016	0.0882
23	0.0012	0.0014	-.0001	0.0028	-.0317	0.0003
33	0.0305	-.0012	-.0003	0.1045	-.0008	0.0201

CO13A   CO13B   CO13C
CO13D   CO13E   CO13F
CO14A   CO14B   CO14C
CO14D   CO14E   CO14F

MEAN DEFORMATION RATE
INTEGRAL SCALES   MICROSCALES
REYNOLDS-STRESS BUDGET
"FAST" PRESSURE-STRAIN TENSOR

Page content consists of twelve dense numerical data blocks (turbulence statistics). Due to the very low image quality, only the block structure is reliably legible.

Each block is headed by a label (CO21A, CO21B, CO21C, CO21D, CO21E, CO21F, CO22A, CO22B, CO22C, CO22D, CO22E, CO22F) and contains the following sections:

- **MEAN DEFORMATION RATE** (with parameters T, VISC, RII, PII, DII, II, III and X, Y, Z components for U, V, W)
- **INTEGRAL SCALES** and **MICROSCALES** (X, Y, Z for U, V, W)
- **REYNOLDS-STRESS BUDGET** (IJ, RIJ/RII, RATE = PROD + P2S + P1S + DISS for rows 11, 12, 13, 22, 23, 33)
- **"FAST" PRESSURE-STRAIN TENSOR** (LJ/MI, columns 11, 12, 13, 22, 23, 33)

********************** BSH12F **********************

T	2.000E-01		MEAN DEFORMATION RATE		
			X	Y	Z
VISC	5.000E-03				
RII	1.701E 01	U	0.00	20.00	0.00
PII	1.079E 02	V	0.00	0.00	0.00
DII	1.113E 02	W	0.00	0.00	0.00
II	4.501E-02				
III	-9.862E-03				

INTEGRAL SCALES   MICROSCALES

	X	Y	Z	X	Y	Z
U	.2289	.1405	.0560	.1126	.0625	.0614
V	.0947	.2192	.1045	.0146	.0742	.0522
W	.0599	.0690	.1047	.0144	.0535	.0812

REYNOLDS-STRESS BUDGET

IJ	RIJ/RII	RATE =	PROD	+ P2S	+ P1S	+ DISS
11	0.419	0.014	0.499	-0.142	-0.210	-0.384
12	-0.159	0.030	-0.755	0.424	0.255	0.076
13	0.001	0.001	0.001	0.001	-0.002	0.001
22	0.247	0.044	0.000	-0.072	0.296	-0.271
23	-0.000	0.004	0.000	0.004	-0.000	0.000
33	0.334	0.021	0.000	0.344	-0.040	-0.347

"FAST" PRESSURE-STRAIN TENSOR

IJ/MI	11	12	13	22	23	33
11	0.1171	-.0560	0.0003	0.1681	0.0005	0.2017
12	-.0144	-.6293	-.0014	-.0036	0.0008	-.1221
13	0.0004	-.0001	-.0878	0.0004	0.0998	-.0011
22	0.2910	-.0634	0.0021	0.1073	-.0010	0.3063
23	0.0000	-.0002	0.0783	0.0004	-.0730	0.0021
33	0.4291	-.1678	-.0002	0.2257	-.0004	0.1608

********************** BSH12E **********************

T	3.000E-01		MEAN DEFORMATION RATE		
			X	Y	Z
VISC	5.000E-03				
RII	1.759E 01	U	0.00	20.00	0.00
PII	1.128E 02	V	0.00	0.00	0.00
DII	9.314E 01	W	0.00	0.00	0.00
II	7.739E-02				
III	1.030E-03				

INTEGRAL SCALES   MICROSCALES

	X	Y	Z	X	Y	Z
U	.3119	.1443	.0570	.1246	.0702	.0699
V	.1149	.2142	.1067	.0187	.0800	.0555
W	.0647	.0640	.1059	.0031	.0577	.0886

REYNOLDS-STRESS BUDGET

IJ	RIJ/RII	RATE =	PROD	+ P2S	+ P1S	+ DISS
11	0.483	0.127	1.174	-0.383	-0.275	-0.392
12	-0.194	-0.016	-0.823	0.452	0.280	0.076
13	-0.001	-0.001	-0.002	0.004	-0.003	0.000
22	0.223	0.003	0.000	-0.031	0.299	-0.266
23	0.001	0.007	0.000	0.004	0.001	0.000
33	0.324	0.007	0.030	0.414	-0.023	-0.344

"FAST" PRESSURE-STRAIN TENSOR

IJ/MI	11	12	13	22	23	33
11	0.1148	-.0518	0.0203	0.1450	0.0016	0.1816
12	-.0286	-.0248	0.0007	-.0042	-.0003	-.1206
13	0.0010	-.0002	-.0900	0.0013	0.0562	0.0006
22	0.3158	-.0838	-.0027	0.0947	-.0001	0.3075
23	0.0014	-.0012	0.0964	0.0004	-.0499	-.0006
33	0.4763	-.2029	0.3000	0.2034	-.0004	0.1630

********************** BSH12L **********************

T	4.000E-01		MEAN DEFORMATION RATE		
			X	Y	Z
VISC	5.000E-03				
RII	1.999E 01	U	0.00	20.00	0.00
PII	1.279E 02	V	0.00	0.00	0.00
DII	9.317E 01	W	0.00	0.00	0.00
II	8.551E-02				
III	2.435E-03				

INTEGRAL SCALES   MICROSCALES

	X	Y	Z	X	Y	Z
U	.3930	.2264	.0606	.1420	.0744	.0774
V	.1321	.2626	.1168	.0032	.0841	.0587
W	.0707	.0791	.1139	.0087	.0038	.0945

REYNOLDS-STRESS BUDGET

IJ	RIJ/RII	RATE =	PROD	+ P2S	+ P1S	+ DISS
11	0.473	0.201	1.369	-0.432	-0.341	-0.394
12	-0.154	-0.058	-0.911	0.435	0.308	0.072
13	-0.001	-0.003	0.003	-0.007	0.000	0.002
22	0.212	0.065	0.000	-0.020	0.351	-0.262
23	-0.001	-0.002	0.000	0.003	-0.006	0.000
33	0.314	0.088	0.000	0.451	-0.010	-0.344

"FAST" PRESSURE-STRAIN TENSOR

IJ/MI	11	12	13	22	23	33
11	0.1108	-.0503	0.0005	0.1358	-.0011	0.1692
12	-.0283	-.0251	-.0007	0.0023	0.0004	-.1177
13	0.0026	-.0007	-.0857	0.0004	0.0526	-.0010
22	0.3352	-.0645	-.0026	0.0914	0.0000	0.3031
23	0.0037	-.0025	0.0928	0.0010	-.0463	0.0007
33	0.5009	-.2042	-.0001	0.1976	-.0003	0.1521

********************** BSH12D **********************

T	5.000E-01		MEAN DEFORMATION RATE		
			X	Y	Z
VISC	5.000E-03				
RII	2.440E 01	U	0.00	20.00	0.00
PII	1.504E 02	V	0.00	0.00	0.00
DII	9.875E 01	W	0.00	0.00	0.00
II	8.792E-02				
III	3.591E-03				

INTEGRAL SCALES   MICROSCALES

	X	Y	Z	X	Y	Z
U	.4812	.2833	.0657	.1524	.0818	.0844
V	.1587	.3087	.1752	.0889	.2894	.0630
W	.0825	.0732	.1163	.0920	.0034	.1044

REYNOLDS-STRESS BUDGET

IJ	RIJ/RII	RATE =	PROD	+ P2S	+ P1S	+ DISS
11	0.485	0.202	1.523	-0.441	-0.383	-0.191
12	-0.156	-0.099	-1.018	0.466	0.311	0.087
13	-0.000	0.008	-0.000	-0.003	0.010	0.001
22	0.204	0.108	0.000	-0.018	0.387	0.261
23	0.000	0.001	0.000	0.001	0.002	-0.000
33	0.305	0.133	0.000	0.445	-0.004	-0.348

"FAST" PRESSURE-STRAIN TENSOR

IJ/MI	11	12	13	22	23	33
11	0.1102	-.0480	0.0002	0.1404	-.0010	0.1628
12	-.0325	-.0245	-.0020	-.0018	0.0016	-.1147
13	-.0004	0.0004	-.0851	-.0004	0.0498	-.0013
22	0.3422	-.0637	0.0000	0.0841	0.0004	0.2984
23	-.0037	0.0016	0.0959	-.0011	-.0448	0.0016
33	0.5107	-.2015	-.0010	0.1902	0.0007	0.1506

********************** BSH12R **********************

T	6.000E-01		MEAN DEFORMATION RATE		
			X	Y	Z
VISC	5.000E-03				
RII	2.493E 01	U	0.00	20.00	0.00
PII	1.781E 02	V	0.00	0.00	0.00
DII	1.201E 02	W	0.00	0.00	0.00
II	8.443E-02				
III	3.482E-03				

INTEGRAL SCALES   MICROSCALES

	X	Y	Z	X	Y	Z
U	.4959	.2803	.0700	.1524	.0824	.0844
V	.1641	.3342	.1796	.0863	.0885	.0618
W	.0848	.0764	.1376	.0954	.0647	.1001

REYNOLDS-STRESS BUDGET

IJ	RIJ/RII	RATE =	PROD	+ P2S	+ P1S	+ DISS
11	0.483	0.230	1.483	-0.463	-0.402	-0.389
12	-0.151	0.070	-1.036	0.487	0.355	0.064
13	0.000	0.033	0.001	0.010	0.023	-0.001
22	0.211	0.105	0.000	-0.028	0.435	-0.271
23	-0.000	-0.008	0.000	-0.009	0.004	-0.001
33	0.305	0.147	0.000	0.491	-0.005	-0.319

"FAST" PRESSURE-STRAIN TENSOR

IJ/MI	11	12	13	22	23	33
11	0.1079	-.0472	0.0010	0.1435	-.0011	0.1642
12	-.0375	-.0238	-.0033	-.0029	0.0001	-.1114
13	-.0083	0.0031	-.0631	-.0019	0.0501	-.0035
22	0.3464	-.0498	0.3090	0.0888	0.0020	0.2970
23	-.0377	0.0332	0.0961	-.0017	-.0650	0.0013
33	0.5122	-.1847	0.0029	0.1903	-.0014	0.1492

BR3A ··················

MEAN DEFORMATION RATE
INTEGRAL SCALES   MICROSCALES
REYNOLDS-STRESS BUDGET
RIJ/RII   RATE = PROD + P2S + P1S + DISS
"FAST" PRESSURE-STRAIN TENSOR

BR3B ··················

BR3C ··················

BR3D ··················

BR3E ··················

BR3F ··················

BR4A ··················

BR4B ··················

BR4C ··················

BR4D ··················

BR4E ··················

BR4F ··················

```
T    4.719E-02           MEAN DEFORMATION RATE
VISC 7.071E-03              X      Y      Z
RII  1.334E 00        U    0.00   0.00  40.00
PII    0.000         V    0.00   0.00   0.00
DII  8.880E 00        W  -40.00   0.00   0.00
II   1.293E-04
III  4.105E-07

        INTEGRAL SCALES          MICROSCALES
         X      Y      Z         X      Y      Z
U      .1601  .0792  .0879     .1016  .0765  .0709
V      .0841  .1490  .0847     .0713  .1076  .0710
W      .0749  .0853  .1613     .0712  .0766  .1019

        REYNOLDS-STRESS BUDGET
IJ  RIJ/RII  RATE =  PROD  +  P2S  +  P1S  +  DISS
11  0.327   -0.349  -0.015   0.005  -0.015  -0.324
12 -0.001   -0.007  -0.008   0.005   0.000  -0.001
13  0.001   -0.012  -0.021   0.010  -0.000  -0.000
22  0.342   -0.334   0.000  -0.013   0.034  -0.190
23  0.000   -0.001  -0.004   0.004  -0.000  -0.001
33  0.331   -0.318   0.015   0.012  -0.019  -0.326

         "FAST" PRESSURE-STRAIN TENSOR
IJ/KL  11      12      13      22      23      33
11  0.1351  1.0CC1  0.0002  0.2744  0.0003  0.2743
12 -.0001  -.0639  -.0897  -.0011  -.0016  -.0021
13 -.0003  -.0903  -.0698  0.0014  0.0011  0.0014
22  0.2479  0.00C6  0.0019  0.1300  0.0002  0.2511
23  0.0008  -.0002  0.0002  0.0002  -.0061  0.0005
33  0.2727  -.0019  0.0004  0.2801  0.0001  0.1359
```

```
T    1.011E-01           MEAN DEFORMATION RATE
VISC 7.071E-03              X      Y      Z
RII  9.876E-01        U    0.00   0.00  40.00
PII    0.000         V    0.00   0.00   0.00
DII  4.706E 00        W  -40.00   0.00   0.00
II   3.195E-04
III  2.234E-06

        INTEGRAL SCALES          MICROSCALES
         X      Y      Z         X      Y      Z
U      .1678  .0934  .0866     .1197  .0925  .0831
V      .0997  .1830  .0921     .0841  .1376  .0836
W      .0874  .1025  .1951     .0830  .0922  .1192

        REYNOLDS-STRESS BUDGET
IJ  RIJ/RII  RATE =  PROD  +  P2S  +  P1S  +  DISS
11  0.326   -0.312  -0.035   0.033  -0.011  -0.321
12  0.002   -0.025   0.007  -0.029  -0.003  -0.001
13  0.001   -0.009  -0.003  -0.003  -0.002  -0.000
22  0.348   -0.314   0.000  -0.044   0.027  -0.357
23 -0.001   0.010   0.017  -0.002   0.000   0.001
33  0.326   -0.313   0.013   0.012  -0.018  -0.323

         "FAST" PRESSURE-STRAIN TENSOR
IJ/KL  11      12      13      22      23      33
11  0.1346  0.0031  0.0005  0.2707  -0.0009  0.2738
12 -.0406  -.0648  -.0009  -.0036  -.0020  -.0001
13 -.0014  0.00C8  -.07C1  0.0033  0.0003  0.0014
22  0.2431  0.00C5  0.0001  0.1301  0.0004  0.2436
23  0.0009  0.00C7  C.00C3  0.0005  -.0653  0.0005
33  0.2741  0.00C4  C.0007  0.2764  -.0012  0.1354
```

```
T    1.693E-01           MEAN DEFORMATION RATE
VISC 7.071E-03              X      Y      Z
RII  7.591E-01        U    0.00   0.00  40.00
PII    0.000         V    0.00   0.00   0.00
DII  2.779E 00        W  -40.00   0.00   0.00
II   3.467E-04
III  2.756E-06

        INTEGRAL SCALES          MICROSCALES
         X      Y      Z         X      Y      Z
U      .1966  .1116  .1072     .1355  .1039  .0940
V      .1003  .1444  .0967     .0955  .1457  .0949
W      .0896  .1192  .2043     .0943  .1061  .1359

        REYNOLDS-STRESS BUDGET
IJ  RIJ/RII  RATE =  PROD  +  P2S  +  P1S  +  DISS
11  0.324   -0.302  -0.012  -0.003  -0.007  -0.320
12  0.000   -0.016   0.001  -0.018   0.003  -0.000
13  0.001   -0.053  -0.024  -0.026  -0.003   0.000
22  0.349   -0.364   0.000   0.001   0.014  -0.359
23 -0.000  -0.009   0.303  -0.014   0.001  -0.001
33  0.327   -0.274   0.012   0.012  -0.008  -0.321

         "FAST" PRESSURE-STRAIN TENSOR
IJ/KL  11      12      13      22      23      33
11  0.1347  0.0010  -.0018  0.2804  0.0002  0.2743
12 -.0007  -.0638  0.00C6  -.0025  -.0002  -.0009
13  0.0002  0.0001  -.0710  0.0034  0.0015  0.0020
22  0.2374  -.00C7  0.0028  0.1297  -.0010  0.2421
23  0.0022  -.00C3  0.0013  -.00C7  -.0654  0.0006
33  0.2747  0.00C6  0.0001  0.2877  0.0006  0.1364
```

```
T    2.411E-01           MEAN DEFORMATION RATE
VISC 7.071E-03              X      Y      Z
RII  5.852E-01        U    0.00   0.00  40.00
PII    0.000         V    0.00   0.00   0.00
DII  1.564E 00        W  -40.00   0.00   0.00
II   5.082E-04
III  1.720E-06

        INTEGRAL SCALES          MICROSCALES
         X      Y      Z         X      Y      Z
U      .2147  .1237  .1122     .1517  .1101  .1045
V      .1139  .2077  .1041     .1042  .1619  .1053
W      .0926  .1354  .2266     .1042  .1184  .1505

        REYNOLDS-STRESS BUDGET
IJ  RIJ/RII  RATE =  PROD  +  P2S  +  P1S  +  DISS
11  0.324   -0.316   0.090  -0.103  -0.013  -0.323
12 -0.003  -0.032  -0.012  -0.023   0.062   0.001
13 -0.002   0.008   0.065  -0.055  -0.002   0.001
22  0.347   -0.38C   0.000  -0.243   0.020  -0.358
23  0.001   0.012  -0.037   0.048   0.001  -0.000
33  0.324   -0.23C  -0.050   0.144  -0.007  -0.320

         "FAST" PRESSURE-STRAIN TENSOR
IJ/KL  11      12      13      22      23      33
11  0.1341  -.0004  -.0027  0.2171  0.0024  0.2779
12 -.0006  -.066C  -.0018  -.0013  -.0010  -.0024
13  0.0011  0.0010  -.0700  0.0018  0.0016  0.0037
22  0.2419  -.0001  0.0008  0.1290  0.0003  0.2365
23  0.0012  0.00C6  0.00L7  -.0002  -.0650  0.0015
33  0.2920  -.0051  -.0018  0.2815  -.0000  0.1350
```

```
T    3.244E-01           MEAN DEFORMATION RATE
VISC 7.071E-03              X      Y      Z
RII  4.7C4E-01        U    0.00   0.00  40.00
PII    0.000         V    0.00   0.00   0.00
DII  1.175E 0C        W  -40.00   0.00   0.00
II   3.081E-06
III  1.514E-06

        INTEGRAL SCALES          MICROSCALES
         X      Y      Z         X      Y      Z
U      .2234  .1357  .1230     .1602  .1299  .1137
V      .1219  .2195  .1179     .1134  .1774  .1154
W      .1055  .1504  .2337     .1142  .1280  .1639

        REYNOLDS-STRESS BUDGET
IJ  RIJ/RII  RATE =  PROD  +  P2S  +  P1S  +  DISS
11  0.330   -0.354  -0.024  -0.097  -0.010  -0.323
12 -0.003  -0.062  -0.001  -0.063   0.003   0.002
13  0.001  -0.C73   0.104  -0.178  -0.001   0.000
22  0.347   -0.354   0.00C  -0.010   0.013  -0.357
23  0.000  -0.067  -0.037  -0.023   0.002   0.001
33  0.323   -0.341  -0.024   0.1C8  -0.004  -0.314

         "FAST" PRESSURE-STRAIN TENSOR
IJ/KL  11      12      13      22      23      33
11  2.1343  -.0C21  -.0013  0.2812  0.3517  0.2738
12  0.0001  -.0633  -.00C8  0.0004  -.0016  -.0004
13  0.0017  0.0020  -.0710  0.0031  0.0021  0.0028
22  0.2405  -.00C0  0.0034  0.1275  -.0020  0.2376
23  0.0030  -.0011  0.00J4  -.0024  -.0642  0.0028
33  0.2848  -.0012  -.5006  0.2891  0.0004  0.1352
```

```
T    4.172E-01           MEAN DEFORMATION RATE
VISC 7.071E-03              X      Y      Z
RII  3.803E-01        U    0.00   0.00  40.00
PII    0.000         V    0.00   0.00   0.00
DII  9.762E-04        W  -40.00   0.00   0.00
II   8.762E-04
III  2.591E-06

        INTEGRAL SCALES          MICROSCALES
         X      Y      Z         X      Y      Z
U      .2273  .1513  .1157     .1766  .1384  .1231
V      .1312  .2252  .1291     .1206  .1915  .1240
W      .1190  .1647  .2591     .1237  .1385  .1777

        REYNOLDS-STRESS BUDGET
IJ  RIJ/RII  RATE =  PROD  +  P2S  +  P1S  +  DISS
11  0.323   -0.353   0.294  -0.291  -0.008  -0.320
12  0.002   -0.119  -0.012  -0.107   0.002  -0.002
13 -0.307  -0.C44  -0.012  -0.035  -0.001   0.004
22  0.353   -0.328   0.300   0.023   0.010  -0.361
23  0.001  -0.C24   0.031  -0.052  -0.005   0.000
33  0.324   -0.317  -0.264   0.267  -0.002  -0.319

         "FAST" PRESSURE-STRAIN TENSOR
IJ/KL  11      12      13      22      23      33
11  0.1370  0.0009  -.0056  0.2746  0.0009  0.2723
12 -.0020  -.0643  -.0C09  -.0008  0.0029  -.0007
13  0.0022  0.0008  -.0707  0.0039  -.0002  0.0031
22  0.2354  0.0C12  -.0045  0.1303  0.0016  0.2410
23  0.0045  0.0019  0.0C08  0.0000  -.0640  -.0007
33  0.2742  0.0C12  -.0041  0.2356  -.0009  0.1347
```

RX11/2   RX11A4   RX12A2

RX12A4   RX13A2   RX13A4

RX14A2   RX14A4   RX21A2

RX21A4   RX12A2   RX22A4

(Each panel contains the following labeled data blocks: T, VISC, RII, PII, DII, II, III; MEAN DEFORMATION RATE with X, Y, Z columns for U, V, W; INTEGRAL SCALES and MICROSCALES with X, Y, Z for U, V, W; REYNOLDS-STRESS BUDGET with columns IJ, RIJ/RII, RATE, PROD, P2S, P1S, DISS; and "FAST" PRESSURE-STRAIN TENSOR with columns IJ/MI, 11, 12, 13, 22, 23, 33.)

RX23A2

RX23A4

RX14A2

MEAN DEFORMATION RATE

INTEGRAL SCALES   MICROSCALES

REYNOLDS-STRESS BUDGET

"FAST" PRESSURE-STRAIN TENSOR

RX24A4

RX11C2

RX11C4

RX12C2

RX12C4

RX13C2

RX13C4

RX14C2

RX14C4

```
*****************     RX13F2     *****************

T      7.875E-02              MEAN DEFORMATION RATE
VISC   7.071E-03               X       Y       Z
RII    3.371E 00       U     0.00    0.00    0.00
PII        0.000       V     0.00    0.00    0.00
DII    3.624E 01       W     0.00    0.00    0.00
II     7.870E-02
III   -9.007E-03

          INTEGRAL SCALES             MICROSCALES
          X       Y       Z          X       Y       Z
U       .0516   .0666   .0631      .0818   .0430   .0429
V       .2163   .1308   .0173      .1222   .0766   .0441
W       .2038   .0168   .1274      .1227   .0462   .0770

                 REYNOLDS-STRESS BUDGET
IJ  RIJ/RII   RATE =   PROD  +  P2S  +   P1S  +  DISS
11   0.104   -0.023   0.000   0.000   0.146  -0.169
12  -0.001   -0.001   0.000   0.000  -0.001  -0.000
13   0.001   -0.001   0.000   0.000  -0.000  -0.001
22   0.446   -0.487   0.000   0.000  -0.073  -0.415
23  -0.001    0.004   0.000   0.000   0.004   0.000
33   0.450   -0.489   0.000   0.000  -0.071  -0.416

            "FAST" PRESSURE-STRAIN TENSOR
IJ/MI  11       12       13       22       23       33
11  0.0388  -.0002   0.0002   0.1082   0.0011   0.1089
12  -.0002  -.0196   -.0003   -.0002   0.0003   -.0016
13  0.0001  -.0004   -.0192   0.0009   0.0004   -.0004
22  0.3851  0.0001   0.0015   0.2066   -.0009   0.5854
23  -.0001  -.0004   0.0001   0.0019   -.1879   0.0017
33  0.0847  -.0015   0.0003   0.5162   -.0015   0.2062
```

```
*****************     RX13F4     *****************

T      1.398E-01              MEAN DEFORMATION RATE
VISC   7.071E-03               X       Y       Z
RII    2.016E 00       U     0.00    0.00    0.00
PII        0.000       V     0.00    0.00    0.00
DII    1.309E 01       W     0.00    0.00    0.00
II     9.950E-02
III   -9.328E-03

          INTEGRAL SCALES             MICROSCALES
          X       Y       Z          X       Y       Z
U       .0634   .0801   .0750      .0865   .0592   .0551
V       .1909   .1633   .0319      .1118   .0994   .0622
W       .1765   .0314   .1656      .1123   .0625   .1002

                 REYNOLDS-STRESS BUDGET
IJ  RIJ/RII   RATE =   PROD  +  P2S  +   P1S  +  DISS
11   0.141   -0.092   0.000   0.000   0.147  -0.229
12  -0.002    0.000   0.000   0.000  -0.000   0.001
13   0.001   -0.000   0.000   0.000   0.000  -0.000
22   0.426   -0.451   0.000   0.000  -0.073  -0.384
23   0.001    0.000   0.000   0.000   0.001  -0.001
33   0.433   -0.461   0.000   0.000  -0.074  -0.387

            "FAST" PRESSURE-STRAIN TENSOR
IJ/MI  11       12       13       22       23       33
11  0.0651  -.0004   0.0002   0.1637   0.0018   0.1652
12  -.0004  -.0318   -.0005   -.0000   0.0008   -.0017
13  0.0001  -.0006   -.0313   -.0002   0.0005   -.0011
22  0.1059  0.0001   0.0012   0.1886   -.0005   0.5123
23  -.0006  -.0004   0.0003   0.0003   -.1568   0.0010
33  0.1090  -.0015   0.0002   0.5001   0.0003   0.1881
```

```
*****************     RX14F2     *****************

T      3.889E-01              MEAN DEFORMATION RATE
VISC   7.071E-03               X       Y       Z
RII    6.593E-01       U     0.00    0.00    0.00
PII        0.000       V     0.00    0.00    0.00
DII    2.099E 00       W     0.00    0.00    0.00
II     7.109E-02
III   -7.728E-03

          INTEGRAL SCALES             MICROSCALES
          X       Y       Z          X       Y       Z
U       .0809   .1181   .1086      .1302   .0849   .0847
V       .2645   .2127   .0414      .1733   .1439   .0871
W       .2532   .0453   .2275      .1746   .0878   .1442

                 REYNOLDS-STRESS BUDGET
IJ  RIJ/RII   RATE =   PROD  +  P2S  +   P1S  +  DISS
11   0.116   -0.047   0.000   0.000   0.125  -0.172
12   0.000   -0.001   0.000   0.000   0.001  -0.002
13   0.001   -0.002   0.000   0.000  -0.002  -0.000
22   0.440   -0.474   0.000   0.000  -0.059  -0.445
23  -0.000    0.004   0.000   0.000   0.005  -0.001
33   0.444   -0.479   0.000   0.000  -0.065  -0.413

            "FAST" PRESSURE-STRAIN TENSOR
IJ/MI  11       12       13       22       23       33
11  0.0529  -.0001   0.0003   0.1975   0.0023   0.1981
12  -.0009  -.0257   -.0014   0.0002   0.0023   0.0018
13  0.0005  -.0010   -.0272   0.0004   -.0001   -.0026
22  0.0892  0.0011   0.0006   0.1918   -.0003   0.5363
23  0.0004  -.0005   -.0002   0.0032   -.1662   0.0017
33  0.0896  -.0001   0.0001   0.5309   -.0022   0.1935
```

```
*****************     RX14F4     *****************

T      5.246E-01              MEAN DEFORMATION RATE
VISC   7.071E-03               X       Y       Z
RII    4.507E-01       U     0.00    0.00    0.00
PII        0.000       V     0.00    0.00    0.00
DII    1.085E 00       W     0.00    0.00    0.00
II     5.651E-02
III   -5.476E-03

          INTEGRAL SCALES             MICROSCALES
          X       Y       Z          X       Y       Z
U       .0996   .1366   .1200      .1390   .1006   .1003
V       .2331   .2478   .0607      .1668   .1706   .1065
W       .2434   .0678   .2433      .1686   .1015   .1769

                 REYNOLDS-STRESS BUDGET
IJ  RIJ/RII   RATE =   PROD  +  P2S  +   P1S  +  DISS
11   0.139   -0.082   0.000   0.000   0.122  -0.209
12  -0.000   -0.002   0.000   0.000   0.000  -0.002
13  -0.000   -0.002   0.003   0.000  -0.001  -0.000
22   0.428   -0.457   0.000   0.000  -0.058  -0.349
23   0.002    0.005   0.000   0.000   0.006  -0.001
33   0.432   -0.461   0.000   0.000  -0.064  -0.396

            "FAST" PRESSURE-STRAIN TENSOR
IJ/MI  11       12       13       22       23       33
11  0.0695   .0004   0.0001   0.1567   0.0044   0.1990
12  -.0011  -.0335   -.0018   0.0004   0.0026   0.0029
13  0.0011  -.0017   -.0360   0.0006   -.0000   -.0027
22  0.1042  0.0011   -.0007   0.1865   -.0002   0.4826
23  0.0011  -.0012   -.0000   0.0019   -.1470   0.0020
33  0.1049  -.0012   0.0001   0.4756   0.0003   0.1830
```

```
*****************     RX21F2     *****************

T      2.423E-01              MEAN DEFORMATION RATE
VISC   1.414E-02               X       Y       Z
RII    6.566E-01       U     0.00    0.00    0.00
PII        0.000       V     0.00    0.00    0.00
DII    3.370E 00       W     0.00    0.00    0.00
II     8.100E-02
III   -9.390E-03

          INTEGRAL SCALES             MICROSCALES
          X       Y       Z          X       Y       Z
U       .0840   .1380   .1210      .1700   .1035   .1037
V       .2720   .2446   .0391      .2321   .1562   .0919
W       .2380   .0445   .2339      .2308   .0925   .1510

                 REYNOLDS-STRESS BUDGET
IJ  RIJ/RII   RATE =   PROD  +  P2S  +   P1S  +  DISS
11   0.101   -0.052   0.000   0.000   0.071  -0.123
12  -0.002   -0.002   0.000   0.000  -0.001  -0.001
13  -0.003   -0.000   0.000   0.000  -0.000   0.000
22   0.445   -0.470   0.000   0.000  -0.03[illegible]  -0.431
23  -0.001    0.004   0.000   0.000   0.004  -0.000
33   0.454   -0.478   0.006   0.000  -0.038  -0.440

            "FAST" PRESSURE-STRAIN TENSOR
IJ/MI  11       12       13       22       23       33
11  0.0445  -.0022   -.0001   0.1384   0.0022   0.1440
12  -.0002  -.0217   -.0006   0.0011   0.0000   -.0028
13  0.0018  -.0006   -.0229   0.0009   0.0010   0.0001
22  0.0795  -.0000   0.0006   0.1955   -.0030   0.5670
23  -.0009  -.0011   0.0002   0.0020   -.1738   0.0037
33  0.0781  -.0027   -.0005   0.5564   -.0015   0.1967
```

```
*****************     RX21F4     *****************

T      3.884E-01              MEAN DEFORMATION RATE
VISC   1.414E-02               X       Y       Z
RII    3.648E-01       U     0.00    0.00    0.00
PII        0.000       V     0.00    0.00    0.00
DII    1.181E 00       W     0.00    0.00    0.00
II     4.357E-02
III   -6.525E-03

          INTEGRAL SCALES             MICROSCALES
          X       Y       Z          X       Y       Z
U       .1016   .1623   .1430      .1833   .1320   .1319
V       .2256   .3054   .0606      .2251   .2025   .1228
W       .2259   .0793   .2992      .2234   .1235   .2032

                 REYNOLDS-STRESS BUDGET
IJ  RIJ/RII   RATE =   PROD  +  P2S  +   P1S  +  DISS
11   0.128   -0.087   0.000   0.000   0.074  -0.161
12  -0.005    0.001   0.000   0.000   0.001   0.001
13   0.000    0.001   0.000   0.000   0.000   0.001
22   0.432   -0.451   0.000   0.000  -0.035  -0.416
23   0.000    0.001   0.000   0.000   0.003  -0.002
33   0.441   -0.461   0.000   0.000  -0.038  -0.423

            "FAST" PRESSURE-STRAIN TENSOR
IJ/MI  11       12       13       22       23       33
11  0.0651  -.0036   0.0003   0.1913   0.0029   0.2003
12  0.0001  -.0314   -.0007   0.0031   0.0008   -.0024
13  0.0027  -.0007   -.0337   -.0004   0.0005   -.0011
22  0.0954  -.0014   0.0007   0.1807   -.0021   0.4961
23  -.0018  -.0017   0.0013   0.0314   -.1493   0.0028
33  0.0945  -.0050   -.0010   0.4913   -.0007   0.1830
```

```
*****************     RX22F2     *****************

T      1.400E-01              MEAN DEFORMATION RATE
VISC   1.414E-02               X       Y       Z
RII    1.108E 00       U     0.00    0.00    0.00
PII        0.000       V     0.00    0.00    0.00
DII    9.193E 00       W     0.00    0.00    0.00
II     8.259E-02
III   -1.054E-02

          INTEGRAL SCALES             MICROSCALES
          X       Y       Z          X       Y       Z
U       .0717   .1155   .1046      .1510   .0851   .0833
V       .2786   .2068   .0279      .2166   .1256   .0736
W       .2432   .0299   .1935      .2163   .0163   .1266

                 REYNOLDS-STRESS BUDGET
IJ  RIJ/RII   RATE =   PROD  +  P2S  +   P1S  +  DISS
11   0.092   -0.038   0.000   0.000   0.074  -0.111
12  -0.001   -0.002   0.000   0.000  -0.001  -0.001
13  -0.000   -0.001   0.000   0.000  -0.006  -0.000
22   0.450   -0.478   0.000   0.000  -0.036  -0.442
23  -0.001    0.004   0.000   0.000   0.003   0.000
33   0.459   -0.484   0.000   0.000  -0.038  -0.446

            "FAST" PRESSURE-STRAIN TENSOR
IJ/MI  11       12       13       22       23       33
11  0.0366  -.0013   -.0001   0.1149   0.0017   0.1107
12  0.0001  -.0180   -.0001   0.0007   0.0000   -.0029
13  0.0010  -.0009   -.0186   0.0011   0.0006   0.0003
22  0.0760  0.0004   0.0003   0.2029   -.0030   0.5950
23  -.0007  -.0009   -.0005   0.0019   -.1849   0.0037
33  0.0729  -.0012   -.0001   0.5819   -.0013   0.2019
```

```
*****************     RX22F4     *****************

T      2.465E-01              MEAN DEFORMATION RATE
VISC   1.414E-02               X       Y       Z
RII    6.344E-01       U     0.00    0.00    0.00
PII        0.000       V     0.00    0.00    0.00
DII    2.938E 00       W     0.00    0.00    0.00
II     6.618E-02
III   -6.921E-03

          INTEGRAL SCALES             MICROSCALES
          X       Y       Z          X       Y       Z
U       .0883   .1362   .1235      .1503   .1078   .1080
V       .2239   .2616   .0522      .2035   .1674   .1011
W       .2010   .0576   .2508      .2024   .1017   .1606

                 REYNOLDS-STRESS BUDGET
IJ  RIJ/RII   RATE =   PROD  +  P2S  +   P1S  +  DISS
11   0.123   -0.078   0.000   0.000   0.081  -0.160
12  -0.003   -0.001   0.000   0.000  -0.000  -0.000
13  -0.000    0.001   0.000   0.000   0.000   0.000
22   0.433   -0.451   0.000   0.000  -0.040  -0.417
23   0.001    0.003   0.000   0.000   0.004  -0.002
33   0.444   -0.465   0.000   0.000  -0.041  -0.424

            "FAST" PRESSURE-STRAIN TENSOR
IJ/MI  11       12       13       22       23       33
11  0.0595  -.0023   -.0000   0.1315   0.0031   0.1782
12  0.0002  -.0289   -.0006   0.0018   0.0038   -.0030
13  0.0017  -.0006   -.0306   -.0000   0.0005   -.0005
22  0.0944  -.0007   0.0002   0.1861   -.0014   0.5216
23  -.0019   .0011   0.0005   0.0006   -.1572   0.0020
33  0.0929  -.0040   -.0006   0.5665   -.0001   0.1878
```

```
*****************     RX23F2     *****************

T      9.226E-02              MEAN DEFORMATION RATE
VISC   1.414E-02               X       Y       Z
RII    1.724E 00       U     0.00    0.00    0.00
PII        0.000       V     0.00    0.00    0.00
DII    1.751E 01       W     0.00    0.00    0.00
II     9.308E-02
III   -1.157E-02

          INTEGRAL SCALES             MICROSCALES
          X       Y       Z          X       Y       Z
U       .0684   .1022   .0954      .1428   .0725   .0726
V       .2815   .1843   .0215      .2117   .1091   .0638
W       .2504   .0226   .1484      .2120   .0660   .1099

                 REYNOLDS-STRESS BUDGET
IJ  RIJ/RII   RATE =   PROD  +  P2S  +   P1S  +  DISS
11   0.084   -0.028   0.000   0.000   0.073  -0.101
12  -0.000   -0.002   0.000   0.000  -0.001  -0.001
13   0.000   -0.001   0.000   0.000  -0.000  -0.001
22   0.454   -0.482   0.000   0.000  -0.035  -0.447
23  -0.001    0.003   0.000   0.000   0.002   0.000
33   0.462   -0.490   0.000   0.000  -0.038  -0.451

            "FAST" PRESSURE-STRAIN TENSOR
IJ/MI  11       12       13       22       23       33
11  0.0311  -.0010   -.0003   0.0989   0.0013   0.1014
12  0.0002  -.0194   -.0001   0.0006   -.0000   -.0027
13  0.0007  -.0004   -.0197   0.0013   0.0004   0.0004
22  0.0692  0.0004   0.0005   0.2083   -.0029   0.6192
23  -.0005  -.0068   -.0007   0.0017   -.1928   0.0030
33  0.0683  -.0004   0.0001   0.6001   -.0013   0.2085
```

```
*****************     RX23F4     *****************

T      3.867E-01              MEAN DEFORMATION RATE
VISC   1.414E-02               X       Y       Z
RII    8.870E-01       U     0.00    0.00    0.00
PII        0.000       V     0.00    0.00    0.00
DII    4.139E 00       W     0.00    0.00    0.00
II     6.832E-02
III   -7.264E-03

          INTEGRAL SCALES             MICROSCALES
          X       Y       Z          X       Y       Z
U       .0809   .1717   .1136      .1662   .0992   .0934
V       .2286   .2188   .0436      .1937   .1688   .0894
W       .1995   .0462   .2245      .1932   .0899   .1500

                 REYNOLDS-STRESS BUDGET
IJ  RIJ/RII   RATE =   PROD  +  P2S  +   P1S  +  DISS
11   0.120   -0.032   0.000   0.000   0.085  -0.137
12  -0.002   -0.001   0.000   0.000  -0.001  -0.000
13  -0.000   -0.000   0.000   0.000   0.000  -0.000
22   0.435   -0.461   0.000   0.000  -0.042  -0.419
23   0.001    0.005   0.000   0.000   0.004  -0.001
33   0.445   -0.467   0.000   0.000  -0.043  -0.424

            "FAST" PRESSURE-STRAIN TENSOR
IJ/MI  11       12       13       22       23       33
11  0.0995  -.0036   -.0004   0.1565   0.0026   0.1621
12  0.0032  -.0271   -.0002   0.0012   0.0009   -.0029
13  0.0013  -.0068   -.0282   0.0018   0.0006   -.0006
22  0.0972  -.0076   0.0002   0.1901   -.0016   0.5172
23  -.0015  -.0062   0.0002   0.0007   -.1630   0.0018
33  0.0919  -.0029   -.0004   0.5227   -.0000   0.1913
```

```
*****************     RX24F2     *****************

T      4.355E-01              MEAN DEFORMATION RATE
VISC   1.414E-02               X       Y       Z
RII    5.125E-01       U     0.00    0.00    0.00
PII        0.000       V     0.00    0.00    0.00
DII    4.989E-01       W     0.00    0.00    0.00
II     7.812E-02
III   -8.900E-03

          INTEGRAL SCALES             MICROSCALES
          X       Y       Z          X       Y       Z
U       .1523   .1680   .1660      .2018   .1361   .1351
V       .2885   .2476   .0551      .2723   .2000   .1173
W       .2821   .0639   .2919      .2711   .1182   .2009

                 REYNOLDS-STRESS BUDGET
IJ  RIJ/RII   RATE =   PROD  +  P2S  +   P1S  +  DISS
11   0.105   -0.061   0.000   0.000   0.065  -0.124
12  -0.004   -0.005   0.000   0.000   0.000  -0.000
13   0.000   -0.001   0.000   0.000  -0.001  -0.000
22   0.465   -0.481   0.000   0.000  -0.030  -0.437
23  -0.002    0.002   0.000   0.000   0.003  -0.001
33   0.450   -0.471   0.000   0.003  -0.033  -0.438

            "FAST" PRESSURE-STRAIN TENSOR
IJ/MI  11       12       13       22       23       33
11  0.0496  -.0030   -.0006   0.1556   0.0017   0.1619
12  -.0308  -.0241   -.0032   0.0031   0.0002   -.0028
13  0.0027  -.0006   -.0295   0.0011   0.0009   0.0031
22  0.0812  -.0007   0.0015   0.1906   -.0043   0.5165
23  -.0006  -.0016   0.0016   0.0024   -.1800   0.0042
33  0.0796  -.0041    .0011   0.5429   -.0023   0.1921
```

```
*****************     RX24F4     *****************

T      6.451E-01              MEAN DEFORMATION RATE
VISC   1.414E-02               X       Y       Z
RII    1.818E-01       U     0.00    0.00    0.00
PII        0.000       V     0.00    0.00    0.00
DII    3.879E-01       W     0.00    0.00    0.00
II     6.415E-02
III   -6.615E-03

          INTEGRAL SCALES             MICROSCALES
          X       Y       Z          X       Y       Z
U       .1162   .1978   .1790      .2248   .1669   .1660
V       .2500   .3871   .0887      .2688   .2313   .1310
W       .2840   .1058   .3712      .2680   .1528   .2317

                 REYNOLDS-STRESS BUDGET
IJ  RIJ/RII   RATE =   PROD  +  P2S  +   P1S  +  DISS
11   0.127   -0.092   0.000   0.000   0.063  -0.155
12  -0.006    0.002   0.000   0.000   0.001   0.001
13  -0.000    0.000   0.000   0.000  -0.000   0.000
22   0.431   -0.453   0.000   0.000  -0.031  -0.422
23  -0.002    0.004   0.000   0.000   0.004  -0.000
33   0.441   -0.455   0.000   0.000  -0.032  -0.424

            "FAST" PRESSURE-STRAIN TENSOR
IJ/MI  11       12       13       22       23       33
11  0.0470  -.0044   -.0007   0.2029   0.0022   0.2132
12  -.0008  -.0322   0.0008   0.0040   0.0011   -.0007
13  0.0001  -.0017   -.0348   0.0010   0.0004   -.0044
22  0.0939  -.0018   0.0023   0.1706   -.0049   0.4867
23  -.0008  -.0028   0.0027   0.0017   -.1464   0.0041
33  0.0925  -.0057   -.0021   0.4139   -.0015   0.1813
```

DETAILS OF THE NUMERICAL ALGORITHM

THE EQUATIONS OF MOTION FOR HOMOGENEOUS TURBULENCE

We begin with the Navier-Stokes equations for a fluid of uniform density and viscosity:

$$\frac{\partial u_i}{\partial t} + u_j u_{i,j} + p_{,i} = \nu u_{i,jj} \tag{B1}$$

$$u_{i,i} = 0$$

The velocity field is decomposed into mean and turbulence components

$$u_i = U_i(\underline{x}) + u_i'(\underline{x}') , \qquad p = P(\underline{x}) + p'(\underline{x}')$$

where $\underline{x}'$ is related linearly to $\underline{x}$, and the mean is restricted to a spatially linear form

$$U_i = U_{i,j} x_j \tag{B2}$$

where $U_{i,j}$ depends only on time.

The explicit appearance of U_i (but not its gradient) in the equations of motion for the turbulence field is eliminated by the use of a spatial coordinate system that moves with the mean flow. This eliminates the terms, which contain $\underline{x}$ explicitly, that represent convection of the turbulence by the mean velocity.

This moving coordinate system is linearly related to an inertial laboratory frame by the relation

$$x_i' = B_{ij} x_j \tag{B3}$$

where $\underline{\underline{B}}$ is determined by the constraint that the new coordinates move with the mean flow or

$$\frac{\bar{D} x_i'}{\bar{D} t} = \frac{\partial x_i'}{\partial t} + U_k \frac{\partial x_i'}{\partial x_k} - (\dot{B}_{ij} + B_{ik} U_{k,j}) x_j = 0$$

so that

$$\dot{B}_{ij} + B_{ik} U_{k,j} = 0 \tag{B4}$$

The Navier-Stokes equations then become

$$(\dot{U}_{i,k} + U_{i,j}U_{j,k})x_k + P_{,i} + \frac{\partial u_i'}{\partial t} + u_j'U_{i,j} + B_{kj}(u_i'u_j')_{,k} + B_{ki}P_{,k}' - \nu B_{kj}B_{\ell j}u_{i,k\ell}' = 0$$

$$U_{i,i} + B_{ji}u_{i,j}' = 0$$

Note that differentiation of $\underline{U}$ is with respect to $\underline{x}$ while that of $\underline{u}'$ is with respect to $\underline{x}'$. The time variable for both is t.

To separate the mean from the fluctuation parts we take the ensemble average of the Navier-Stokes equations, using the ergodic hypothesis to replace ensemble averages of spatially homogeneous terms by their volume averages:

$$(\dot{U}_{i,k} + U_{i,j}U_{j,k})x_k + P_{,i} = 0$$

$$U_{i,i} = 0 \tag{B5}$$

This gives the equations for the turbulent component.

$$\frac{\partial u_i'}{\partial t} + U_{i,j}u_j' + B_{kj}(u_i'u_j')_{,k} + B_{ji}P_{,j}' = \nu B_{kj}B_{\ell j}u_{i,k\ell}' \tag{B6}$$

$$B_{ji}u_{i,j}' = 0$$

The mean-momentum equation implies that $-P$ must be quadratic in $\underline{x}$ (ignoring an arbitrary additive function of time), that is,

$$P = C_{jk}x_j x_k$$

so that

$$P_{,i} = (C_{ik} + C_{ki})x_k \equiv P_{ik}x_k$$

where $\underline{\underline{P}}$ is a symmetric tensor.

The mean-momentum equations then require

$$\dot{U}_{i,k} + U_{i,j}U_{j,k} + P_{ik} = 0$$

When the mean deformation is decomposed into strain and vorticity tensors

$$U_{i,j} = S_{ij} + \Omega_{ij}$$

we find upon separation into symmetric and antisymmetric parts that

$$\dot{S} + S^2 + \Omega^2 + P = 0$$

$$\dot{\Omega} + S\Omega + \Omega S = 0$$

This is simply a statement that the strain rate $\underline{\underline{S}}$ may be specified as an arbitrary

39

function of time subject only to the constraint $S_{11} = 0$. The second equation determines $\underset{\approx}{\Omega}$, and the first equation determines the mean pressure field. The initial value of $\underset{\approx}{\Omega}$ is arbitrary.

The basic equations for the turbulence field (B6) can be solved in a straightforward manner in principle, but in practice one is usually constrained by computer memory size, and it is advantageous, and in our case absolutely necessary, to reduce the number of words per node to the minimum. For this reason, the general case of (B6) with arbitrary mean-deformation tensor $U_{i,j}$ was not implemented. The current program allows a velocity deformation tensor of the form (rotation is handled as a special case)

$$U_{i,j} = \begin{pmatrix} a(t) & s(t) & 0 \\ 0 & b(t) & 0 \\ 0 & 0 & c(t) \end{pmatrix}, \qquad a + b + c = 0 \qquad\qquad (B7)$$

If the mesh is given at $t = 0$ by

$$B_{11}(0) = \beta_1 , \qquad B_{22}(0) = \beta_2 , \qquad B_{33}(0) = \beta_3 , \qquad \text{rest of } \underset{\approx}{B} \text{ zero}$$

the time variation of the metric tensor $\underset{\approx}{B}$ is determined by (B4) as

$$B_{11} = \beta_1 \, e^{-\int_0^t a\,dt} \qquad\qquad B_{22} = \beta_2 \, e^{-\int_0^t b\,dt}$$

$$\qquad\qquad\qquad\qquad\qquad\qquad\qquad\qquad\qquad\qquad\qquad (B8)$$

$$B_{33} = \beta_3 \, e^{-\int_0^t c\,dt} \qquad\qquad B_{12} = \frac{-s(0)}{\beta_1\beta_2} B_{22}(t) \int_0^t B_{11}^2(t)\,dt$$

$$\text{, rest of } \underset{\approx}{B} = \text{zero}$$

The use of β_i other than unity allows the mesh spacing to vary with direction. We have made use of (B7) to find that

$$s(t) = s(0)e^{\int_0^t c\,dt} = \frac{s(0)\beta_3}{B_{33}(t)}$$

RAPID-DISTORTION THEORY

Substitution of (B7) into (B6) gives (taking for the moment $s = 0$)

40

$$u_t + au + B_{11}P_x = \Big\}$$
$$v_t + bv + B_{22}P_y = \Big\} \quad \text{nonlinear + viscous terms}$$
$$w_t + cw + B_{33}P_z = \Big/$$
$$B_{11}u_x + B_{22}v_y + B_{33}w_z = 0$$

In the rapid-distortion limit the strain rates a, b, and c become infinite but integrable, so that the metric tensor $\underline{\underline{B}}$ has a finite discontinuity. During this straining period, $0 < t < T$, and (B9) degenerates to

$$u_t + au + B_{11}P_x = B_{11} \frac{\partial}{\partial t}(B_{11}^{-1}u + \phi_x) = 0 \tag{B10}$$

where
$$\phi = \int_0^t p\, dt$$

with similar equations for v and w.

This suggests the introduction of the scaled velocities

$$(u\,',v\,',w\,') = (B_{11}^{-1}u,\ B_{22}^{-1}v,\ B_{33}^{-1}w)$$

and new dependent variables $u\,' + \phi_x$, $v\,' + \phi_y$, $w\,' + \phi_z$

that remain continuous during a rapid distortion. In terms of these new variables, the rapid-distortion process is simply

$$u\,'(T) = u\,'(0) - \phi_x(T)$$
$$v\,'(T) = v\,'(0) - \phi_y(T) \tag{B11}$$
$$w\,'(T) = w\,'(0) - \phi_z(T)$$

where $\phi(T)$ is found by applying the continuity condition (B9) at $t = T$:

$$B_{11}^2\phi_{xx} + B_{22}^2\phi_{yy} + B_{33}^2\phi_{zz} = B_{11}^2 u_x'(0) + B_{22}^2 v_y'(0) + B_{33}^2 w_z'(0)$$

When the shear rate s is not zero, the metric $\underline{\underline{B}}$ varies with time and the pressure cannot be completely absorbed into a new dependent variable as it was above. The equations analogous to (B9) are

$$u_t + au + B_{11}P_x = \Big\}$$
$$v_t + bv + B_{22}P_y + B_{12}P_x = \Big\} \quad \text{nonlinear + viscous terms} \tag{B12}$$
$$w_t + cw + B_{33}P_z = \Big/$$
$$B_{11}u_x + B_{12}v_x + B_{22}v_y + B_{33}w_z = 0$$

and we take as new dependent variables

$$u' + \phi_x , \qquad v' + \phi_y + \frac{B_{12}}{B_{22}} \phi_x , \qquad w' + \phi_z$$

In these variables equation (B10) remains valid for the x and z directions, but in the y direction

$$v_t + bv + B_{22}p_y + B_{12}p_x = B_{22} \frac{\partial}{\partial t}\left(B_{22}^{-1}v + \phi_y + \frac{B_{12}}{B_{22}}\phi_x\right) - B_{22}\phi_x \frac{d}{dt}\left(\frac{B_{12}}{B_{22}}\right)$$

where, from (B8) ,

$$\frac{d}{dt}\left(\frac{B_{12}}{B_{22}}\right) = \frac{-s(0)}{\beta_1\beta_2} B_{11}^2$$

so that $B_{22}\phi_x \dfrac{d}{dt}\left(\dfrac{B_{12}}{B_{22}}\right)$ remains bounded during a rapid-distortion.

The new dependent variables above are therefore continuous through a rapid distortion, and, as before, the state of the velocity field following the distortion is found directly from the continuity condition (B12).

The numerical advantage of the new dependent variables is that the strain rate no longer imposes a stability limit on the time-advance step size, and that rapid-distortion theory is exactly captured by the simulation.

THE VISCOUS TERMS

In the moving coordinate system, the Laplacian becomes

$$\nabla^2 u_i = B_{mj}B_{\ell j}u_{i,m\ell}$$

and the diffusion operator in wave space becomes

$$\left(\frac{\partial}{\partial t} + \nu B_{mj}B_{\ell j}k_m k_\ell\right)\hat{u}_i = F^{-1}(\underline{k},t) \frac{\partial}{\partial t}[F(\underline{k},t)\hat{u}_i]$$

where F is the integrating factor

$$\log F = \nu k_i k_\ell \int B_{mj}B_{\ell j}\, dt$$

We again re-define the dependent variables to include the integrating factor and eliminate the diffusion term as a numerical stability constraint. The use of the integrating factor also permits us to carry fewer words per node for some time-advance algorithms (e.g., fourth-order Runge-Kutta) than the explicit treatment would allow.

In addition to the more or less "classical" transformations above, we have made a few simple modifications of the algorithm that pertain to data management. The primary consideration here is the reduction of the number of words per node required for the simulation. A secondary consideration is the cost reduction that results from lowered operation counts and lowered I/O operations between fast memory and backing store.

The necessity for these modifications and their actual form is largely dictated by the size and architecture of the Illiac computer, and the data-base structure chosen by the author. These modifications are presented for the basic Navier-Stokes operator in Cartesian coordinates; their application to the transformed system of equations is straightforward.

PSEUDODERIVATIVE

We use as dependent variables

$$\hat{u}(0,k_2,k_3) , \quad ik_1\hat{u}(\underline{k}) , \quad k_1 \neq 0$$
$$\hat{v}(k_1,0,k_3) , \quad ik_2\hat{v}(\underline{k}) , \quad k_2 \neq 0$$
$$\hat{w}(k_1,k_2,0) , \quad ik_3\hat{w}(\underline{k}) , \quad k_3 \neq 0$$

rather than the usual Fourier coefficients:

$$\hat{u}(\underline{k}) , \quad \hat{v}(\underline{k}) , \quad \hat{w}(\underline{k})$$

In physical space the equivalent information is

$$\hat{u}(0,k_2,k_3) \longleftrightarrow \frac{1}{2\pi} \int_0^{2\pi} u(x,y,z)dx \qquad \text{etc.}$$

$$ik_1\hat{u}(\underline{k}) \longleftrightarrow \frac{\partial}{\partial x} u(x,y,z) \qquad \text{etc.}$$

The basic variables are then u_x, v_y, and w_z. The integrals determine the constants of integration required to recover u, v, and w by integration. These variables are rather natural for the Navier-Stokes equations because their use leads to

$$u_{xt} + (uu)_{xx} + (uv)_{xy} + (uw)_{xz} + \ldots$$
$$v_{yt} + (uv)_{xy} + (vv)_{yy} + (vw)_{yz} + \ldots$$
$$w_{zt} + (uw)_{xz} + (vw)_{yz} + (ww)_{zz} + \ldots$$

in which the "matrix" of nonlinear terms is symmetric, even when the differentiation

43

operations are included. In the usual variables we would have nine different nonlinear terms rather than the six above.

An additional benefit of these variables is the ease of enforcing the continuity condition. Thus it is practical to discard w_z from the database on backing store altogether since it can be simply recovered from u_x and v_y. Of course we must save $\tilde{w}(k_1,k_2,0)$, but this is only a two-dimensional array.

MODIFIED PRESSURE

The nonlinear terms are formed (in physical space) when (x,z) planes are in fast memory. Thus we can form the nonlinear terms:

$$(uu)_{xx} + (uw)_{xz} , \qquad (uv)_x , \qquad (vv) , \qquad (vw)_z , \qquad (uw)_{xz} + (ww)_{zz}$$

The y differentiation must wait for a pass over the database bringing $(x-y)$ planes into fast memory, and this prevents further summing of terms. Thus we would have to carry five words per node to calculate the nonlinear terms. This can be reduced to four words per node by simply introducing the modified pressure $p + v^2$. The required nonlinear terms are then

$$(u^2 - v^2)_{xx} + (uw)_{xz} , \qquad (uv)_x , \qquad (vw)_z , \qquad (w^2 - v^2)_{zz} + (uw)_{xz}$$

Because of Illiac constraints, an implementation of five words per node for the calculation of the convective terms would have been difficult and considerably less efficient than that for four words per node.

The disadvantage of the modified pressure is that we have lost the ability to form output statistics containing pressure, because we only have the modified pressure and not the v^2 information necessary to recover physical pressure from it. When the pressure is required for output statistics a separate calculation must be made.

FINITE FOURIER TRANSFORMS

The use of fast-Fourier-transform techniques in the simulation of isotropic turbulence was pioneered by Orszag and Patterson (1972). Because we have departed a little from their treatment, it is worthwhile to cover some of the details of our implementation.

For purposes of analysis it is advantageous to work with general complex transforms, even though the physical data are real. In practice, of course, the complex transform is not used as such because it doubles the time and space requirements. (One can, however, use the complex algorithm on two real fields simultaneously, or use a half-length complex transform on full-length real data.)

The only subtle aspect of the use of discrete Fourier transforms is the aliasing problem. Although it has been discussed by many other authors, it seems appropriate to give a short exposition of it here.

The one-dimensional discrete Fourier transform of length M is defined as

$$M\tilde{a}_n = \sum_{j=0}^{M-1} a_j \, e^{-2\pi i (jn/M)}$$

with inverse

$$a_j = \sum_{n=0}^{M-1} \tilde{a}_n \, e^{2\pi i (jn/M)}$$

Suppose we have data a_j given by

$$a_j = \beta \, e^{2\pi i (j/M) k}$$

a wave having integer wave number k. The discrete transform of these data gives for M values of n :

$$M\tilde{a}_n = \beta \sum_{j=0}^{M-1} e^{2\pi i (j/M)(k-n)} = M\beta\delta[(k-n)\bmod M]$$

so that

$$\tilde{a}_n = \beta\delta[(k-n)\bmod M]$$

Thus a wave having wave number k in physical space is transformed into the Fourier coefficient at wave number $k \bmod M$ in wave space. This can also be seen by noting that the discrete data

$$a_j = \beta \, e^{2\pi i (j/M) k} = \beta \, e^{2\pi i (j/M)(k+NM)}$$

for any integer N.

Thus the data at M equidistant points of the period in physical space is the same for any value of N. Wave numbers $k+NM$ are said to be "aliased" to wave number k.

The aliasing problem occurs when operations on data (usually occurring in physical space) with a wave-number span of M produce a wave-number span greater than M.

In the Navier-Stokes equations, the nonlinear (bi-linear products) terms act to increase the span of wave-numbers. Consider a product in one dimension,

$$c_j = a_j b_j = \sum_{n=0}^{M-1} \tilde{a}_n\, e^{2\pi i (jn/M)} \sum_{m=0}^{M-1} \tilde{b}_m\, e^{2\pi i (jm/M)}$$

$$= \sum_{n=0}^{M-1} \sum_{m=0}^{M-1} \tilde{a}_n \tilde{b}_m\, e^{2\pi i (j/M)(n+m)}$$

which has the discrete Fourier transform

$$\tilde{c}_k = \sum_{n=0}^{M-1} \sum_{m=0}^{M-1} \tilde{a}_n \tilde{b}_m \delta[(n + m - k)\bmod M]$$

The most common transforms used (and those used in the current program) have M equal to a power of 2, and the wave-numbers spanned without alias are $1-M/2 \leq k \leq M/2$. Products of two such series result in the wave-number range $2-M \leq \overline{k} \leq \overline{M}$. This is illustrated by the following diagram which illustrates how the product of waves with positive wave-numbers n and m can produce the aliased wave at n+m-M rather than at the correct wave number n+m. In a similar way products of waves both having negative wave-numbers can be aliased to a positive wave-number in the result.
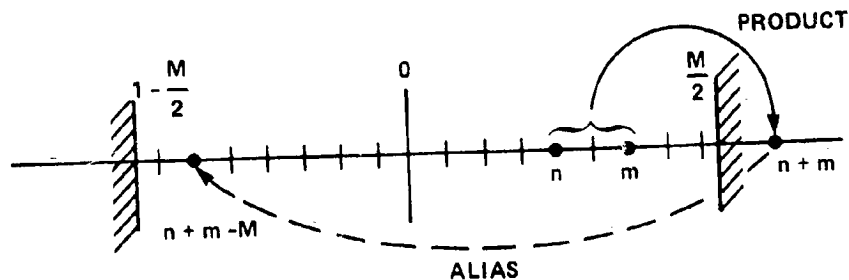
The alias error resulting from bi-linear products can be removed by two different methods (Patterson and Orszag (1971)).

ALIAS REMOVAL BY TRUNCATION

We want to form the length M alias-free product of two Fourier series of length M ($1-M/2 \leq k \leq M/2$). As we have seen the product will result in a Fourier series of length $2M-1$. It is then obvious that an alias-free product can be obtained by using a Fourier transform of length 2M. The process is carried out as follows: (1) form the length 2M transforms $\tilde{a}$, $\tilde{b}$, using the given M data for $1-M/2 \leq k \leq M/2$ and zeroes for the remaining k; (2) invert the transform to obtain the length 2M

46

physical space; (3) form the length 2M product ab ; and (4) return to length 2M wave space, using a length 2M transform. At this point we have the length 2M alias-free Fourier transform of the product. We now simply discard the modes in the result outside our length M original data to obtain the length M alias-free product.

The same result can be achieved using transforms of length 3M/2 rather than 2M, with a resulting time and space savings. Because we are going to retain in the results only those waves $1-M/2 \leq k \leq M/2$ we pose the following problem: What is the shortest length (L) transform that will not alias the product into modes $1-M/2 \leq k \leq M/2$? The limiting product is that between modes both having wave-number M/2 resulting in wave-number M aliased by the length L transform to wave-number M-L, which must be outside the span $1-M/2 \leq k \leq M/2$. Thus we have

$$M-L < 1-M/2 \quad \text{or} \quad L > 3M/2-1$$

Similarly, the lowest wave-number $1-M/2$ at worst produces wave-number 2-M in the result and is thus aliased to L+2-M which must be greater than M/2. This requires $L > 3M/2-2$.

In practice, the length of the Fourier transform (M) is determined by computer size and the wave-numbers carried are reduced from $1-M/2 \leq k \leq M/2$ to $-M/3 \leq k \leq M/3$ in order to achieve alias-free products. (Note that by M/3 we mean the truncated integer value.) This procedure is popularly referred to as the 2/3 rule.

ALIAS REMOVAL BY PHASE SHIFTS

We can rewrite the transform of an aliased product as

$$c_k = \sum_{\substack{n,m \\ n+m=k}} \tilde{a}_n \tilde{b}_m + \sum_{\substack{n,m \\ n+m=k\pm M}} \tilde{a}_n \tilde{b}_m$$

where the first sum is the alias-free result, and the second sum is the alias error at wave-number k. Consider the effect of a shifted physical space grid. In wave space the shift is achieved by multiplying each Fourier mode $\tilde{a}_n$ by the phase factor $e^{in\Delta}$. If we form the product on the shifted mesh and then shift the result back to the original mesh we obtain

$$\tilde{c}_k = e^{-ik\Delta} \left\{ \sum_{n+m=k} \tilde{a}_n e^{in\Delta} \tilde{b}_m e^{im\Delta} + \sum_{n+m=k\pm M} \tilde{a}_n e^{in\Delta} \tilde{b}_m e^{im\Delta} \right\}$$

or

$$\tilde{c}_k = \sum_{n+m=k} \tilde{a}_n \tilde{b}_m + e^{\pm iM\Delta} \sum_{n+m=k\pm M} \tilde{a}_n \tilde{b}_m$$

The alias-free sum is unchanged by the shifts, but the alias error is multiplied by the phase factor $e^{\pm iM\Delta}$. This offers several possibilities for eliminating the error, the first of which is that of evaluating $\tilde{c}_k$ on two meshes, one shifted from the other by exactly half a grid cell. Then $\Delta^{(2)} = \Delta^{(1)} + \pi/M$, which gives

$$e^{\pm iM\Delta^{(2)}} = -e^{\pm iM\Delta^{(1)}}$$

and the alias-free sum is one half the sum of the two evaluations.

This method allows one to retain all of the Fourier modes associated with a length M transform, but requires two evaluations.

A second possibility, which does not exactly eliminate the error and does not require double evaluations, is the use at each evaluation of the time advance of a random value of $e^{iM\Delta}$ taken from a uniform distribution around the unit circle.

The current code, as we will see shortly, uses both truncation and shifts in concert to effectively eliminate alias error at little cost.

MULTIDIMENSIONAL ALIAS ERROR

The multidimensional discrete Fourier transform is simply the product over the dimensions of one-dimensional transforms. Similarly, the aliased wave-number in a given direction depends only on the wave-numbers in that direction of the modes being multiplied. Thus a product of two modes in three-dimensional space has eight possible outcomes as far as aliasing is concerned. That is, the result may be aliased or not in each of the three directions independently.

When independent shifts are applied to each direction, we have

$$\tilde{c}_{\underline{k}} = S_{000} + \theta_1 S_{100} + \theta_2 S_{010} + \theta_3 S_{001} + \theta_1 \theta_2 S_{110} + \theta_2 \theta_3 S_{011} + \theta_1 \theta_3 S_{101} + \theta_1 \theta_2 \theta_3 S_{111}$$

where

$\theta_1 = e^{\pm iM_1\Lambda_1}$ (etc. for θ_2, θ_3) are the phase factors,

$$S_{000} = \sum_{\underline{m}+\underline{n}=\underline{k}} \tilde{a}(\underline{n})\tilde{b}(\underline{m})$$

$$S_{100} = \sum_{\underline{m}+\underline{n}=\underline{k}+M_1\underline{e}_1} \tilde{a}(\underline{n})\tilde{b}(\underline{m}) , \qquad \underline{e}_1 \text{ is a unit vector in the } x \text{ direction}$$
etc. for S_{010}, S_{001}

$$S_{110} = \sum_{\underline{m}+\underline{n}=\underline{k}+M_1\underline{e}_1+M_2\underline{e}_2} \tilde{a}(\underline{n})\tilde{b}(\underline{m}) , \qquad \underline{e}_2 \text{ is a unit vector in the } y \text{ direction}$$
etc. for S_{011}, S_{101}

$$S_{111} = \sum_{\underline{m}+\underline{n}=\underline{k}+\underline{M}} \tilde{a}(\underline{n})\tilde{b}(\underline{m})$$

The alias-free result is S_{000}; S_{100}, S_{010}, and S_{001} are sums aliased in the 1, 2, and 3 directions, as indicated by the subscripts; S_{110}, S_{011}, and S_{101} are aliased in two directions, and S_{111} is aliased in all three directions.

We use a combination of truncation and phase shifting similar to that of Patterson and Orszag to eliminate all of the alias errors. Recall that truncation by the 2/3 rule consists of zeroing wave-numbers k_i with $|k_i| > M/3$ prior to inversion of the transform, and their discard upon return to wave space following formation of the bi-linear product.

In three dimensions, truncation of wave vectors having any component greater than M/3 results in the elimination of all the alias-error sums S for the remaining wave vectors. If only those wave vectors having two or more components greater than M/3 are truncated, only the double and triple aliases are eliminated. If only those vectors having all three components greater than M/3 are truncated, only the triple alias sums are eliminated. We have followed Patterson and Orszag and eliminated the double and triple aliases by truncating wave vectors having two or more components greater than M/3 (Patterson and Orszag truncate modes with $k^2 > 2(M/3)^2$, a more severe truncation). We are then left with only the single aliases:

$$\tilde{c}_k = S_{000} + \theta_1 S_{100} + \theta_2 S_{010} + \theta_3 S_{001}$$

These can be eliminated by summing evaluations from shifted grids as outlined

49

previously. If the __exact__ elimination of the single-alias error is not required, we can avoid the extra evaluation and perform the phase shifting as the time-advance proceeds. Thus the alias error from one step will be nearly cancelled at the next step. In the Runge-Kutta methods used in the current algorithm, the residual alias error is of the order of the square of the time-step (h). Each cancelling pair of evaluations is made at the same time level of the advance, and the shifts in the three directions are uncorrelated with one another, that is

$$\theta_i^{(1)} = -\theta_i^{(2)} = \mathcal{R}_i$$

where $\mathcal{R}_i$ are three random complex numbers chosen at each time-level from a uniform distribution around the unit circle. The alias errors act as a random forcing function of small amplitude (which is formally $O(h^2)$, but also depends on the energy spectrum).

RE-MESHING THE FIELD

The computational coordinates move with the mean flow and can become greatly distorted from their initial form. When the mean flow is an irrotational strain, the coordinates remain orthogonal, but the mesh aspect ratio grows indefinitely. Because they are influenced by the nonlinear terms in the Navier-Stokes equations, the length scales of the turbulence field are not simply stretched and rotated by the mean field. As the mesh becomes distorted, the range of scales of the turbulence in some direction may not be contained within the resolved range of scales in that direction even though it was at earlier times. We have not yet studied the general re-mesh problem, and the current code re-meshes only the shear flows. The process is illustrated by the following diagram for the case $\beta_1 = \beta_2 = \beta_3 = 1$. The extension to general β is straightforward.
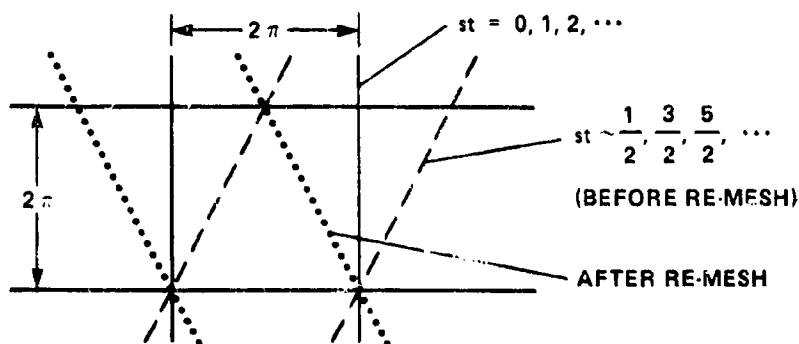
The calculation begins at st = 0 on a Cartesian mesh, shown above as the solid vertical line. At time st = 1/2 the mesh has become skewed to the right as shown by the dashed line. The field is then interpolated onto the mesh skewed to the left (the dotted line), and the time-advance proceeds. At time st = 1, the mesh is again orthogonal, and at st = 3/2 the remesh process is carried out again.

50

The re-mesh process in physical space appears simple, but in fact it results in alias errors unless those errors are explicitly eliminated. Denoting the coordinates before and after re-mesh by superscripts (1) and (2), we define the re-mesh process as

$$\underline{u}^{(2)}[\underline{x}'^{(2)}(\underline{x})] = \underline{u}^{(1)}[\underline{x}'^{(1)}(\underline{x})]$$

where

$$\underline{x}'^{(2)}(\underline{x}) = \underline{x}'^{(1)}(\underline{x}) + x_2' \underline{e}_1$$

$$\underline{e} \text{ is the x unit vector}$$

so that

$$\underline{u}^{(2)}[\underline{x}'^{(2)}] = \underline{u}^{(1)}[\underline{x}'^{(2)} - x_2' \underline{e}_1]$$

To carry out the re-mesh in physical space we would simply shift the data in x-z planes right (end-around due to the periodicity of $\underline{u}$) by the amount y. The first plane is not shifted; the second plane is shifted by one node, etc. The (M+1) plane, which is implicitly equal to the first plane by periodicity in y and not actually present, would be shifted by M nodes (one full period) and remain equal to the first y plane. In terms of Fourier modes the re-mesh operation is

$$\tilde{\underline{u}}^{(2)}[\underline{k}^{(2)}]e^{i\underline{k}^{(2)}\cdot\underline{x}'^{(2)}} = \tilde{\underline{u}}^{(1)}[\underline{k}^{(1)}]e^{i\underline{k}^{(1)}\cdot(\underline{x}'^{(2)}-x_2'\underline{e}_1)}$$

$$= \tilde{\underline{u}}^{(1)}[\underline{k}^{(1)}]e^{i(\underline{k}^{(1)}-k_1^{(1)}\underline{e}_2)\cdot\underline{x}'^{(2)}}$$

Thus a wave with wave-number (k_1,k_2,k_3) on the old mesh has wave-number (k_1,k_2+k_1,k_3) on the new mesh and is aliased if $k_2+k_1 > M/2$.

The alias errors during re-mesh are eliminated by inverting the length M wave space data $\tilde{\underline{u}}$ to a length 2M physical space in the y direction, leaving the x and z directions in an M length wave space. The data are then shifted in x, using the appropriate phase factor, and the shifted result is returned to wave space in y using 2M length transforms. The data for wave-numbers $k_2 > M/2$ are then discarded and the re-mesh is complete. Because we have discarded modes, we lose both energy and dissipation (both being positive-definite), the loss of dissipation being by far the larger because we lose primarily high-wave-number information.

THE INITIAL CONDITIONS

The Fourier transform of the velocity field is initialized to an isotropic state, satisfying continuity, and having a given energy spectrum.

The continuity condition is satisfied by taking

$$\underline{u} = \tilde{u}_1\underline{e}_1 = \alpha(\underline{k})\underline{e}_1' + \beta(\underline{k})\underline{e}_2'$$

where $\underline{e}_i$ is the computation vector basis and $\underline{e}_i'$ is any vector basis having $\underline{e}_3'$ parallel to $\underline{k}$. The complex components α and β in general are random in amplitude and phase, subject only to the constraint that

$$\int \langle \underline{u} \cdot \underline{u}^* \rangle \, dA(k) = E(k) = \int \langle \alpha\alpha^* + \beta\beta^* \rangle \, dA(k)$$

where $E(k)$ is the desired energy spectrum and the brackets $\langle \ \rangle$ denote the expected value. We have not implemented this general form because we feared that the deviation of the energy spectrum from its expected value could be large at low wave-numbers where the sample of modes in $A(k)$ is small.

The form implemented is

$$\alpha = \left(\frac{E(k)}{4\pi k^2}\right)^{1/2} e^{i\theta_1} \cos\phi \ , \qquad \beta = \left(\frac{E(k)}{4\pi k^2}\right)^{1/2} e^{i\theta_2} \sin\phi$$

where θ_1, θ_2, and ϕ are uniformly distributed random numbers on the interval $(0, 2\pi)$. This form results from the stronger constraint on (α, β)

$$E(k) = (\alpha\alpha^* + \beta\beta^*) \int dA(k)$$

where the energy of each mode separately is required to have exactly the expected value. The modes are still random with respect to spatial phase (θ_1, θ_2) and velocity component distribution (ϕ).

To complete the formulation we need only to relate the basis $\underline{e}_i'$ to the computational basis $\underline{e}_i$. Any basis subject to the constraint

$$k\underline{e}_3' = k_1\underline{e}_1 + k_2\underline{e}_2 + k_3\underline{e}_3 = \underline{k}$$

will do, since rotations about $\underline{e}_3'$ can be absorbed into the random phase ϕ. We choose arbitrarily a basis having

$$\underline{e}_1' \cdot \underline{e}_3 = 0$$

which leads to a solution for $\underline{e}_i'$:

$$(k_1^2 + k_2^2)^{1/2} \, \underline{e}_1' = k_2\underline{e}_1 - k_1\underline{e}_2$$

$$k(k_1^2 + k_2^2)^{1/2} \, \underline{e}_2' = k_1k_3\underline{e}_1 + k_2k_3\underline{e}_2 - (k_1^2 + k_2^2)\underline{e}_3$$

Thus we find

$$\tilde{u} = \left(\frac{\alpha k k_2 + \beta k_1 k_3}{k(k_1^2 + k_2^2)^{1/2}}\right) \underline{e}_1 + \left(\frac{\beta k_2 k_3 - \alpha k k_1}{k(k_1^2 + k_2^2)^{1/2}}\right) \underline{e}_2 + \left(\frac{\beta(k_1^2 + k_2^2)^{1/2}}{k}\right) \underline{e}_3$$

The initialization process above does not produce the higher velocity moments (e.g., skewness) characteristic of real turbulence. To relax the flow to a more realistic state we usually allowed it to decay isotropically until the energy cascade was developed and the spectra became fairly smooth. The resulting isotropic fields were stored to be used as the starting conditions for various anisotropic runs. This procedure was used for all of the irrotational-strain runs in which the experiments presumably also had fairly well-developed and nearly isotropic turbulence prior to passage through the straining section of the tunnel. For the shear cases, in which we were primarily interested in the later stages of development having growing energy, we simply ran from a square-pulse spectrum.

REFERENCES

1. Batchelor, G. K. (1953)
The Theory of Homogeneous Turbulence
Cambridge University Press

2. Batchelor, G. K. and Proudman, I. (1954)
The effect of rapid distortion of a fluid in turbulent motion
Quart. J. Mech. and Applied Math. 7 83-103

3. Champagne, F. H., Harris, V. G., and Corrsin S. (1970)
Experiments on nearly homogeneous turbulent shear flow
J. Fluid Mech. 41 81-139

4. Comte-Bellot, G. and Corrsin, S. (1966)
The use of a contraction to improve the isotropy of grid-generated turbulence
J. Fluid Mech. 25 657-682

5. Deissler, R. G. (1961)
Effects of inhomogeneity and of shear flow in weak turbulent fields
Physics of Fluids 4 1187-1198

6. Deissler, R. G. (1970)
Effects of initial condition on weak homogeneous turbulence with uniform shear
Physics of Fluids 13 1868-1869

7. Deissler, R. G. (1972)
Growth of Turbulence in the presence of shear
Physics of Fluids 15 1918-1920

8. Fox, J. (1964)
Velocity correlations in weak turbulent shear flow
Physics of Fluids 7 562-564

9. Harris, V. G., Graham, A. H., and Corrsin, S. (1977)
Further experiments in nearly homogeneous turbulent shear flow
J. Fluid Mech. 81 657-687

10. Hussain, A. K. M. F. and Ramjee, V. (1976)
Effects of the axisymetric contraction shape on incompressible turbulent flow
J. of Fluids Engr. 98 58-69

11. Launder, B. E., Reece, G. J. and Rodi, W. (1975)
Progress in the development of a Reynolds-stress turbulence closure
J. Fluid Mech. 68 537-566

12. Leslie, D. C. (1980)
Analysis of a strongly sheared, nearly homogeneous turbulent shear flow
J. Fluid Mech. 98 435-448

13. Lumley, J. L. and Newman, G. R. (1977)
The return to isotropy of homogeneous turbulence
J. Fluid Mech. 82 161-178

14. Lumley, J. L. (1978)
    Computational modeling of turbulent flows
    Advances in Applied Mechanics 18 123-176

15. Lumley, J. L. (1979)
    Prediction methods for turbulent flows
    VKI lecture series 1979-2

16. Mulhearn, P. J. and Luxton, R. E. (1975)
    The development of turbulence structure in a uniform shear flow
    J. Fluid Mech. 68 577-590

17. Orszag, S. A. and Patterson, G. S. (1972)
    Numerical simulation of three-dimensional homogeneous isotropic turbulence
    Phys. Rev. Lett.

18. Patterson, G. S. and Orszag, S. A. (1971)
    Spectral calculations of isotropic turbulence:
    efficient removal of aliasing interactions
    Physics of Fluids 14 2538-2541

19. Pearson, J. R. A. (1959)
    The effect of uniform distortion on weak homogeneous turbulence
    J. Fluid Mech. 5 274-288

20. Rose, W. G. (1966)
    Results of an attempt to generate a homogeneous shear flow
    J. Fluid Mech. 25 97-120

21. Rotta, J. (1951)
    Statistical theory of inhomogeneous turbulence
    NASA TT F-14,560 (1972)

22. Stewart, R. W. and Townsend, A. A. (1951)
    Similarity and self-preservation in isotropic turbulence
    Philos. Trans. A 243 359-386

23. Tavoularis, S. and Corrsin, S. (1981)
    Experiments in nearly homogeneous turbulent shear
    flow with a uniform mean temperature gradient. Part 1
    J. Fluid Mech. 104 311-347

24. Taylor, G. I. (1935)
    Turbulence in a contracting stream
    Z. angew. Math. Mech. 15 91

25. Townsend, A. A. (1954)
    The uniform distortion of homogeneous turbulence
    Quart. Journ. Mech. and Applied Math. 7 104-127

26. Tucker, H. J. and Reynolds, A. J. (1968)
    The distortion of turbulence by irrotational plane strain
    J. Fluid Mech. 32 657-673

27. Uberoi, M. S. (1956)
     Effect of wind-tunnel contraction on free-stream turbulence
     J. Aero. Sci. 23 754-764

28. Wigeland, R. A. and Nagib, H. M. (1978)
     Grid generated turbulence with and without rotation
     about the streamwise direction.
     Report R78-1, Illinois Inst. of Tech.
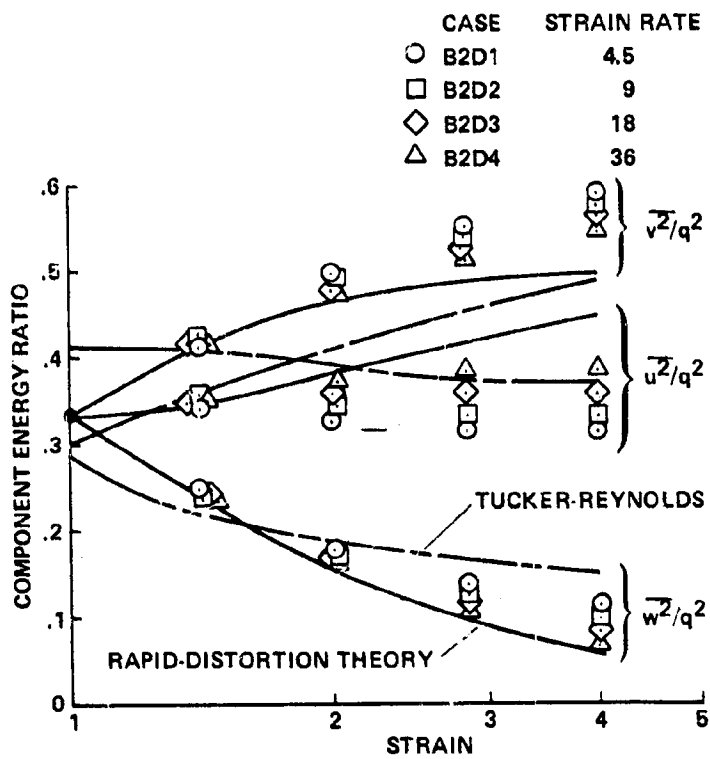
Figure 1.- Component-energy ratios for homogeneous turbulence subjected to plane strain.
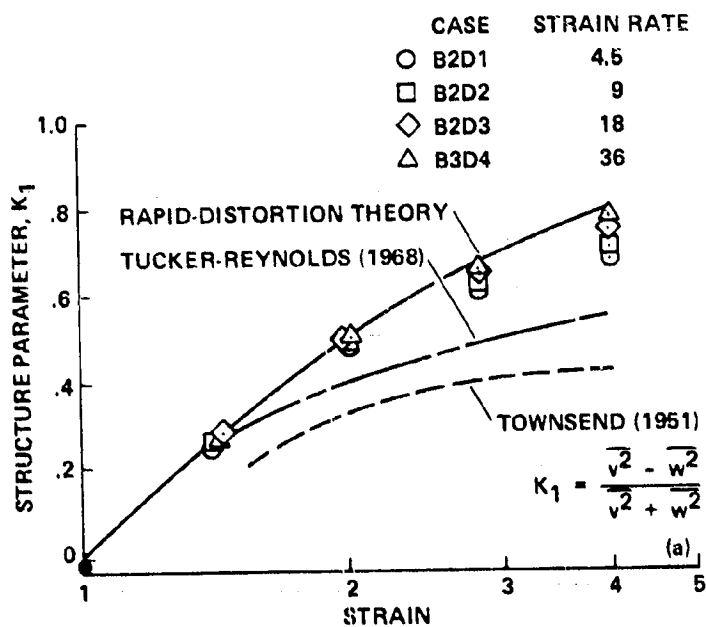
Figure 2.- Anisotropy of velocity components in homogeneous turbulence subjected to plane strain.
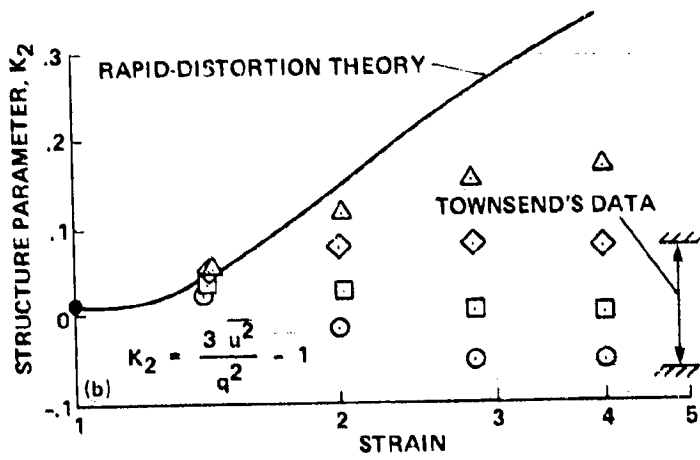
Figure 2.- Concluded.
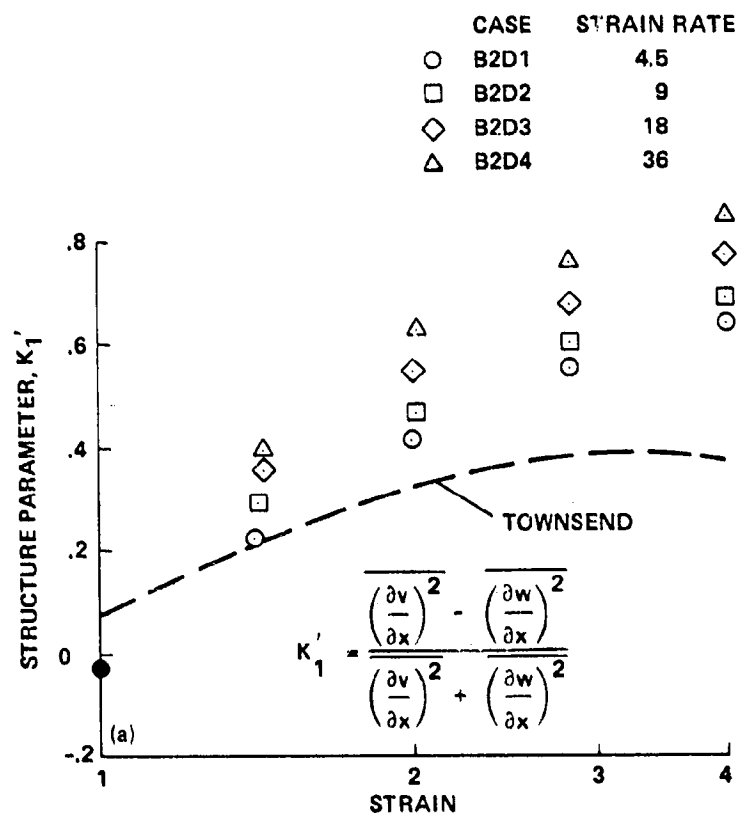
Figure 3.- Anisotropy of velocity gradient in homogeneous turbulence subjected to plane strain.

Figure 3.- Concluded.

	CASE	STRAIN RATE	VISCOSITY
●	CD23	40	0.014
○	CD13	40	0.007
◇	CD12	20	0.007
△	CD11	10	0.007
□	CD14	5	0.007
——	RAPID-DISTORTION		
— —	HUSSAIN-RAMJEE		
—·—	UBEROI		
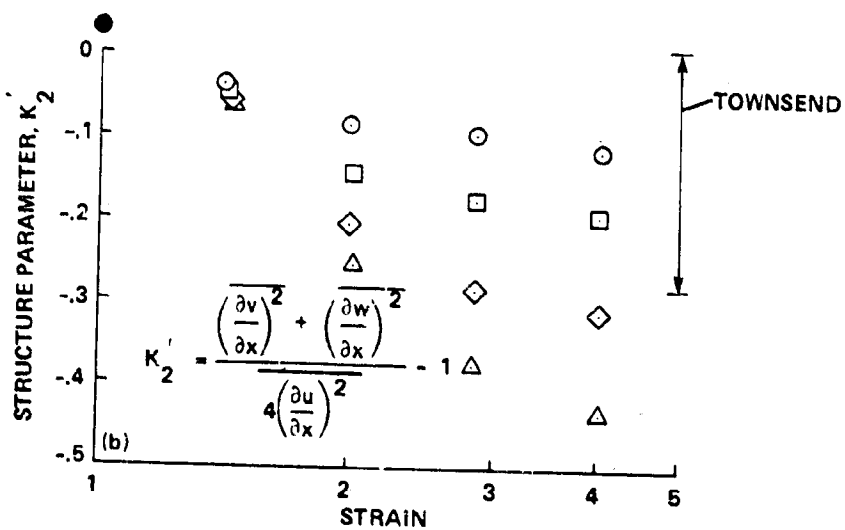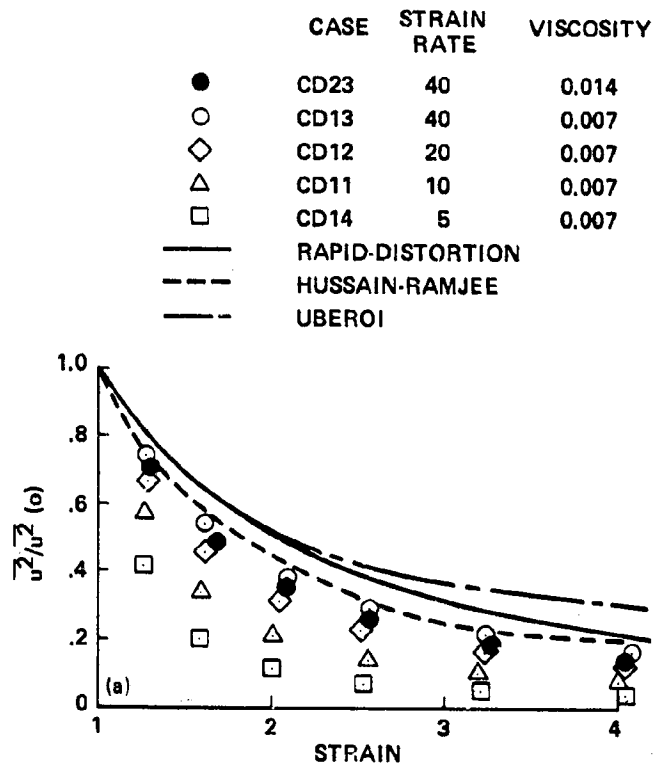
Figure 4.- History of the component energies in homogeneous turbulence subjected to axisymmetric strain.

Figure 4.- Concluded.

	CASE	SHEAR RATE	VISCOSITY
O	BSH9	28	0.007
□	BSH10	28	0.014
◇	BSH11	57	0.014
△	BSH12	20	0.005
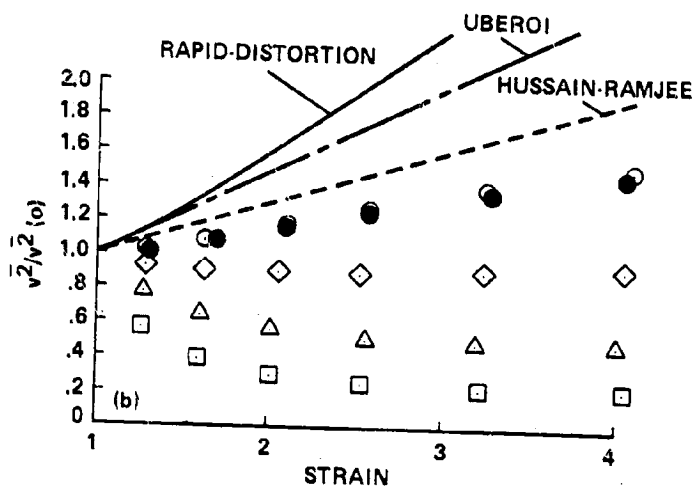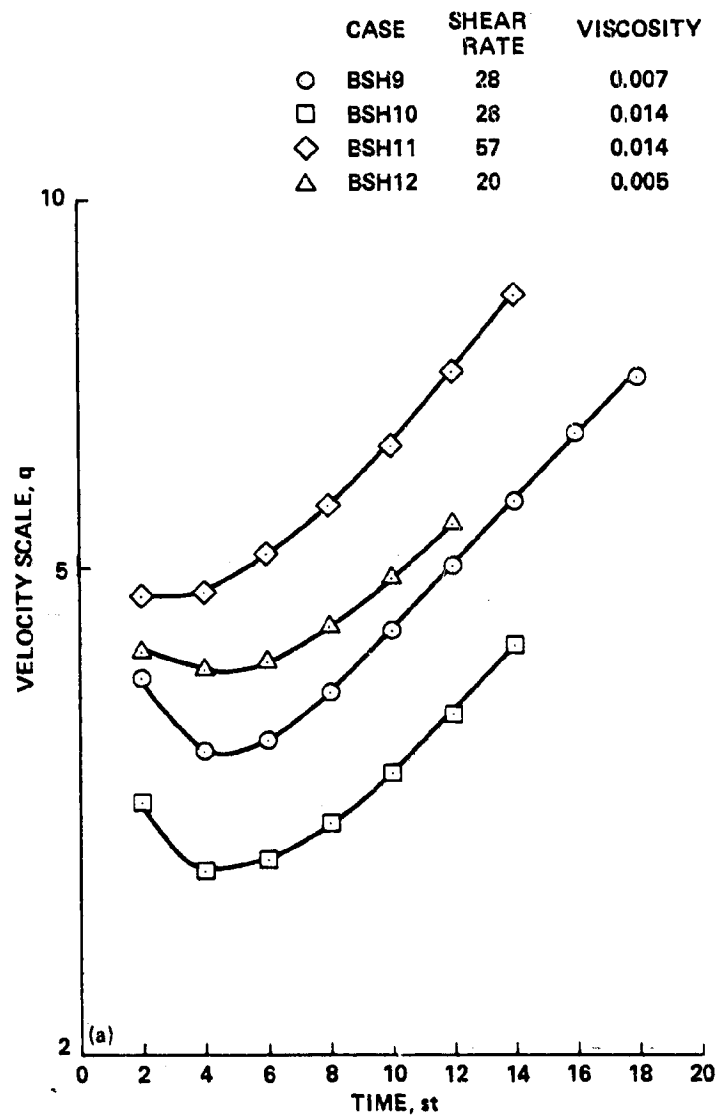
(a) Velocity scale growth.

Figure 5.- Homogeneous shear turbulence.

CASE	SHEAR RATE	VISCOSITY
◯ BSH9	28	0.007
☐ BSH10	28	0.014
◇ BSH11	57	0.014
△ BSH12	20	0.005
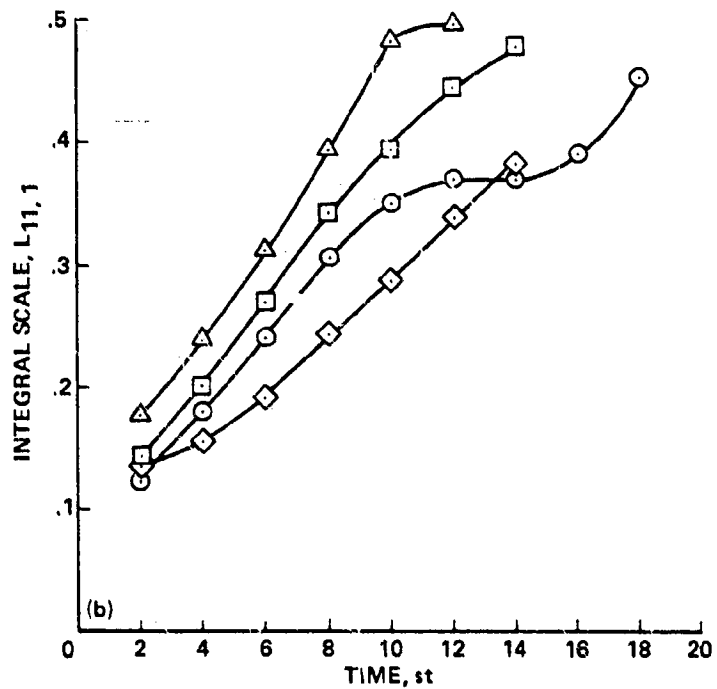
(b) Growth of the streamwise integral scale.

Figure 5.-- Concluded.

65
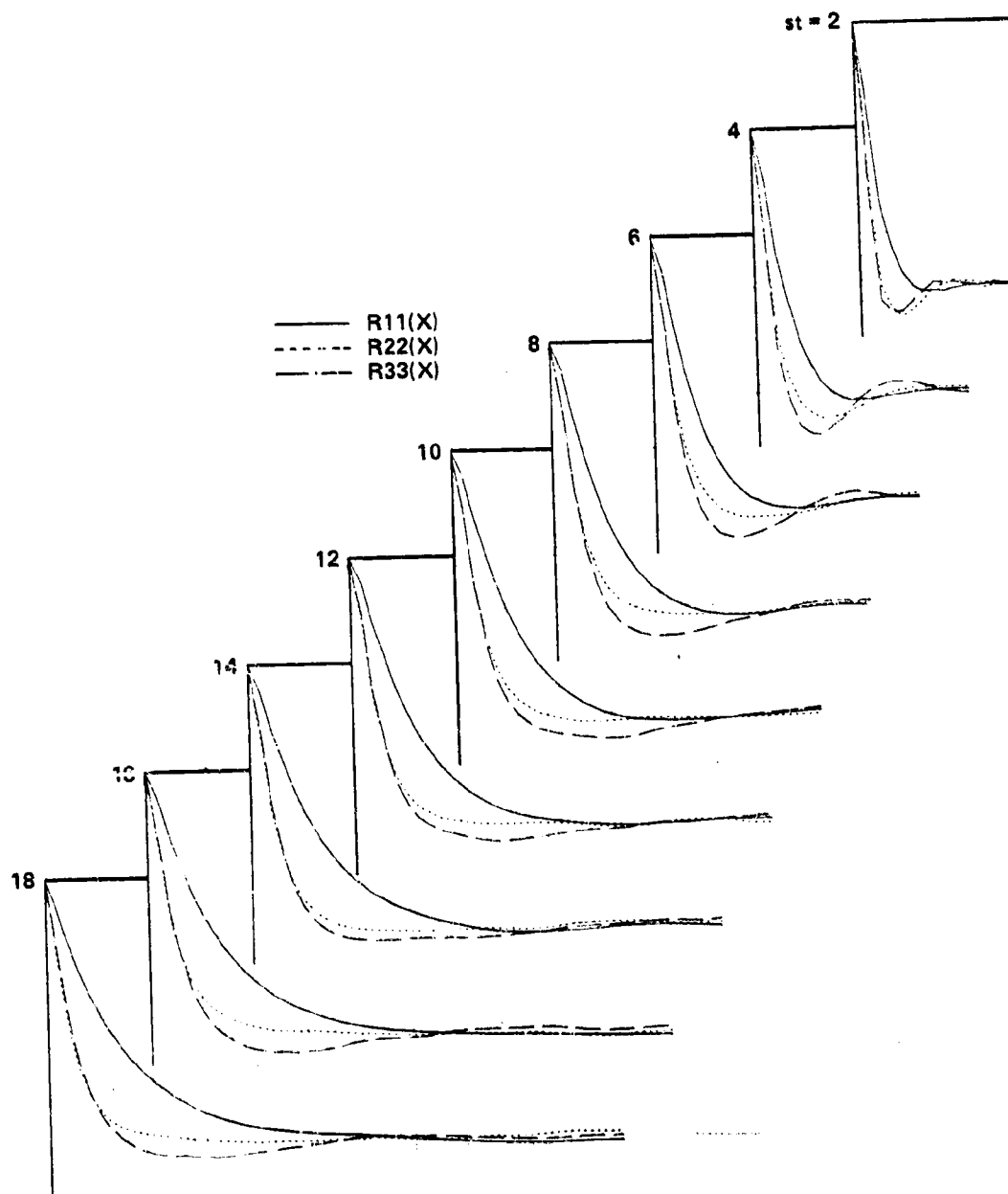
Figure 6.- Velocity autocorrelation for homogeneous shear turbulence (separation in mean stream direction), run BSH9.
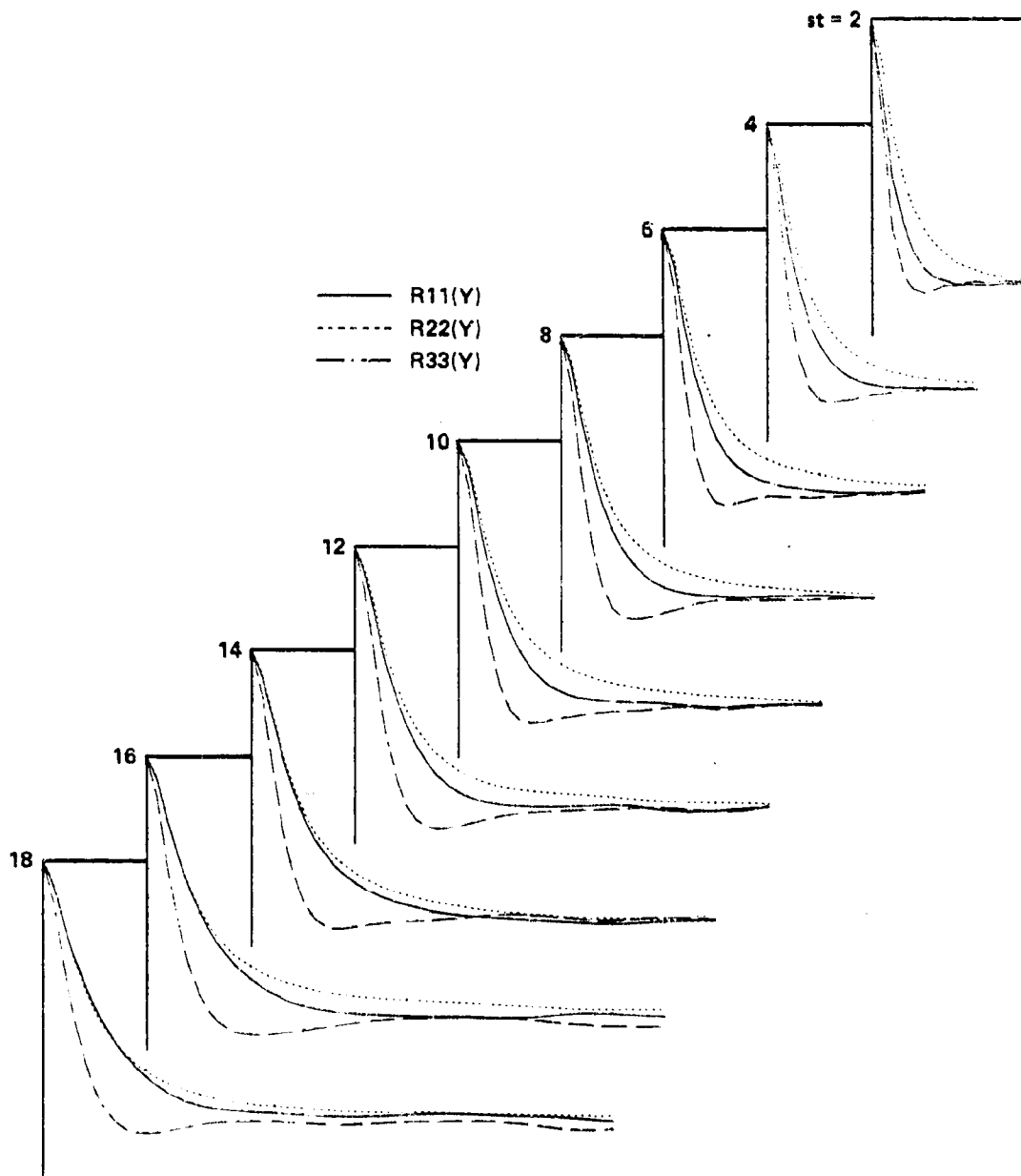
Figure 7.- Velocity autocorrelation for homogeneous shear turbulence
(separation in mean gradient direction), run BSH9.
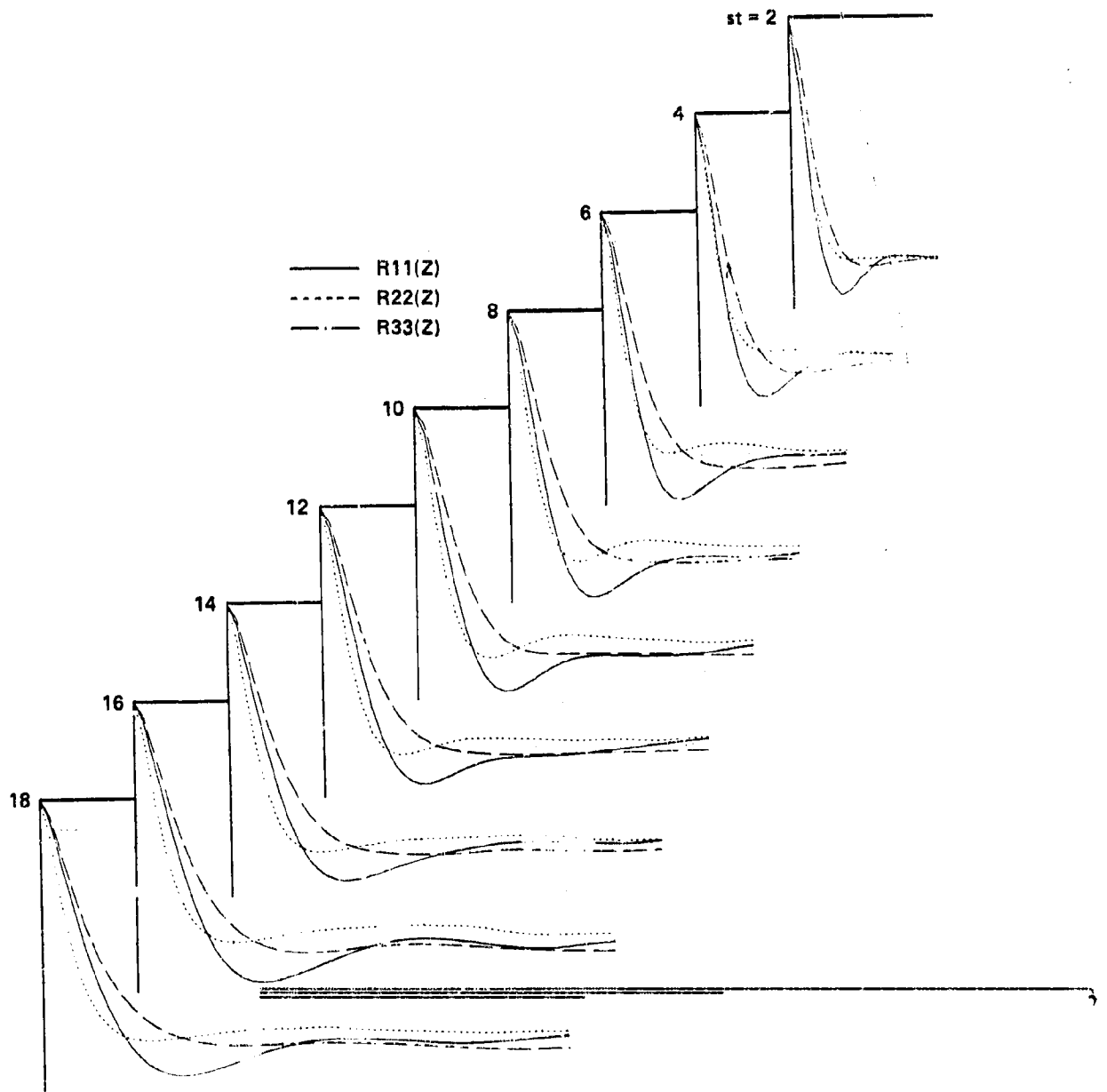
Figure 8.- Velocity autocorrelation for homogeneous shear turbulence
(separation normal to mean stream and gradient), run BSH9.
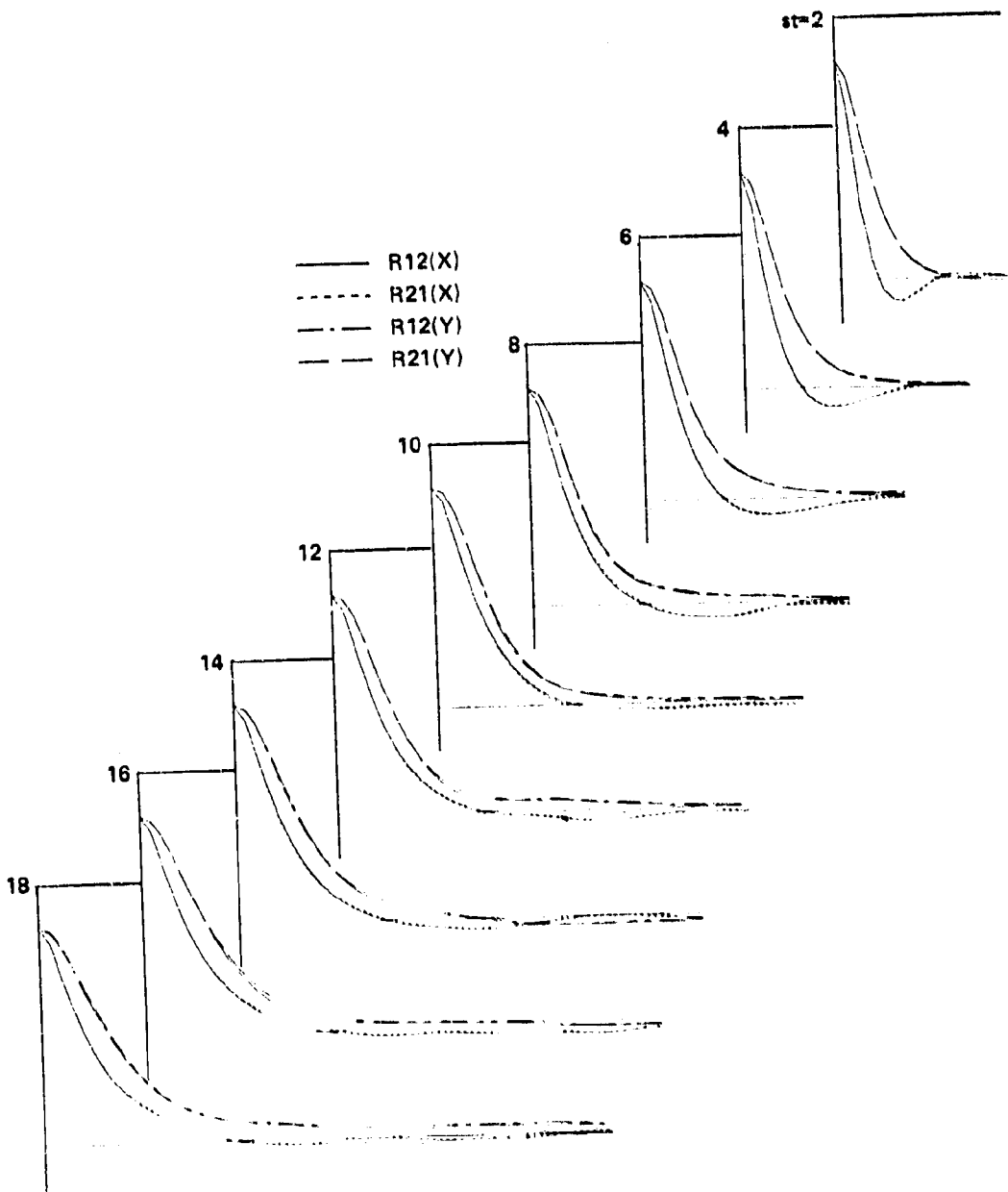
Figure 9.- Velocity cross-correlation for homogeneous shear turbulence (separation in mean stream and gradient directions), run BSH9.
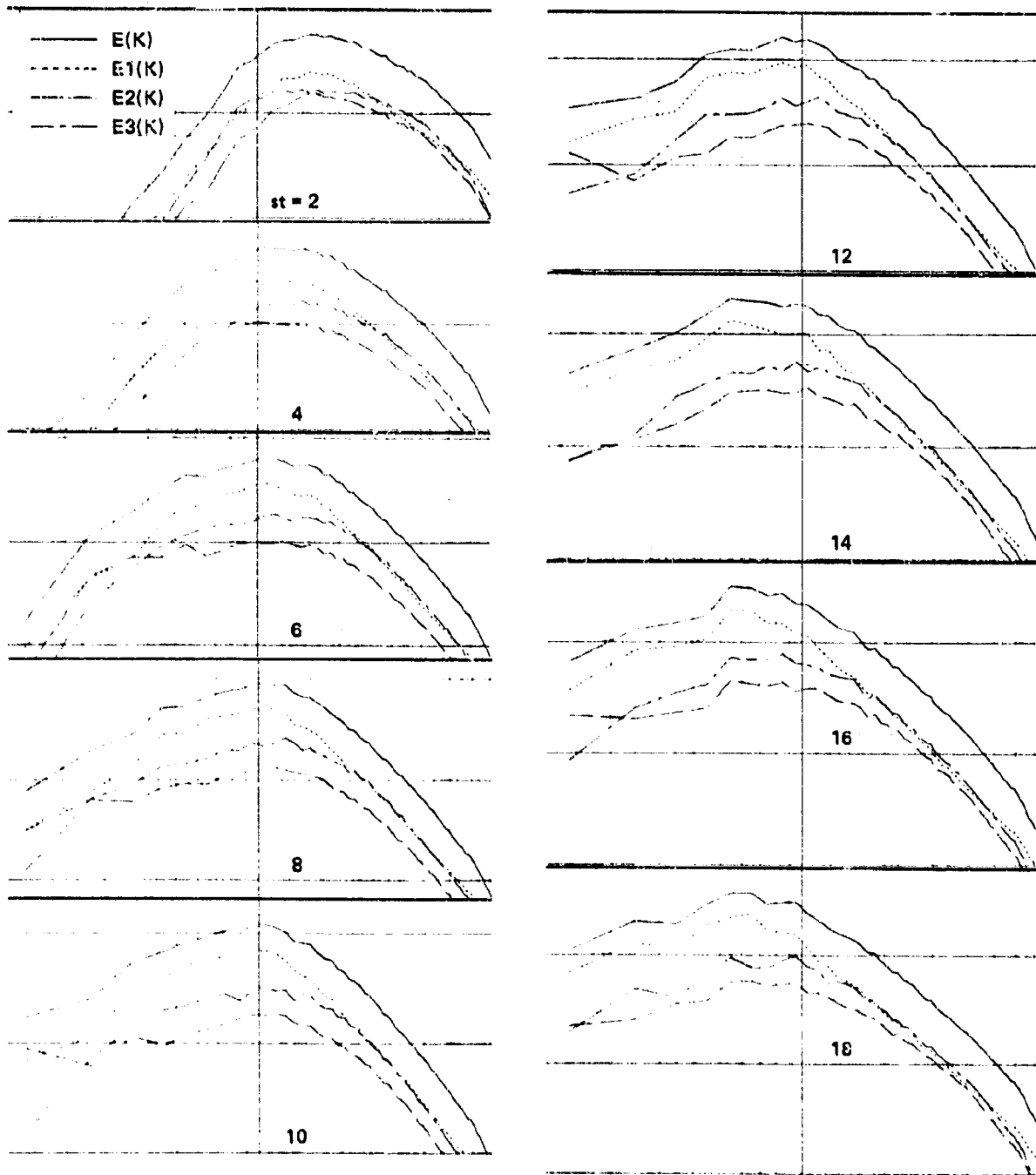
Figure 10.- Three-dimensional energy spectra for homogeneous shear turbulence, run BSH9.
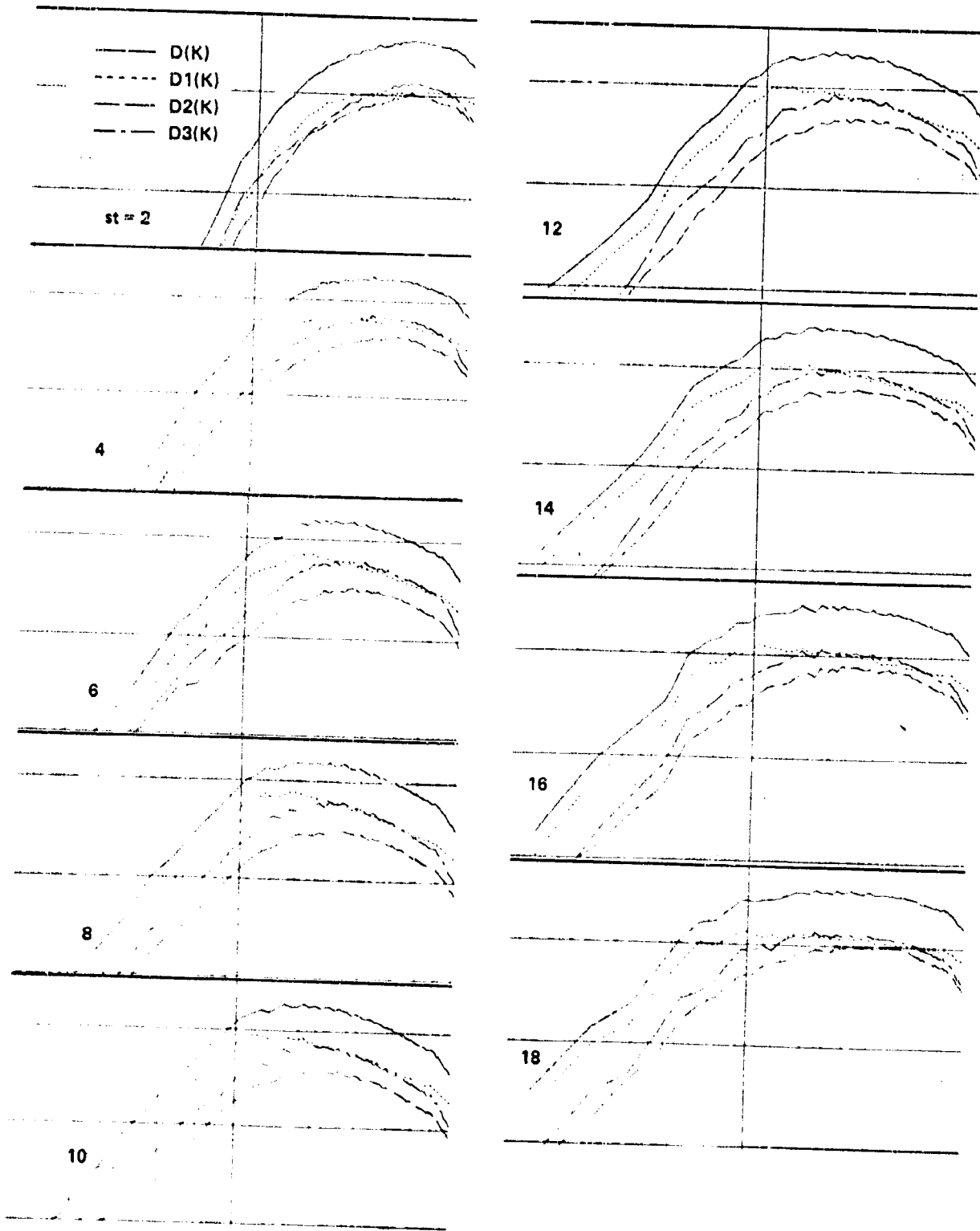
Figure 11.- Three-dimensional dissipation spectra for homogeneous
shear turbulence, run BSH9.

71
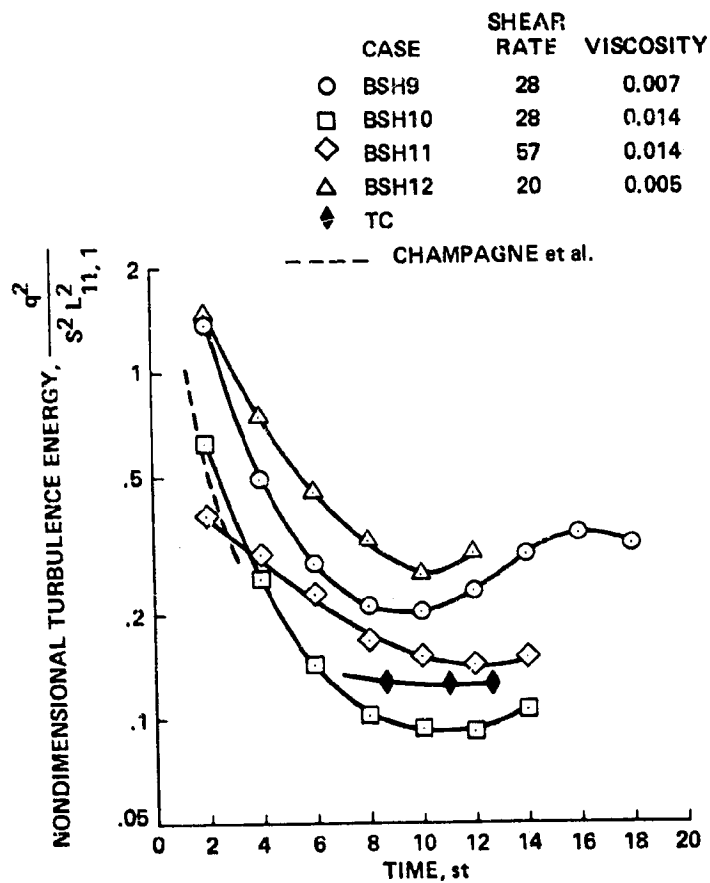
Figure 12.- The tendency toward equilibrium of the turbulence and shear time scales for homogeneous shear turbulence.

CASE	SHEAR RATE	VISCOSITY
○ BSH9	28	0.007
□ BSH10	28	0.014
◇ BSH11	57	0.014
△ BSH12	20	0.005
◆ TC		

TURBULENCE REYNOLDS NUMBER, $qL_{11,1}/\nu$

TIME, st
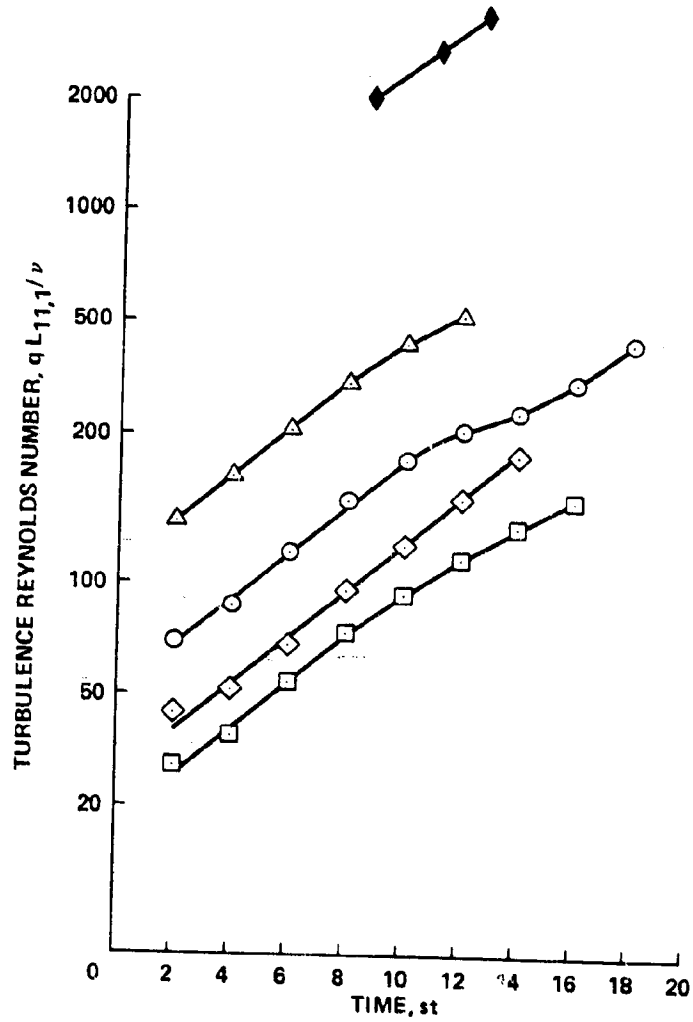
Figure 13.- Growth of the turbulence Reynolds number in homogeneous shear turbulence.

73

	CASE	SHEAR RATE	VISCOSITY
◯	BSH9	28	0.007
☐	BSH10	28	0.014
◇	BSH11	57	0.014
△	BSH12	20	0.005

$$l_y = \frac{\overline{uv}}{S\sqrt{\overline{v^2}}}$$
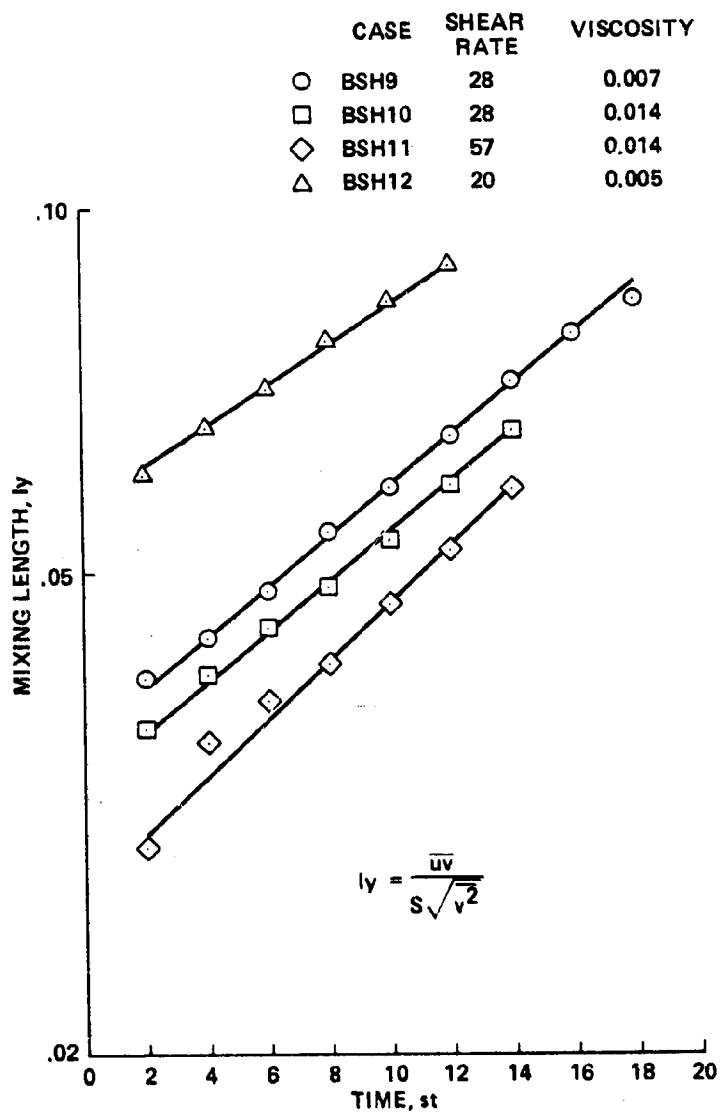
Figure 14.- Growth of the "mixing length" in homogeneous shear turbulence.
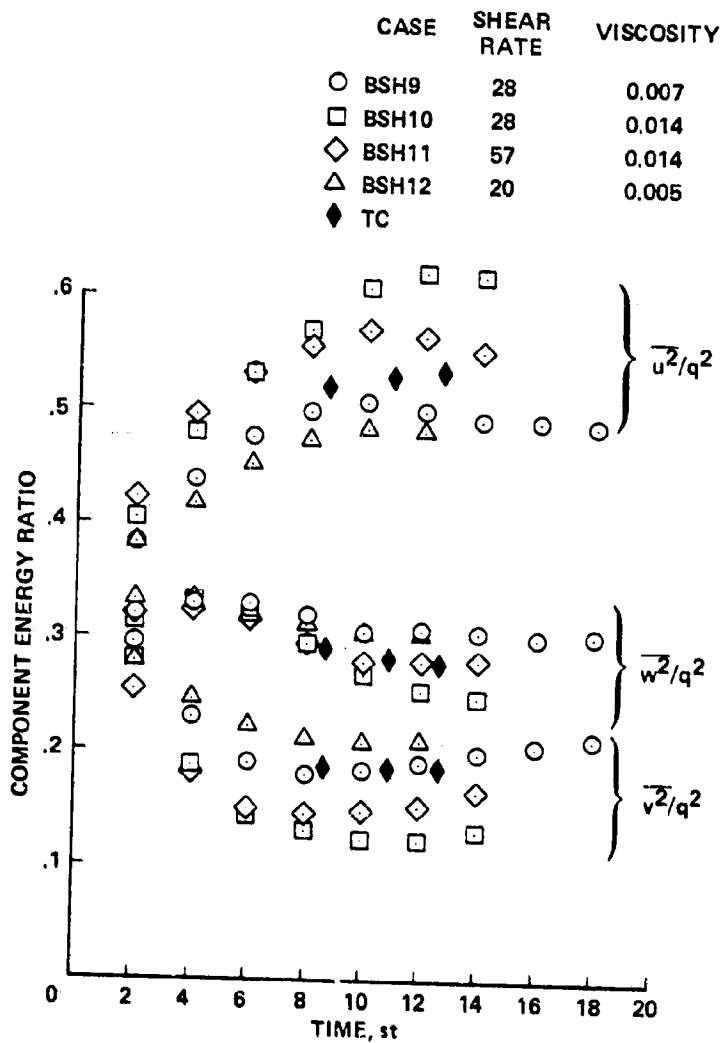
Figure 15.- History of the component energy ratios of homogeneous
shear turbulence.

	CASE	SHEAR RATE	VISCOSITY
○	BSH9	28	0.007
□	BSH10	28	0.014
◇	BSH11	57	0.014
△	BSH12	20	0.005
◆	TC		

$$b_{ij} = \left(\frac{q}{S\,L_{11}}\right)\left(\frac{\overline{u_i\,u_j}}{q^2} - \frac{1}{3}\,\delta_{ij}\right)$$

b_{11}

b_{ij}

b_{33}

b_{22}

st
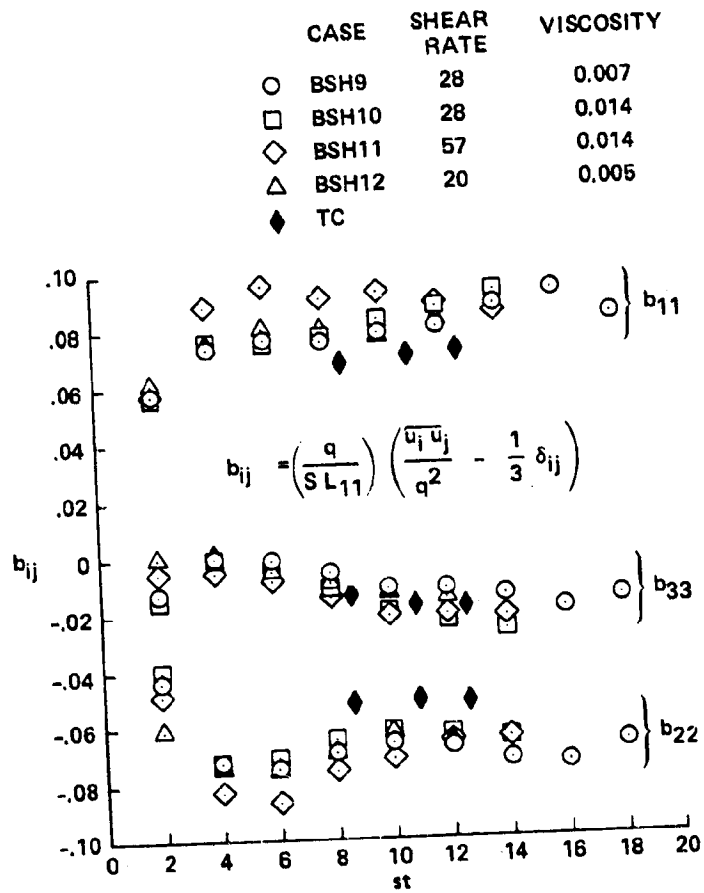
Figure 16.- Anisotropy of the normal stresses in homogeneous shear turbulence.

	CASE	SHEAR RATE	VISCOSITY
○	BSH9	28	0.007
□	BSH10	28	0.014
◇	BSH11	57	0.014
△	BSH12	20	0.005
◆	TC		
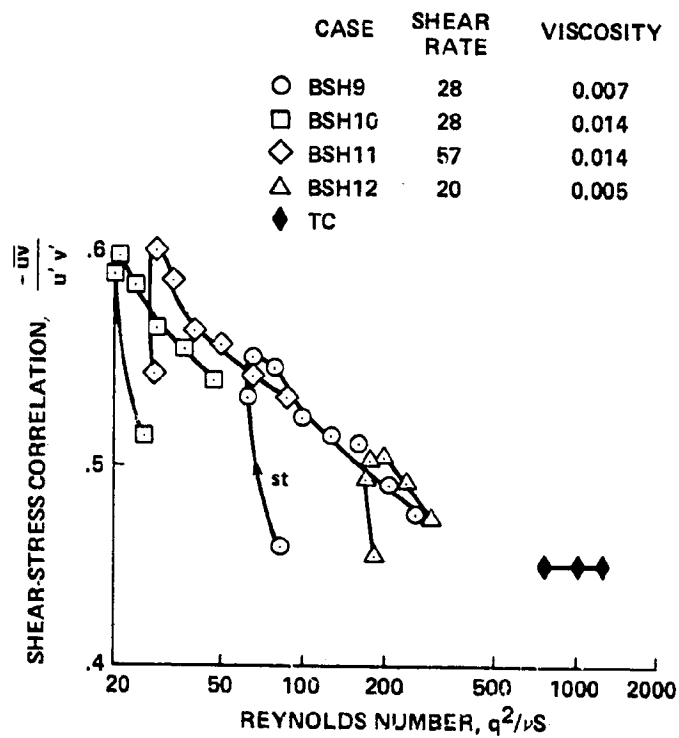
Figure 17.- Dependence of shear-stress correlation on Reynolds number in homogeneous shear turbulence.

Figure 18.- Self-similarity of the autocorrelations in homogeneous shear turbulence.

78

CASE | SHEAR RATE | VISCOSITY

	CASE	SHEAR RATE	VISCOSITY
○	BSH9	28	0.007
□	BSH10	28	0.014
◇	BSH11	57	0.014
△	BSH12	20	0.005

TRANSVERSE MICROSCALE, λ_{12}

LONGITUDINAL MICROSCALE, λ_{11}

$$\lambda_{ij}^2 = \overline{u_i^2} \Big/ \overline{\left(\frac{\partial u_i}{\partial x_j}\right)^2}$$

.1

0

.2

.1

0   2   4   6   8   10   12   14   16   18   20

TIME, st
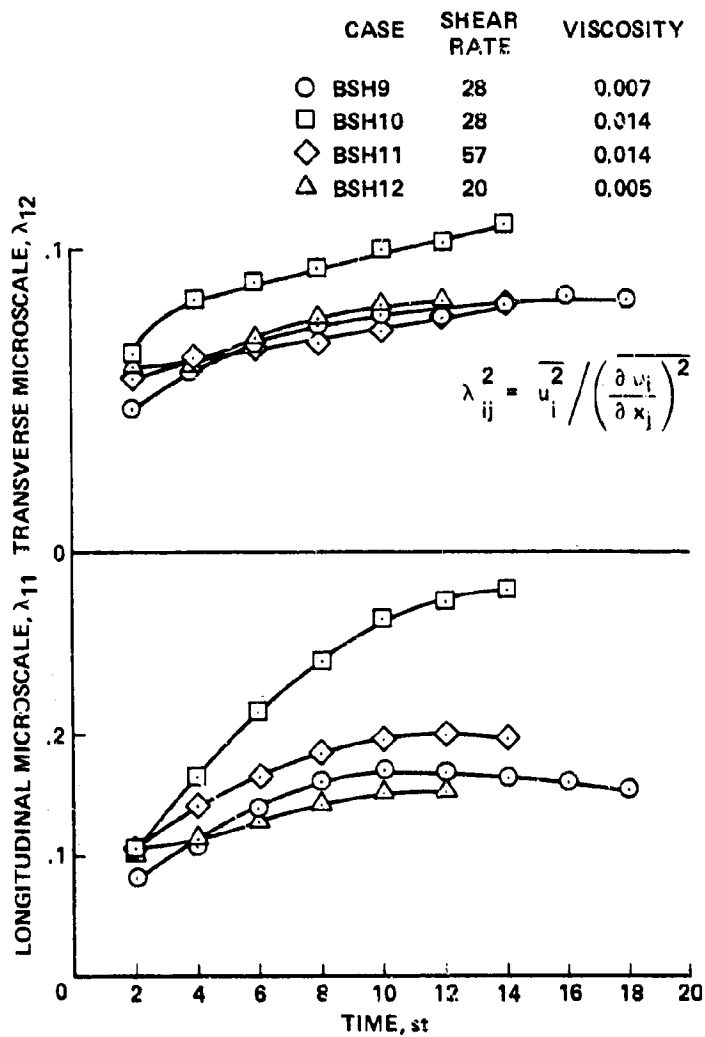
Figure 19.- Growth of the microscales in homogeneous shear turbulence.
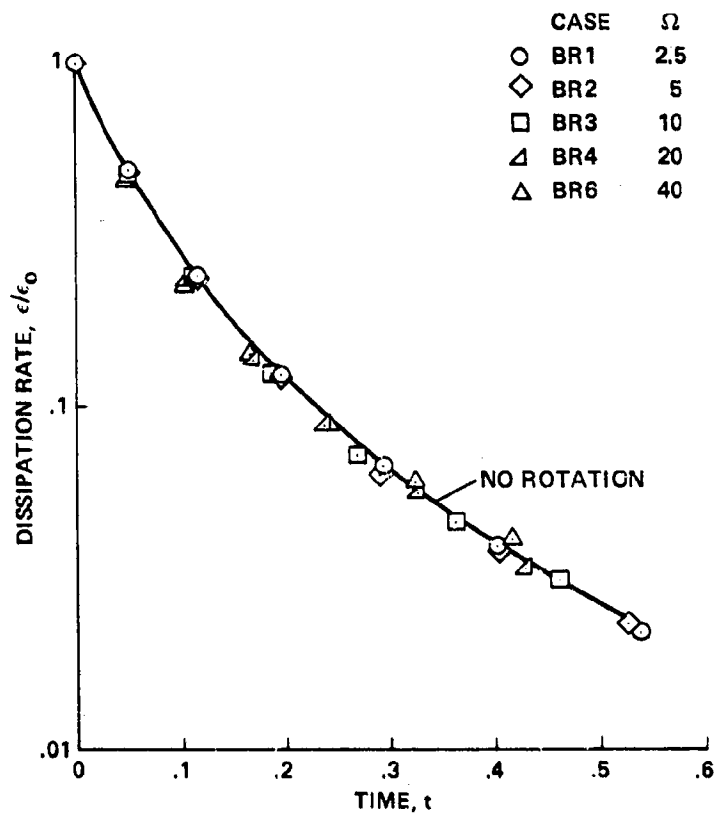
Figure 20.- Decay of the dissipation of homogeneous turbulence in uniform rotation.
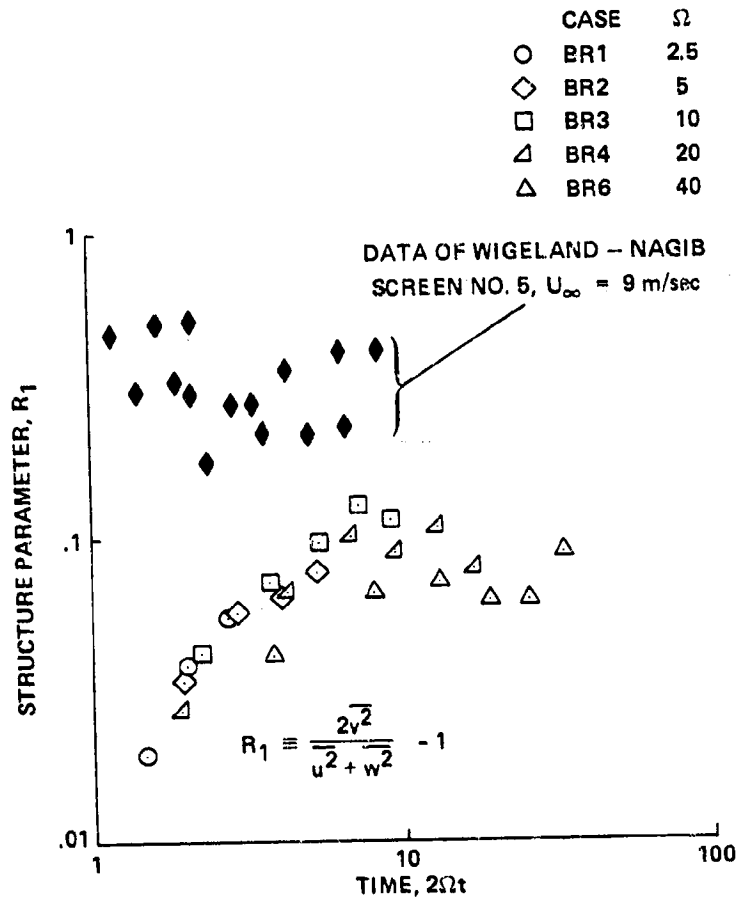
Figure 21.- Development of velocity anisotropy of homogeneous turbulence in uniform rotation.
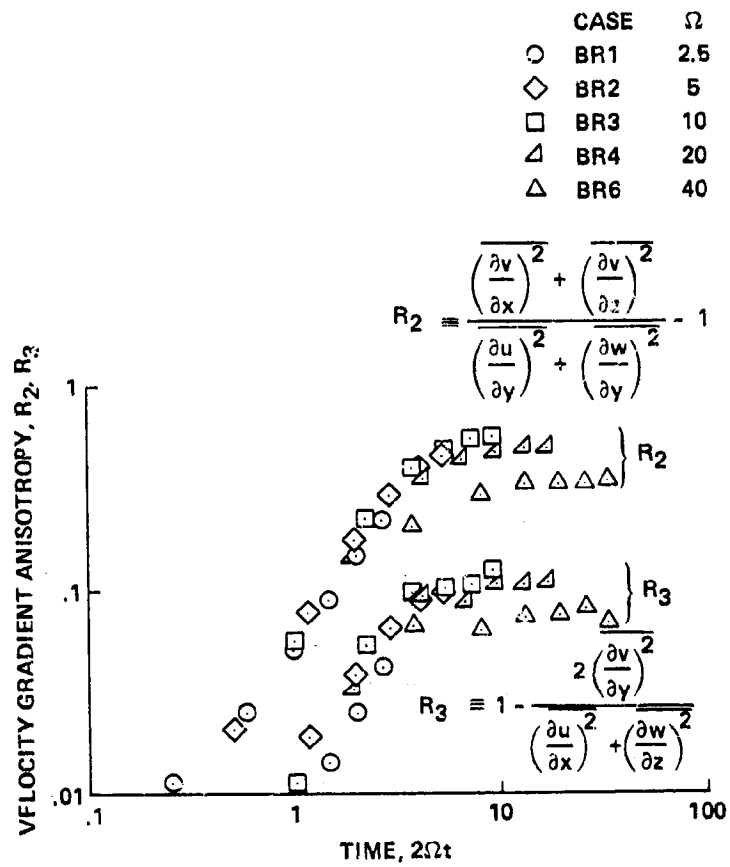
Figure 22.- Velocity gradient anisotropy of homogeneous turbulence in uniform rotation.

(a)

(b)

(c)
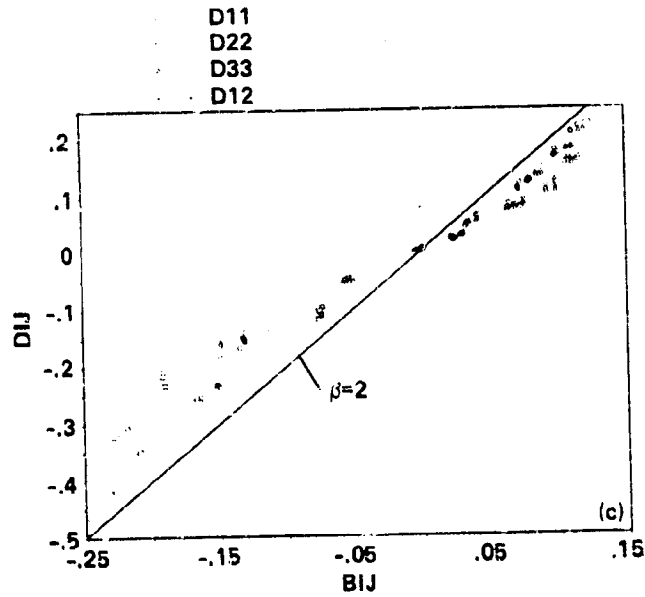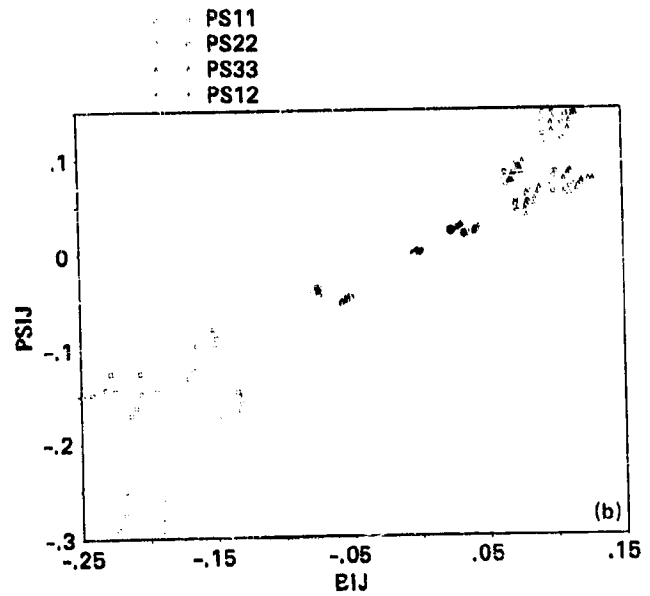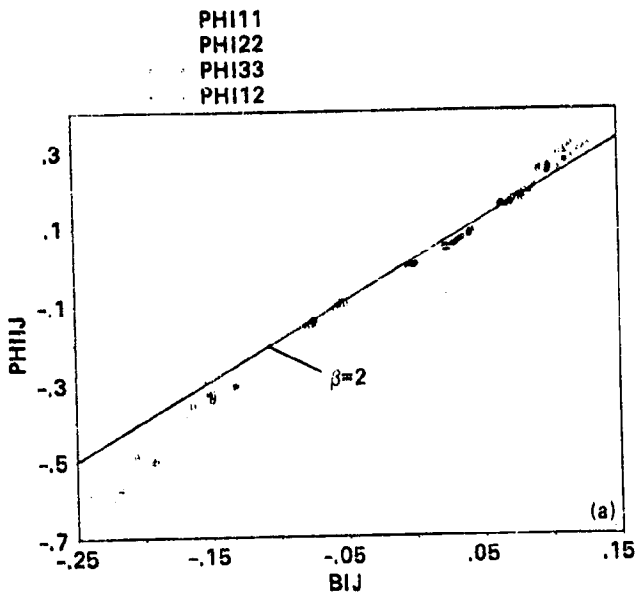
Figure 23.- Anisotropy during relaxation from axisymmetric strain.

PHIJ

DIJ

FSIJ
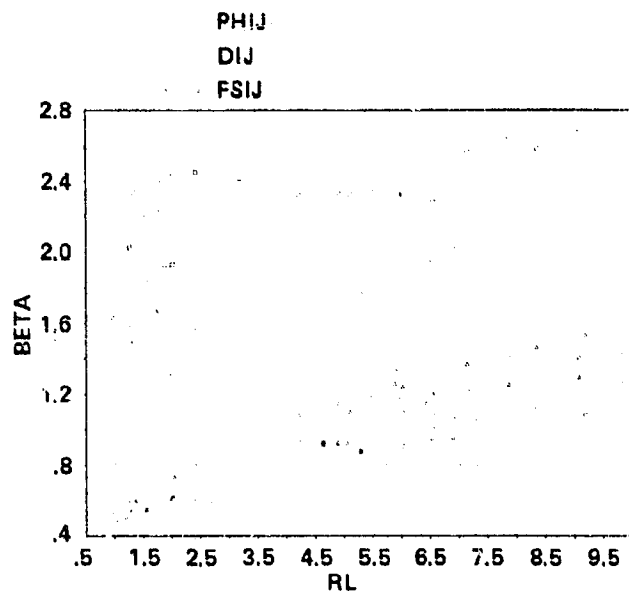
Figure 24.- Variation of Rotta coefficient with Reynolds number during
relaxation from axisymmetric strain.

PHIIJ

DIJ

PSIJ
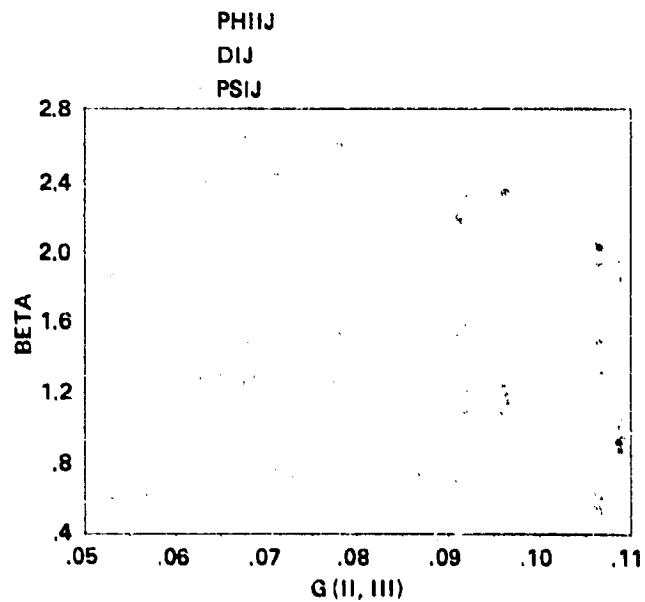
Figure 25.- Variation of Rotta coefficient with anisotropy during
relaxation from axisymmetric strain.
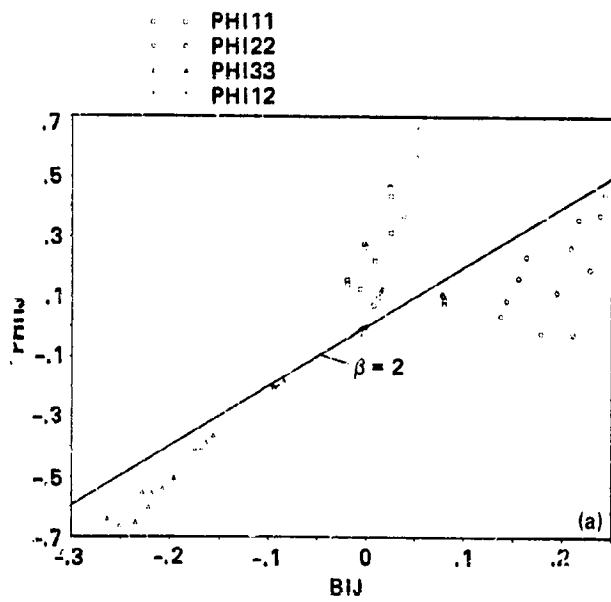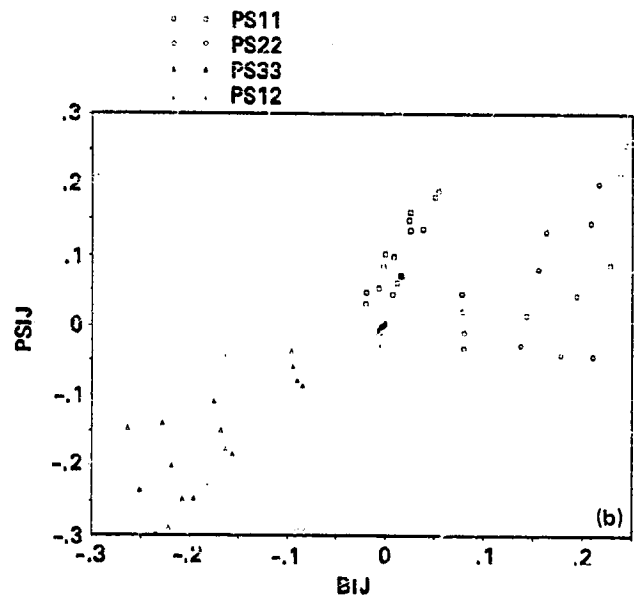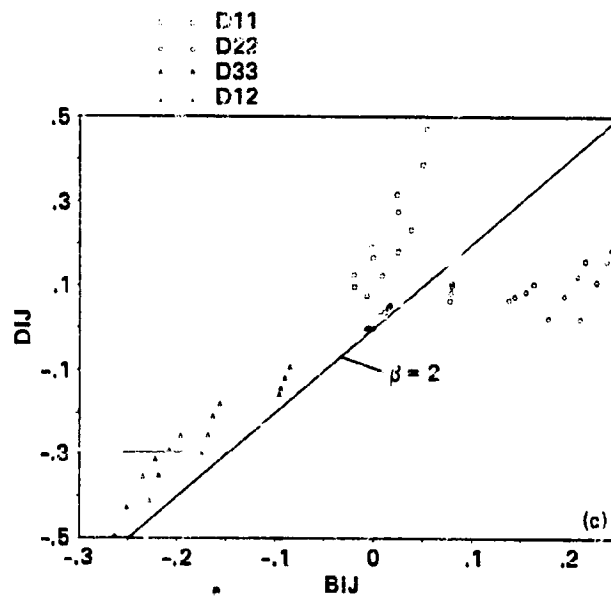
Figure 26.- Anisotropy of homogeneous turbulence subjected to plane strain.
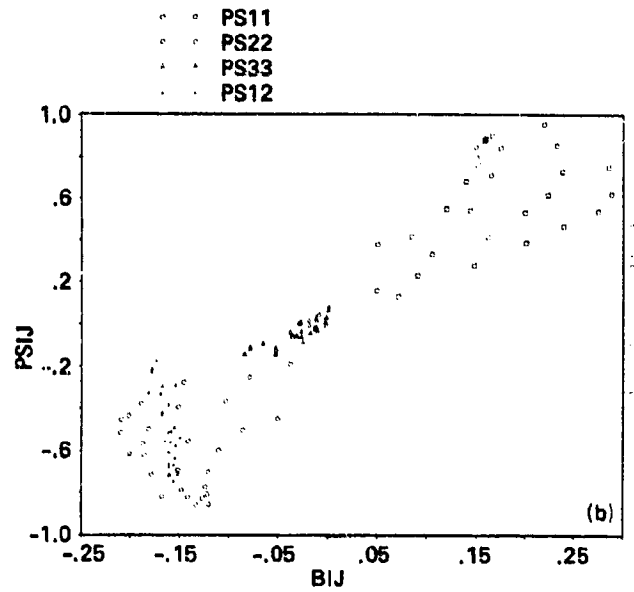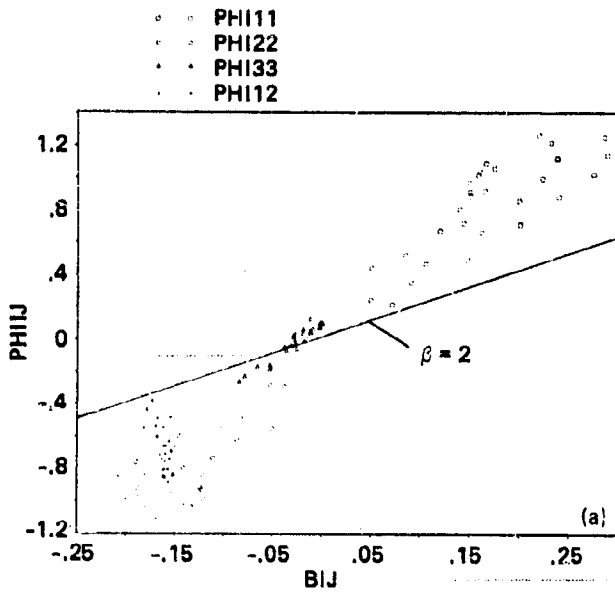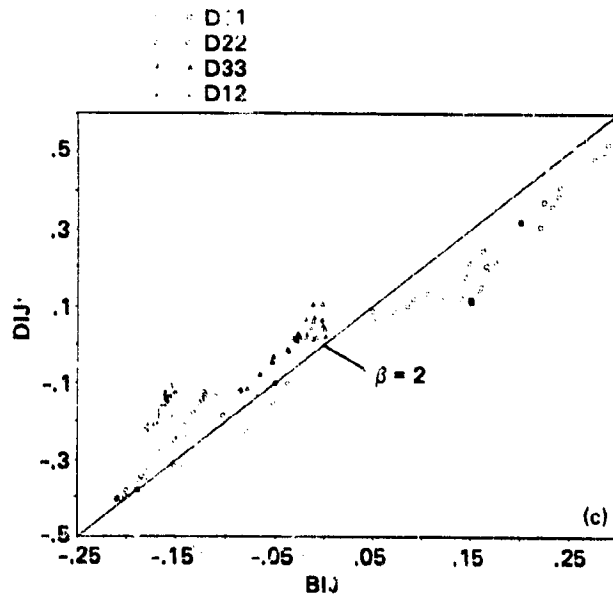
Figure 27 – Anisotropy of homogeneous shear turbulence.

(a)

(b)

(c)
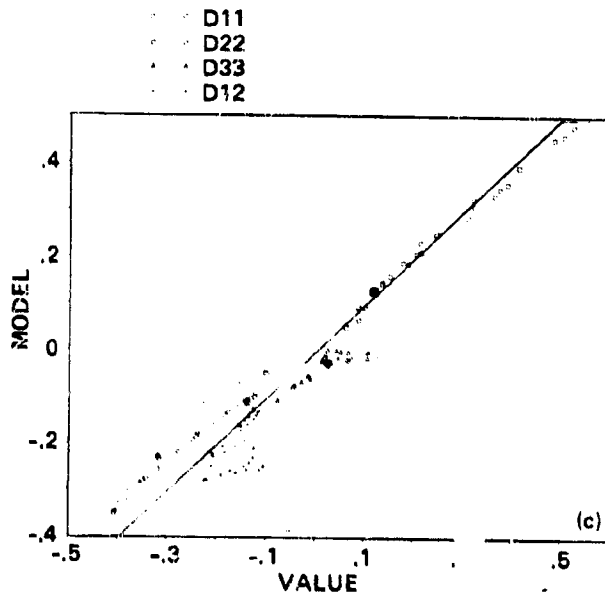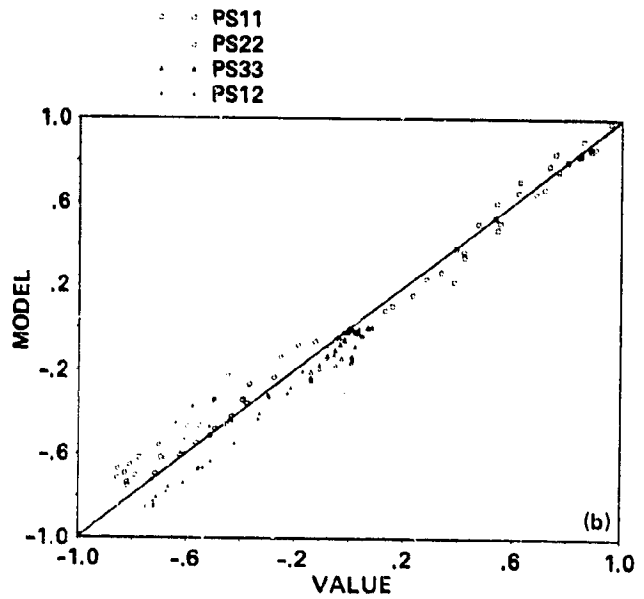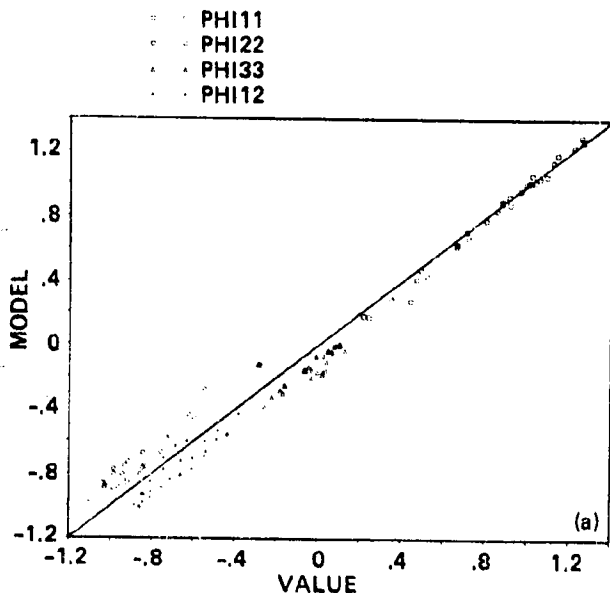
Figure 28.- Comparison of measured and modeled terms in the Reynolds stress
equations for homogeneous shear turbulence.
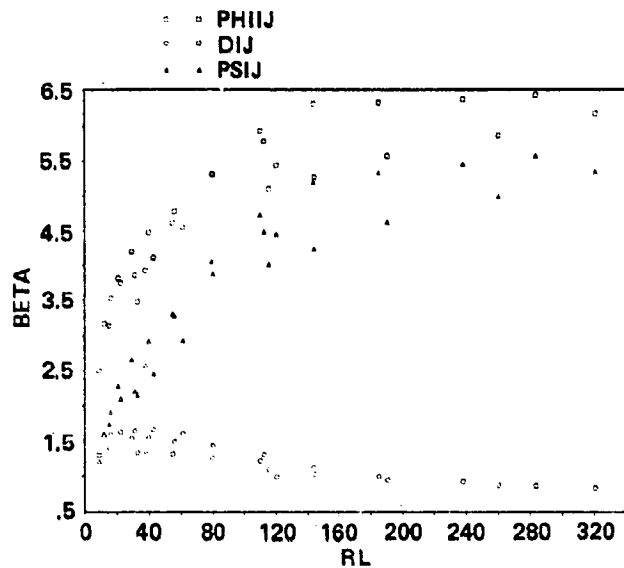
Figure 29.- Variation of Rotta coefficient with Reynolds number
in homogeneous shear turbulence.
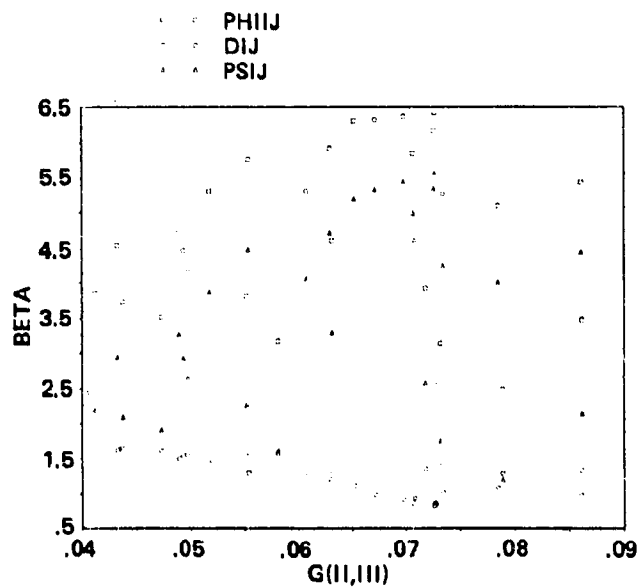
Figure 30.- Variation of Rotta coefficient with anisotropy
in homogeneous shear turbulence.
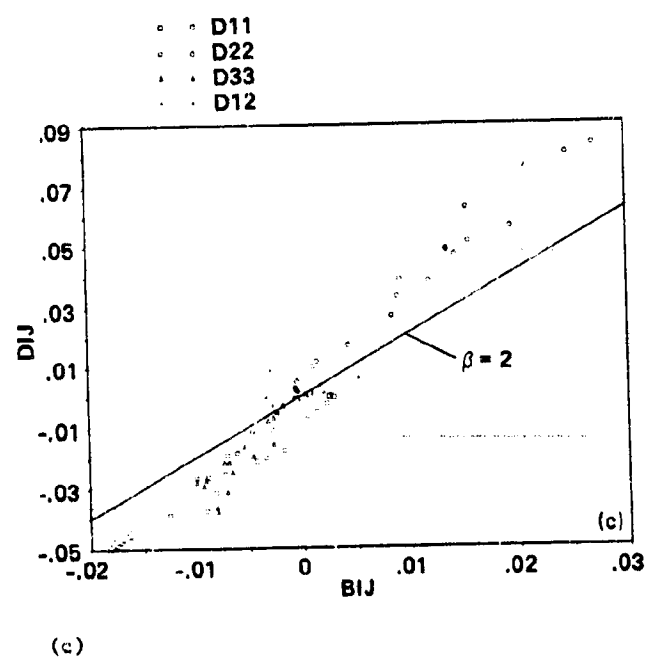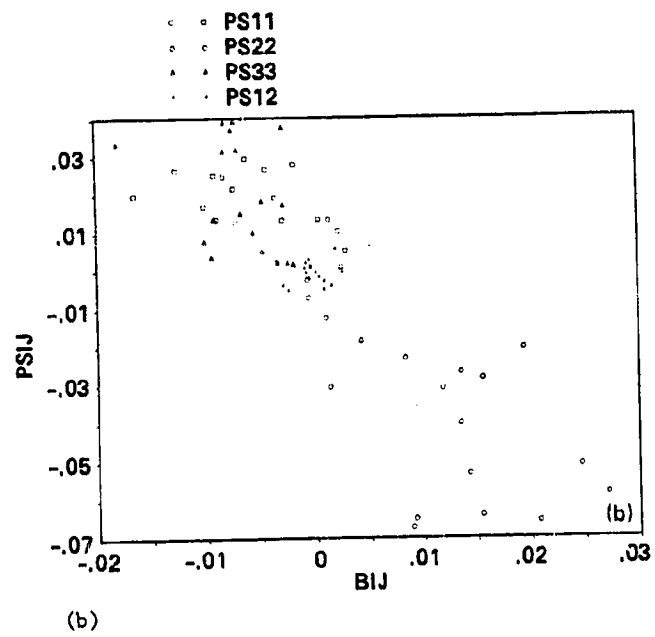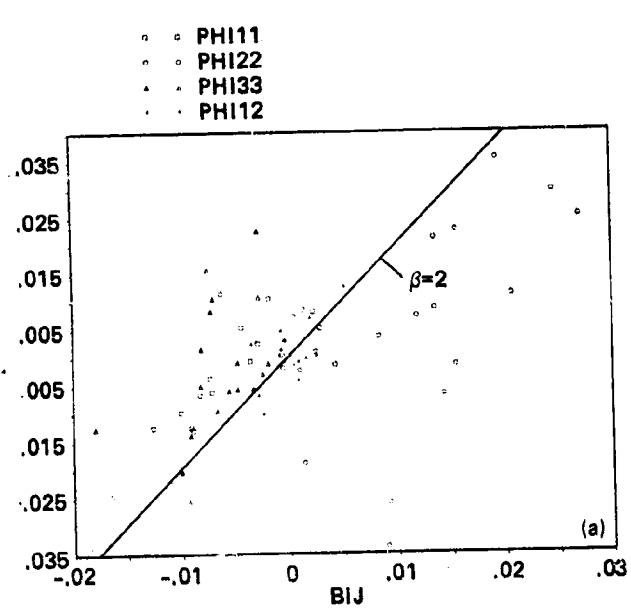
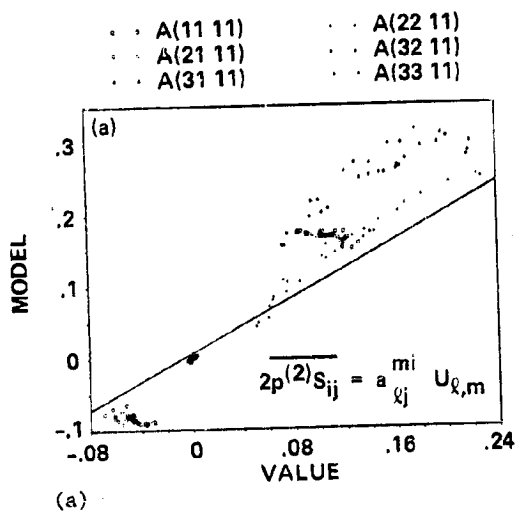Figure 31.- Anisotropy of homogeneous turbulence in uniform rotation.
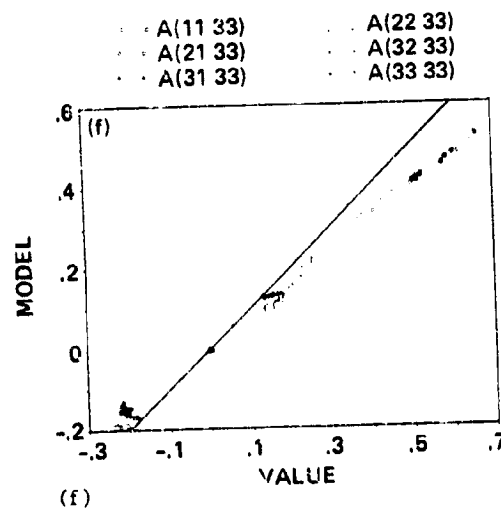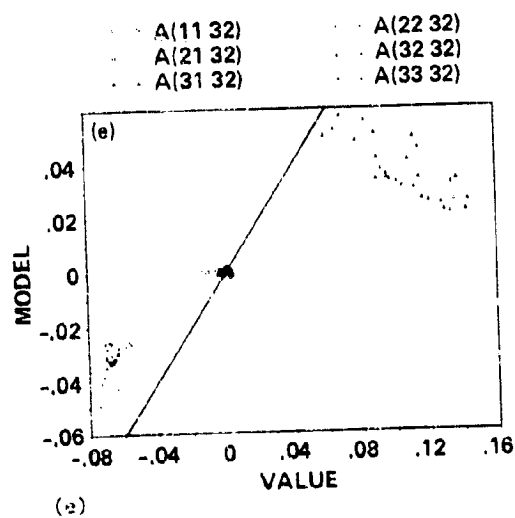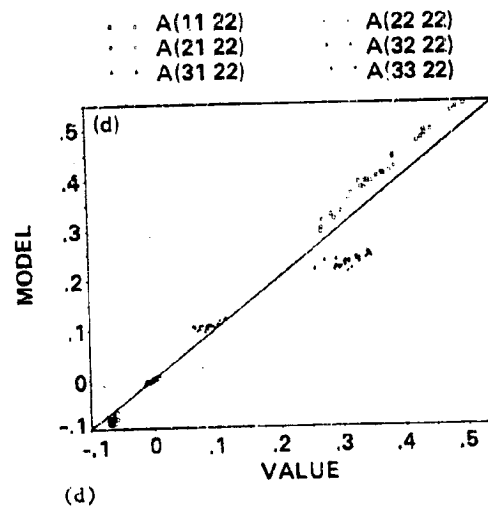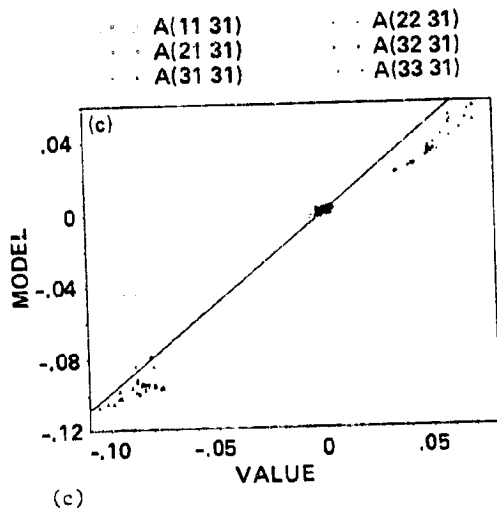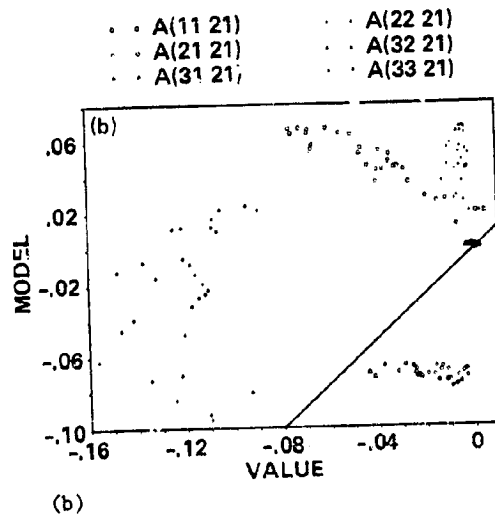
Figure 32.— Comparison of measured and modeled values of the "fast-pressure-strain" tensor a_{1j}^{mi} using the Launder-Reece-Rodi model in homogeneous shear turbulence.
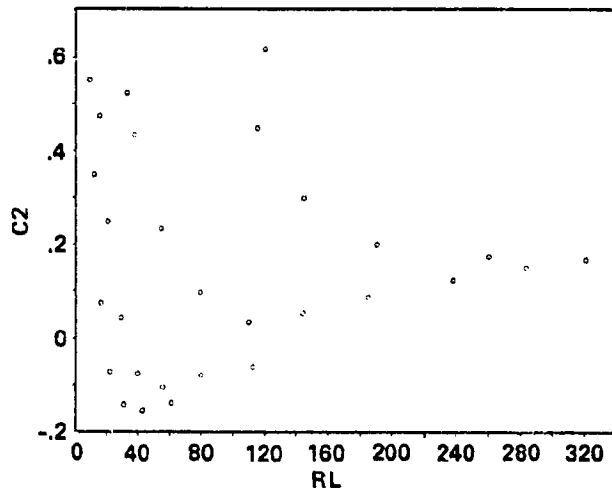
90

Figure 33.- Variation of the Launder-Reece-Rodi coefficient with Reynolds
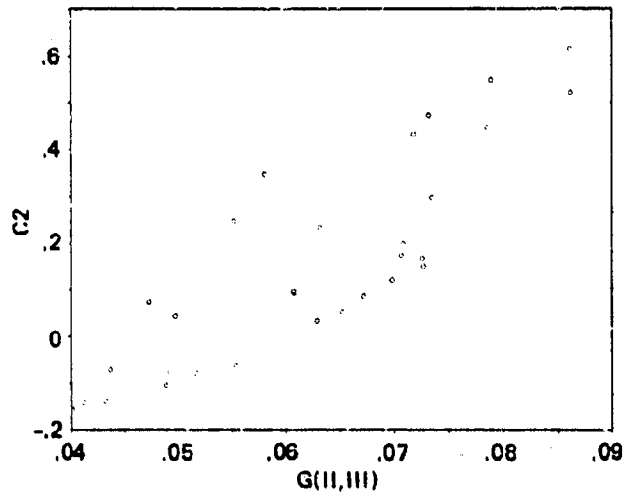number in homogeneous shear turbulence.

Figure 34.- Variation of the Launder-Reece-Rodi coefficient with anisotropy
level in homogeneous shear turbulence.

91